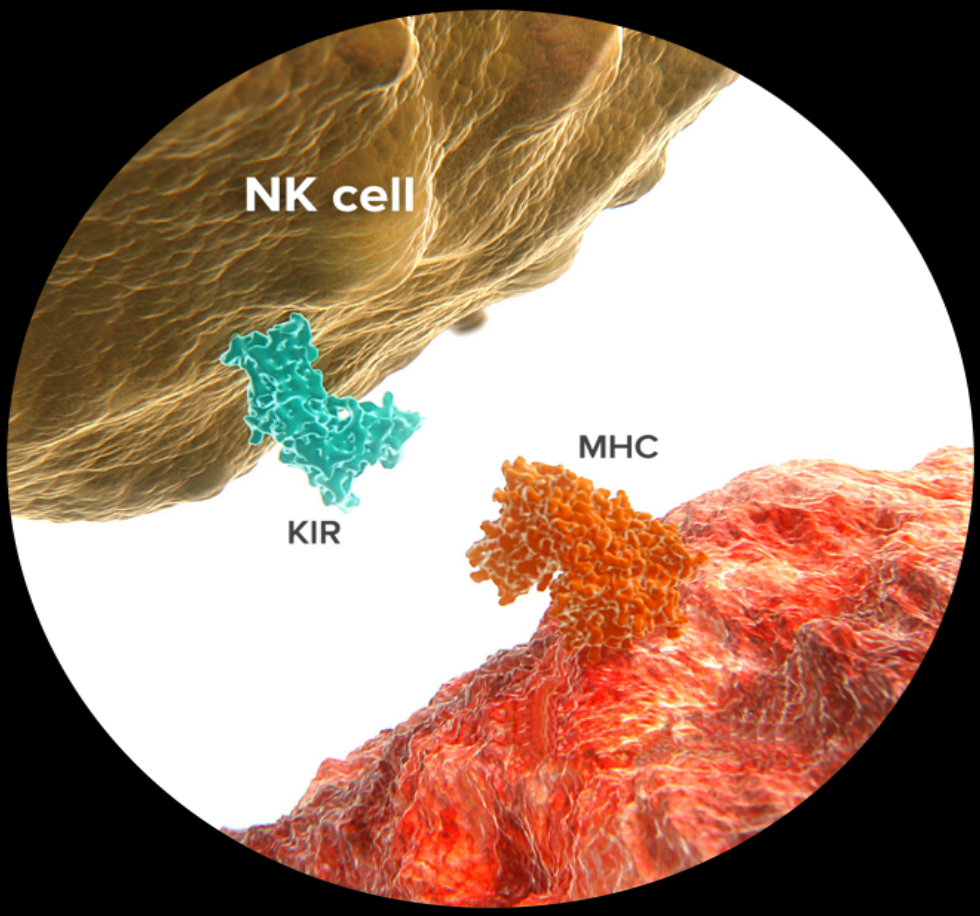

Kátia Ribeiro de Jesus

Immunology and genetics in nonhuman primates: Study of KIR3DL02 interaction with MHC-class-I ligands of rhesus macaques

Dissertação para a obtenção do grau de Mestre em Investigação Biomédica sob orientação científica da Professora Doutora Maria Joana Lima Barbosa de Melo e do Professor Doutor Lutz Walter e apresentada à Faculdade de Medicina da Universidade de Coimbra.

Maio 2018

· U C ·

Universidade de Coimbra

Immunology and genetics in nonhuman primates:

Study of KIR3DL02 interaction with MHC-class-I ligands of rhesus macaques

Kátia Ribeiro de Jesus

Dissertation for the attribution of the Masters degree in the specialty field of Biomedical Research, submitted to the Faculty of Medicine of the University of Coimbra, Portugal. The research work presented in this dissertation was performed at the German Primate Center (Deutsches Primatenzentrum - Leibniz-Institut für Primatenforschung, GmbH), under the supervision of Professor Doctor Maria Joana Lima Barbosa de Melo, Professor Doctor Lutz Walter and Doctor Beatrix Petersen.

Dissertação apresentada à Faculdade de Medicina da Universidade de Coimbra para cumprimento dos requisitos necessários à obtenção do grau de Mestre em Investigação Biomédica. Este trabalho foi realizado no German Primate Center (Deutsches Primatenzentrum - Leibniz-Institut für Primatenforschung, GmbH), sob orientação científica da Professora Doutora Maria Joana Lima Barbosa de Melo, do Professor Doutor Lutz Walter e da Doutora Beatrix Petersen.

Universidade de Coimbra

2018

Front cover:

Interactions between killer cell immunoglobulin-like receptors (KIRs) and major histocompatibility complex class I (MHC-I) molecules in target cells are key regulators in the cytotoxic response of natural killer (NK) cells. Illustration adapted from Immuno-Oncology, Bristol Myers Squibb.

“Success is not final, failure is not fatal:

It is the courage to continue that counts”

Winston Churchill

Acknowledgments

The development of this master work and the writing of my master thesis was made possible thanks to many people. To everyone who supported and encoureged me in any way in this last year, I would like to leave my appreciation. This was a year full of challenges but also full of accomplishemnts.

I would like to thank Professor Doctor Joana Melo for all the support and help thoughout this year abroad. For enabeling this opportunity, for her total availability and concern for the development of this work, I thank her.

To Professor Doctor Lutz Walter, I would also like to show my gratitude, for accepting me in the Primate Genetics Laboratory and for giving me the opportunity of developing me master work in the German Primate Centre (DPZ). Thank you for all the orientation during the development of my project and the guidance while discussing the results. This was an extraordinary experience and I am extremely grateful.

I would also like to leave a very special thank you to Trixi, for all the support, help and patience during my research and for all the reviews and constructive critiques to my work. She was a great mentor an even greater inspiration and was fundamental in my development as a researcher and the improvement of the scientific quality of this work. Thank you for pushing me and teaching me how to do great research and also for all your help and kindness.

Working at the Primate Genetics Laboratory (DPZ) was very pleasant thanks to several colleagues. To Ellen, thank you for all the lab tips and teachings. To Christiane, thank you for all the support, help and constructive comments on my lab work, even more, thank you for making the lab such a nice and friendly place. My fellow master students, Julia, Wiebke and Lisbet, thank you for all the lunches and laughters that made the most stressfull days easier to handle. A very special thank you to Delphine, for all the help and support, for pushing me to do more and for believing in me.

Finally, I would like to leave my graditude to the people who have stood by my side from the beginning of this journey. To all my friends, in special, Carlos, Sofia, Ana and Patricia, my familly and most of all to my parents, Nela and Vitor, for always believing and supporting me.

Summary

Natural killer (NK) cells are lymphocytes that are able to kill virus infected or transformed target cells. The activation of the NK cell mediated target cell lysis is achieved by the action of NK cell receptors. An important group of receptors are the killer cell Ig-like receptors (KIR), which are known to bind members of the polymorphic family of MHC-class-I molecules. The rhesus macaque has been considered of great importance as a nonhuman primate model of human infectious diseases. During experimental simian immunodeficiency virus (SIV) infection, a connection has been established between the presence of certain KIR and MHC-class-I alleles with higher or lower viral load, and consequently to faster or slower progression of the disease. Interestingly, the expression of *KIR3DL02* transcripts was shown to be associated with low viral loads and elite controller animals. However, the specificity of interaction between KIR3DL02 and MHC-class-I ligands is unknown. The aim of the present work was, for one, study the interaction between KIR3DL02 and certain Mamu alleles using multimerized KIR-Fc recombinant proteins to stain Mamu expressing cells. Additionally, in order to widen the spectrum of future interaction studies, new Mamu alleles were amplified from cDNA of rhesus macaque and cloned into a mammalian expression vector. The present work allowed the optimization of binding assays using KIR-Fc fusion proteins with K-562 Mamu AcGFP transfected cells. Identification of potential KIR3DL02 ligands as well as production of new Mamu mammalian expression constructs was accomplished. However, further studies need to be conducted to verify results here described and to study interaction between KIR3DL02 and new Mamu alleles amplified. Herein, in special, the known protective Mamu B*008 allele.

Keywords: natural killer (NK) cells; rhesus macaque (*Macaca mulatta*); killer cell immunoglobulin-like receptor (KIR); major histocompatibility complex class I (MHC-class-I); Fc-fusion proteins; expression constructs.

Resumo

Células natural killer (NK) são linfócitos capazes de matar células alvo infectadas ou transformadas por vírus. A ativação da lise de células alvo pelas células NK é mediada pelos receptores presentes nestas células. Um grupo importante de receptores são os receptores tipo imunoglobulina das células killer (KIR), sabe-se que estes ligam a membros da família polimórfica de moléculas MHC-classe-I. O macaco rhesus foi considerado um modelo animal primata não-humano de grande importância para doenças infeciosas nos humanos. Durante infecção experimental com o vírus da imunodeficiência símia (SIV), foi estabelecida uma conexão entre a presença de certos KIR e alelos MHC-classe-I com maiores ou mais baixos níveis virais, e consequentemente com uma mais rápida ou mais lenta progressão da doença. Curiosamente, foi demonstrado que a expressão de *KIR3DL02* está associada com níveis virais mais baixos em animais em ensaios experimentais de infecção. Contudo, as especificações da interação entre KIR3DL02 e ligandos de MHC-classe-I são desconhecidas. O objetivo do presente trabalho, foi, por um lado, estudar a interação entre KIR3DL02 e certos alelos de Mamu, através do uso de proteínas recombinantes de KIR-Fc multimerizadas para marcar células que expressam Mamu. Para além disto, de modo a expandir o espectro de futuros estudos de interação, novos alelos de Mamu foram amplificados de cDNA de macaco rhesus e clonados em vectores de expressão de mamíferos. O trabalho aqui descrito permitiu a otimização dos estudos de ligação com o uso de proteínas KIR-Fc de fusão e células K-562 transfectadas com Mamu AcGFP. Identificação de potenciais ligandos para KIR3DL02 assim como construção de novos vectores de expressão de Mamu foram conseguidos com sucesso. Contudo, é necessária a realização de mais estudos para averiguar os resultados aqui descritos e para estudar a interação entre KIR3DL02 e os novos alelos de Mamu amplificados, com especial interesse no alelo Mamu B*008 por estar associado a um efeito protetivo.

Palavras-chave: células natural killer (NK); macaco rhesus (*Macaca mulatta*); receptores tipo imunoglobulina das células killer (KIR); complexo maior de histocompatibilidade classe I (MHC-classe-I); proteínas de fusão Fc; vectores de expressão.

Index

Index of tables

Index of figures

List of abbreviations

µg	microgram
µL	microliter
µM	Micromolar
Ω	ohm
A	adenine
Amp	Ampicillin
aa	Aminoacid (s)
APC	Allophycocyanin
APS	Ammonium persulfate
bp	base pair(s)
BSA	Bovine Serum Albumin
BV570	Brilliant violet 570
°C	Celsius degree
C	Cytosine
CD	Cluster of differentiation
cDNA	complementary DNA
cm	centimeter
cm^2	Square centimeter
CO_2	Carbon dioxide
dATP	Deoxy adenosintriphosphate
dCTP	Deoxy cytosintriphosphate
ddATP	Dideoxy adenosintriphosphate
ddCTP	Dideoxy cytosintriphosphate
ddGTP	Dideoxy guanosintriphosphate
ddNTP	Dideoxy nukleotidtriphosphate
ddTTP	Dideoxy thymidintriphosphate
dGTP	Deoxy guanintriphosphate
dNTP	Deoxy nucleotidtriphosphate
DMEM	Dulbecco's modified eagle medium
DMSO	Dimethyl sulfoxide
DPZ	Deutsches Primatenzentrum GmbH
dTTP	Deoxy thymidintriphosphate

E. coli	*Escherichia coli*
EDTA	Ethylenediaminetetraacetic acid
e.g.	Example given
et al.	*et alteri*
EtBr	Ethidiumbromid
EtOH	Ethanol
fw	Forward
Fab	Fragment antigen-binding region
FCS	Fetal bovine/calf serum
FACS	Fluorescence activated-cell sorting
Fc	Fragment crystallisable region
FSC	Forward scatter
G	Guanine
g	gram
Genta	Gentamycin
G417	Geneticin
GFP	Green fluorescent protein
Glu	Glutamic acid
h	Hour(s)
H_2O	Water
HCl	Hydrochloric acid
HEK	Human embryonic kidney
HIV	Human immunodeficiency virus
HPLC	High performance liquid chromatography
HRP	Horseradish peroxidase
IgG	Immunoglobulin
IPTG	Isopropyl-β-D-thiogalaktopyranoside
ITAM	Immunoreceptor tyrosine-based activation motif
ITIM	Immunoreceptor tyrosine-based inhibitory motif
ITSM	Immunoreceptor tyrosine-based switch motif
KAc	Potassium acetate
Kana	Kanamycin
KCl	Potassium chloride
kb	kilobase

kD	kilodalton
KH_2PO_4	Potassium hydrogen carbonate
KIR	Killer cell immunoglobulin-like receptor(s)
kV	kilovolt
L	Liter
LRC	Leucocyte receptor complex
M	Molar
mA	Milliampere
MACS	Magnetic-activated cell sorting
mm	Millimeter
mM	Millimolar
mg	Milligram
$MgCl_2$	Magnesium chloride
$MgSO_4$	Magnesium sulfate
MHC	Major histocompatibility complex
min	Minute(s)
mL	Milliliter
NaAc	Sodium acetate
NaCl	Sodium chloride
NaI	Sodium iodade
NaN_3	Sodium azide
NaOH	Sodium hydroxide
ng	Nanogram
NK	Natural killer
nm	Nanometer
Nr.	Number
Pen/Strep	Penicillin/Streptomycin
PCR	Polymerase chain reaction
Pfu	*Pyrococcus furiosus*
g	Gravity
RNA	Ribonucleic acid
RNase	Ribonuclease
RT	Room temperature
s	Second (s)

SAP	Shrimp alkaline phosphatase
SB	Sodium borate
SDS	Sodium dodecyl sulfate
SDS-PAGE	Sodium dodecyl sulfate–polyacrylamide gel electrophoresis
SIV	Simian immunodeficiency virus
SOC	Glucose-yeast-trypton-salt medium
Strep	Streptavidin
SSC	Sideward scatter
T	Thymine
Taq	*Thermus aquaticus*
TEMED	Tetramethylethylenediamine
Tris	Tris hydroxymethyl aminomethane
Tyr	Tyrosine
U	Unit (s)
U/min	rotations per minute
UV	Ultraviolet
Vol	Volume
X-Gal	5-brom-4-chlor-3-indoxyl-β-D-galactopyranoside
YINM	Tyrosine-isoleucine-asparagine-methionine
Zeo	Zeocin

1 Introduction

1.1 The immune system

The human body is constantly exposed to a variety of threats. Its integrity, preservation and protection rely on an adapted response of the immune system, which is very complex and provides defense mechanisms. It is composed by several organs, tissues and cells which act together with the main purpose of defending the body against foreign invaders[1,2]. This is possible due to the capacity of the immune system of distinguishing self from non-self-material. The identification of foreign antigens is accomplished through interactions between receptors present at the membrane surface of immune cells and ligands expressed by the target cell[2–4]. The recognition of non-self-material leads to the labeling of this target material as hazardous and triggers immune responses aiming towards its elimination[1,2]. In this context, the immune system can be divided into an innate and an adaptive part, which present two main response types that can be distinguished by their speed and specificity of reaction[2,3].

1.1.1 The innate and adaptive immune responses

The innate immune system includes the physical, chemical and microbiological barriers of an individual as well as signaling molecules which trigger immediate responses, as are the examples of complement cytokines and acute phase proteins[3]. Moreover, it is composed by the cell types that provide immediate responses upon recognition of foreign antigens, amongst which phagocytic cells (neutrophils, monocytes and macrophages) and natural killer cells[2,3]. The recognition of foreign antigens by these cells relies on a limited subset of germline-encoded receptors which are expressed without gene rearrangement[4,5]. Hence, despite being the first line of defense and presenting the quickest response to infectious material, the innate immune systems' main impairments include its unspecificity in the recognition of foreign material and the inability to enhance upon repeated contact as a result of the lack of memory[5].

In contrast, the hallmarks that characterize the adaptive immunity are its precision, due to antigen specificity, and the presence of memory, which allows the enhancement upon repeated antigen contact[3,4]. Herein, upon infection, antigen presenting cells display the pathogens' digested peptides for B and T lymphocytes to come in contact with. This triggers the expansion of clonal B and T lymphocyte cell lines that express pathogen-specific receptors. The expanded B lymphocytes will secret immunoglobulins, responsible for eliminating extracellular microorganisms, whereas T cells are mainly involved in the defense against intracellular pathogens or rather provide help to other cells in the immune response, depending on the expression of CD8 or CD4 co-receptors.

Due to this, for many years, the adaptive immune system and its responses where the main target for immunologist to study, as the innate immune response was considered to only keep the pathogens at bay while the adaptive immune response was being formulated[6]. Nonetheless, pathogens might be highly variable, being able to quickly alter themselves to better evade and survive the immune system, underlying the importance of a fine-tuned communication between innate and adaptive immune system to provide proper defense mechanisms[7].

1.2 The Major Histocompatibility Complex: the role in immunity

The Major Histocompatibility Complex (MHC) is a genomic region on human chromosome 6 that contains over 200 gene loci, which were at first described as histocompatibility-specific genes[8]. Nowadays, it is known, that genes encoded in the MHC locus also have a major impact in the immune response and can be divided into class I, class II and class III, according to their function [9–11]. It is a highly polymorphic family, characterized by its allelic variability, rapid evolution and polygeny[8,10–12]. These features are likely to be the result of the continuous need of the immune response to adapt when faced with constant evolving pathogens[8].

The classical MHC class I and class II molecules, have been strongly associated with several immune diseases over the years[11,13]. MHC class II molecules, constituted by α and β chains, are only expressed on antigen-presenting cells (APCs), such as dendritic cells, macrophages and B cells and are needed for the induction of CD4+ T helper cell mediated immunity[12,14–17] Upon infection, when an APC phagocytes a pathogen, the latter is degraded intracellularly into peptides which can then be bound to the MHC class II molecule and brought to the cell surface to be presented to CD4+ T helper cells to trigger an immune response[12,14,16].

In contrast, MHC class I proteins are present on the surface of all nucleated cells. These molecules are heterodimers generally composed by a heavy chain (MHC α chain) and a light chain (β2-microglobulin chain) which present a short antigenic peptide[11,12,14]. Herein, the extracellular region of the heavy chain folds into α1, α2 and α3 domains, where α1 and α2 form the groove or binding site for antigenic peptides of 8-10 amino acids[18]. In healthy cells the peptide presented by the MHC molecule is derived from proteins of the cell. Upon infection, MHC class I displays peptides derived from the intracellular pathogen in order to induce the activation of CD8+ T cells[19,20]. In an effort to avoid detection, certain pathogens have developed mechanisms to evade antigen presentation by downregulation of the MHC class I expression[21]. A major example for this is the human immunodeficiency virus (HIV).

1.2.1 The impact of HIV infection on MHC class I expression

According to the world health organization in 2016, 36.7 million people were infected with human immunodeficiency virus (HIV) and in the same year 1.0 million died due to HIV-related disease. Nonetheless, up to date, no cure was yet found for this type of infectious disease. Over the years, many strategies for treatment and prevention have arose, which aim mainly towards controlling the viral loads. Currently, the most common therapy strategy is the use of antiretroviral drugs which impair efficiently the replication of the virus in infected cells thus delaying the onset of the disease[22]. However this type of treatment requires constant drug administration which can leads to several adverse effects and can ultimately lead to the development of drug resistant virus strains[23,24].

In 1986, acquired immunodeficiency syndrome (AIDS) was established to be the result of infection with HIV, which is part of a subgroup of retroviruses, designated lentiviruses. The latter cause chronic and deadly disease which present long incubation periods. Upon infection with HIV, the virus enters the hosts CD4+ T cells, transcribes its RNA into DNA and then uses the cells machinery to replicate, creating new copies of its genome, which are then released to infect further cells[25,26]. This results in the progressive depletion of CD4+ T cells, leading to an increased susceptibility to infections, being the cause for immunodeficiency verified in AIDS patients[27,28]. The ability of HIV to evade the immune system so efficiently derives from many reasons. Besides its genetic variability being one of the key aspects, the capacity of the virus to down regulate the MHC class I and II molecules of the host cell allows evasion of detection by CD8+ T cells as well as NK cells[21,29,30]. Nonetheless, several studies have pointed to the importance of NK cells receptor repertoire and MHC class I ligands in an individual in influencing the infections' outcomes.

It has already been published, that some MHC class I molecules act protectively during HIV infection, whereas others are linked to worse outcome[31,32]. More recently, the interaction between certain NK cell receptors, the killer cell immunoglobulin-like receptors (KIR) and their MHC class I ligands has been shown to be associated with slower progression of the disease[33,34]. This protective effect of KIR/MHC class I interaction has already been described for several other viral infections as is the example of hepatitis C, suggesting that interaction between KIR and their MHC class I ligands might have a fundamental role in NK cell mediated control of viral infections[35].

1.3 Natural killer cells

Natural killer (NK) cells are a population of lymphocytes which have been characterized as part of the innate immune system mainly due to their rapid response and lack of receptor gene rearrangement[36]. It is nowadays known that NK cell cytolytic activity is dependent on the MHC class I expression of the target cell and that this is controlled by signals received through the NK cell

receptors. Additionally over the last few years, evidence has been brought to light that proves that NK cells also present features of the adaptive immune system[37].

NK cells are nowadays characterized as being part of the group 1 of innate lymphoid cells (ILCs). They are responsible for killing virus infected or malignantly transformed cells through the release of granzymes and perforins, and modulating the adaptive immune response thought the release of cytokines and chemokines. Additionally, certain NK cell subsets can expand in a pathogen-specific manner, generating long lasting memory cells that persist after the encounter with the antigen and even mount an enhanced response upon repeated contact[37–39]. Altogether this highlights the importance of NK cells in the immune system, underlying the need for a better understanding of their development, education, training and function.

The first definition for NK cells was, that these where large granular lymphocytes that could kill infected cells without the need of any additional stimulus. For many years NK cells were thought to resemble T cells, with the main difference that these were not restricted to MHC class I expression. In 1984, Kärre postulated the Missing self-Hypothesis, saying that NK cells target an altered MHC class I expression on host cells. Hence, NK cells are activated by a reduced or nonexistent cell surface level of MHC class I molecules[40,41]. Consequently, the NK cells cytolytic activity is dependent on information on the surface of their target cells, which are sensed by a variety of NK cell receptors. It is estimated that the human NK cell population can present from 6 000 up to 30 000 subpopulations according to their phenotypic variability and that this might rise not only from their genetic but also environmental variabilities[42].

1.3.1 NK cell development, licensing and disarming

Despite being a growing topic of research, NK cell development and maturation still raises many questions. NK cells, like all other leucocytes, derive from pluripotent hematopoietic stem cells (HSCs) residing in the bone marrow from a $CD34^+$ common lymphoid progenitor (CLP), which is capable of producing all types of lymphocytes. The process by which these ILCs are matured is composed by a combination of several steps that successively restrict the NK cell population and allow differentiation of mature natural killer cell lineages[39,43,44].

The NK cell development is divided into five stages, illustrated in the figure below, which characterize the restriction and acquisition of NK specific markers.

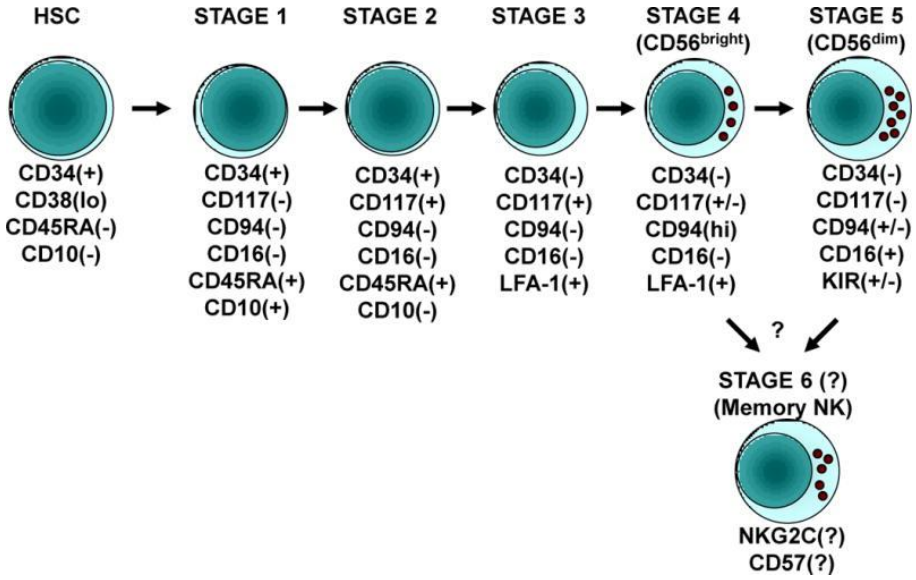

Figure 1 - Schematic representation of the of human natural killer (NK) cell development. *Illustration from Yu et al. (2013), "Location and cellular stages of natural killer cell development", Trends immunol.*

During the first two stages, cells undergoing maturation retain the ability to develop not only into NK cells but also dendritic cells and T cells. It is only on stage three that this developmental potential is lost and immature NK cells are identified[44]. Another important mark in NK cell development is the acquisition of the interleukin (IL)-15 receptor. IL-15 is fundamental for NK cell differentiation and maturation and also throughout NK lifetime for their survival[39,43]. Populations of CLP responsive to IL-15 have been identified during stage 2 and stage 3 of NK cell development[44]. After this, NK cells acquire markers like CD94, necessary for surface expression of NKG2 receptors, and the NK cell marker CD56 as well as functional receptors like NKG2D and killer cell immunoglobulin-like receptors (KIRs)[39,44]. The maturation process is completed when $CD56^{bright}CD16^{+/-}$ cells from stage 4 convert into $CD56^{dim}CD16^{+}$ NK cells[39,44]. Both NK cell populations can be found in human peripheral blood and can be distinguished by their cytolytic capacity and cytokine production ability. $CD56^{bright}$NK cells present a higher capacity for cytokine production and a lower cytolytic capacity. In contrast, $CD56^{dim}$NK cells predominate in the peripheral blood and are characterized by higher cytotoxicity[39,45,46].

At the end of the maturation process, each NK cell presents a variety of receptors which control the cells' activation status. As each cell is equipped with different receptors, each individual possesses several populations of NK cells with a variety of receptors stochastically distributed. This might, lead to the maturation of NK cells which only possess activating receptors and for this reason will not be able to recognize self-molecules in healthy cells[38]. Due to this, NK cells undergo a fine-tuned education process. NK cells that cannot recognize healthy cells are rendered ineffective. Those which

express a subset of receptors capable of distinguishing infected cells are conferred functional capacity[38].

The education process is characterized by the adjustment of NK cells functional and phenotypical response. NK cells with activating receptors that recognize MHC class I molecules are more efficient in the identification of MHC-I devoid cells and are designated as licensed[42,47]. Cells that do not express activation receptors that recognize MHC-I respond poorly to stimulation and are classified as not-licensed. The disarming mechanism explains the licensing model of natural killer cells. This states that at some point in NK cell development, the activating receptors become responsive by default. This leads to the necessity of inhibitory receptors to neutralize activation. Hence, cells that do not express inhibitory receptors become less responsive or disarmed[42,47].

These education processes ultimately determine the threshold of activation of mature NK cells in an individual by conditioning the activation state of the NK cells during development according to the strength of the inhibitory signals recieved[48].

1.3.2 NK cell receptors

NK cell receptors are fundamental players in the education and regulation of the cytolytic capacity of these cells. The receptors can be divided mainly into activating and inhibitory ones and the balance of the signals provided by these determines NK cell activation or inhibition toward a target cell[49–51].

These two groups of NK cell receptors use opposing signaling mechanisms. Inhibitory receptors contain an intercellular immune receptor tyrosine-based inhibitory motif (ITIM) in their cytoplasmic tail[50]. Upon ligand binding, a tyrosine residue in the ITIM is phosphorylated, by an Scr family kinase, being then able to recruit protein tyrosine phosphatase through the SH2 domain[49,50,52]. The type of protein tyrosine phosphatase being recruited, either tyrosine-specific phosphatase (SHP-1 or SHP-2) or phospholipid-specific phosphatase (SHIP), depends on the receptor being engaged[53]. The phosphatases are essential for mediating inhibitory function as these intermediate at a membrane proximal location, leading to the dampening or preventing downstream signals required for activation and therefore, blocking effector functions[53,54]. This explains the prevalence of inhibitory over activatory signals when both receptors of an NK cell are engaged by their ligands[54].

On the contrary, some activating receptors contain a positively charged amino acid in their transmembrane region and are usually non-covalently associated with signal adaptor molecules, like DAP12 and FcγR, which possess an immune receptor tyrosine based activating motif (ITAM)[51]. In this case, after phosphorylation of the tyrosine contained in the ITAM, Scr homology 2 domain containing

kinases (Syc or ZAP70) are recruited, leading to the onset of a signaling cascade which triggers NK cells degranulation and production of cytokines and chemokines[50,55].

The genes encoding NK cell receptors are clustered in two gene complexes which form the two receptor families. The natural killer complex (NKC) encoding C-type lectin like receptors, as are Ly49 and the CD94/NKG2 heterodimers, at chromosome 12, and the leucocyte receptor complex (LRC) encoding the immunoglobulin-like receptors, as are the killer cell immunoglobulin-like receptors (KIRs) and the leucocyte immunoglobulin-like receptors (LIR, ILT or CD85), at chromosome 19[48,50,56,57]. Although both gene clusters are present in different species and there are orthologues as CD94 which are maintained between species, there is evidence for differential development which lead to highly polymorphic genes. For example, in mice the C type lectin like Ly49 family is highly developed, nonetheless in humans this is only a pseudogene. In agreement with this, the KIR family is highly polymorphic in primates, but in mice no trace of this family has been found[58].

1.3.3 The Killer Cell Immunoglobulin-like receptors (KIRs)

The killer cell immunoglobulin-like receptors are type I transmembrane glycoproteins that belong to the immunoglobulin superfamily[11]. They are present in NK cells as well as cytotoxic T cells and have become the main receptors in human NK cells for MHC class I ligands[51]. The expression level of KIR receptors is controlled at the transcriptional level firstly by methylation of the CpG islands surrounding the start site[59,60]. Another way to control KIR expression levels in humans occurs through bidirectional promotors which are able to switch the direction of KIR transcription during NK cell development[59,61].

Up to now, in humans 16 highly polymorphic genes have been identified to encode KIR proteins[62,63]. The polymorphic character of the KIR gene family can be explained by the several expansions and contractions that the region has undergone over time. Next to the MHC region, the KIR region is the most polymorphic of the human genome. This also allows an enormous variability in the subset of KIRs being expressed in any individual[64]. The allelic variability of the KIR gene family occurs mainly due to gene duplication and non-allelic homologous recombination, which derives from high similarity between different KIRs[11,59].

Two distinct haplotypes have been identified in the human population, the class A haplotype only presents one activating KIR and is mainly characterized for having inhibitory KIR genes. This haplotype is considered structurally invariant and usually presents allelic polymorphism[63,65]. In contrast, the class B haplotype presents greater structural variability, containing usually more than one activating KIR and diverse combinations of KIRs in different individuals, but featuring less allelic

polymorphism[63,65]. However, both haplotypes present *KIR2DL4*, *KIR3DL3* and *KIR3DL2*[66,67]. These two classes of KIR haplotypes display different features. Whereas the class A haplotype is linked to a better resistance against infections and pathogens, KIR haplotype class B presents advantageous characteristics on what concerns reproduction as well as other yet unknown functions[63,65].

KIR receptors can be functionally divided into activating and inhibitory ones, and are also key regulators during the development of tolerance in NK cell education[62,68]. Figure 2 illustrates activating and inhibitory KIR receptors as well as their adaptor molecules.

The nomenclature used for KIRs is based on three criteria, the number of extracellular IgG domains, the length of the cytoplasmic tail and the sequence similarity. Regarding the number of extracellular C2 type immunoglobulin-like domains, KIRs can possess two or three IgG domains and are for this designated KIR2D or KIR3D, respectively[11,64]. These extracellular IgG domains are responsible for ligand recognition[62,69].

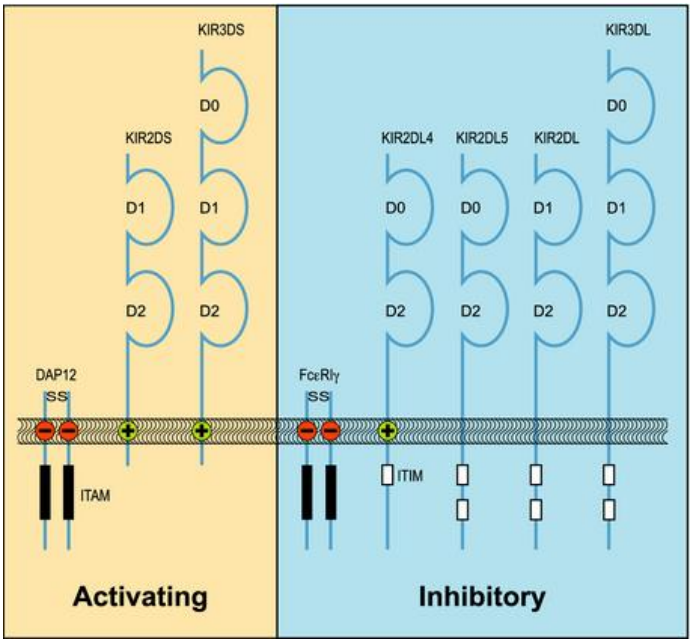

***Figure 2 - Illustration of the different KIR subgroups**. Inhibitory and activating receptors, respectively from the left to the right side. Illustration edited from Groot et al. (2015), Co-evolution of the MHC class I and KIR gene families in rhesus macaques: ancestry and plasticity", Immunological Reviews.*

Further, KIRs can mediate activating or inhibitory signals. This correlates with the length of the cytoplasmic tail. Herein, activating KIRs, designated KIR2DS or KIR3DS, present short cytoplasmic tails and contain a positively charged amino acid, able to onset a cascade which will trigger cytotoxicity as well as cytokine and chemokine release. Inhibitory KIRs present long cytoplasmic tails and contain an ITIM that inhibits the effector functions of the NK cells and are for this designated KIR2DL or KIR3DL[11,62,69].

An exception to this is the KIR2DL4, which despite presenting a long cytoplasmic tail is an activating receptor only expressed in CD56^{bright} NK cells[62,70]. This NK cell receptor associates with ITAM-containing FcεRI-γ adaptor leading to a stronger activation of the production of cytokines rather than cytotoxic capacity[62,70]. Lastly, different KIRs with a sequence divergence of more than 2 % are numbered in series[71].

1.4 MHC class I and KIR interaction in immune disease

There is strong evidence that, due to their functional dependence, MHC class I and KIR genes have coevolved[72]. In fact, MHC-I and KIR interactions have already been associated with diverse diseases, reproduction failure and recently, even with cancer[73–75]. In the context of immune disease, it is becoming clearer that the strength of KIR-MHC-I binding can influence susceptibility to disease. It is known that the stronger the binding between an inhibitory KIR and its ligands, the stronger the signal and the consequent inhibition of the NK cells functional response[59,76]. Herein allelic variability can contribute to stronger interactions, as some allotypes are expressed on higher levels than other, this will ultimately affect the level of binding[77]. Allelic variants can also be expressed in different frequencies by NK cells. Lastly, peptides present in the binding groove of the MHC ligand can also affect interaction[77].

Several epidemiologic studies have provided evidence for the impact of KIR-HLA combinations. For instance, in hepatitis C virus infections, the combination of KIR2DL3/HLA-C1 leads to weaker inhibitory signals and lower activating capacity which is protective in virus clearance[35,78]. Also, during herpes virus infections, it was found that the combination of KIR2DL1/HLA-C2 which is known to lead to strong inhibitory signals, was detrimental resulting in the NK cells inability to mount a proper protective response against the cytomegalovirus (CMV) infection. Moreover, evidence for a protective capacity of activating KIRs has been described for CMV infection[59,79]. Nonetheless, activating KIRs have been associated with predisposition for occurrence of immune restoration disease associated herpes virus infections and during HIV treatment[80,81]. Immune restoration disease are reactivations of quiescent opportunistic infections which occur after the treatment of immunodeficient patients with antiretroviral therapeutic.

All in all, it was found that in the context of viral infections, on the one hand genotypes that lead to lower inhibition and higher activation are beneficial, on the other hand, a higher risk for autoimmunity and cancer seems to be associated.

In the specific case of HIV, the combination of KIR3DS1/HLA-B Bw4-80I is associated with slower progression of the disease, lower viral loads and protection against opportunistic diseases[82,83]. Herein, it has been proven that NK cells strongly expressing KIR3DS1 provide a better functional response to HIV infected cells that present the HLA-B Bw4-80I epitopes[33,84]. These results are in agreement with knowledge that NK cell activation is beneficial during infections. However, it was also found that the presence of the Bw4 80I ligand, KIR3DL1, especially when highly expressed, is associated with slower progression of the disease and lower viral loads[33]. These results seem to contradict the hypothesis that NK cell activation is protective. Nonetheless, this might suggest a new

model. Herein, the importance of inhibition in NK cell education and the protective effect of activation receptors in infections are both acknowledged. Due to this, it becomes important to consider that KIR-MHC class I inhibitory signals are not only vital for NK cell education. These are also important for the maturation of functional effector NK cells. Altogether indicating inhibitory receptors play an important role in the protection and resolution of HIV infection[85–88].

1.5 The rhesus macaque as a model for the study of HIV/AIDS

The ideal animal model system for studying any disease should present similar signals of illness after exposure to the pathogen and comparable infectious doses. The human immunodeficiency virus (HIV) is a direct descendent of the simian immunodeficiency virus (SIV) from central Africa chimpanzees[89]. Nonetheless, chimpanzees cannot be used as a study model for HIV as for one, infection with the virus in captivity does not always result in development of the disease[90]. In addition to this, chimpanzees are considered an endangered species and implicate high costs in maintenance[91].

The search for the optimal animal model for AIDS was at first hampered due to the fact that the HI virus cannot replicate in a vast majority of animal species, including rodents. This comes from the fact that the cellular proteins of these non-primate species do not support viral replication[91,92]. In contrast to most primate species from Africa, which are natural hosts to the SIV and therefore do not develop the diseases as a consequence of the infection, asian macaques became an interesting animal model for studying HIV/SIV infection. Since these are not natural hosts for primate lentiviruses, upon infection with SIV, high viral loads and progressive depletion of CD4+ T cell population, accompanied with rise of opportunistic disease are observed, providing an animal model with great resemblance to human HIV infection[91]. For these reasons, asian macaques have been accepted as the optimal model for studying HIV/AIDS.

The use of asian macaques has allowed a better understanding of the disease, transmission processes and latency as well as the development of several vaccines and microbicides for prevention of HIV, and lastly the development of the antiretroviral therapy[91,93,94]. Within the asian macaques, the rhesus macaque (*Macaca mulatta*) descendent from India is by far the most used and well characterized non-human primate animal model. Presenting similar replication and outcomes with SIV infection, with minimal animal-to-animal variability. Only the rate of progression of SIV differs from the human HIV infection, decreasing from period of 8-10 years in humans to 1-2 years in rhesus macaques, for development of AIDS[91].

1.5.1 MHC class I in humans and in rhesus macaques

The MHC class I genes of the rhesus macaques, designated Mamu, much like humans, are part of a highly polymorphic family of genes located at chromosome 6, that show the same overall structure in both species[11]. Despite being a major animal model for studying human immune disease, there is still much to understand on what concerns non-human primate genetic diversity and genomics, both important factors in the formation of an immune response[11,95].

The class I loci of rhesus macaques has already been target to some studies that allowed the identification of paralogues to HLA A and HLA B, Mamu A and Mamu B, respectively[11,96,97]. Furthermore, orthologues to HLA E and HLA F, Mamu E and Mamu F, respectively as well as a functional orthologue to HLA G, the Mamu AG, were identified [11,98–100]. A striking difference between human and rhesus macaque MHC class I is the size of the loci of this gene family in both species. In humans, the MHC locus spans approximately 3.7 Mb, whereas in rhesus macaques this extends to as much as 5.3 Mb. This considerable expansion is mainly reflected in the MHC class I A and B genes, which in rhesus macaques have been duplicated, presenting as many as two loci for Mamu A and three loci for Mamu B genes[95,97,101]. This genetic diversity lead to an expansion of six MHC class I genes, expressed in one human haplotype, to up to 22 possibly active MHC class I genes in a rhesus macaque haplotype[95].

This clear difference between human and rhesus macaque MHC class I has functional consequences in the immune response presented by both species that have yet to be understood and are of fundamental interest for a better use of the rhesus macaque as an animal model in human immune disease.

1.5.2 KIR in humans and in rhesus macaques

The KIR gene family is present in all simian primate species and features in all a similar structure. In both, human and non-human primates, KIR genes are located at chromosome 19 and are part of a highly polymorphic family with great allelic and copy number variability and a stochastic expression profile on individual NK cells[53,102]. Nonetheless, there is clear evidence for species-specific evolution of this gene family. A good example of this co-evolution of KIR and their MHC class I ligands is the orangutan, in which single lineage III KIR, present in ancestral haplotypes of KIR, expanded into three lineage III KIRs to become the main receptors for MHC-C[103].

In the rhesus macaque, there are some differences to human that need to be taken into account. For one, the activating receptors, unlike in human, show characteristics of both inhibitory KIR3DL and unique activating KIR2DL4. An even more remarkable distinguishing feature is the clear expansion of

the lineage II KIR3D family. In fact, with the exception of KIR2DL4, KIR2DL5 and KIR1D, all rhesus macaque KIRs present three IgG domains, interacting specifically with the Mamu A and B genes in a locus and allelic specific manner[104,105]. Functional studies have already shown that interactions between rhesus macaque lineage II KIR and their MHC A and B ligands are considerably more diverse than those of humans, nonetheless, the depth of this diversity and the consequences of those interactions are yet to be understood[106].

1.5.3 MHC class I and KIR interaction in SIV

Whilst interactions between human MHC class I and KIR have been target of several studies, and growing evidence points towards the importance of these interactions in several aspects of human disease, in rhesus macaques this has been poorly described, and as main animal model for human immune disease this becomes a matter of clear importance.

Up to now, certain Mamu alleles have successfully been characterized as presenting a protective role in the context of SIV, being associated with slower progression of the disease and lower viral loads[91,107]. These include Mamu A1*001, which has been reported to lead to a five-fold decrease in viral loads and also Mamu B*008 and B*017[91,107].

In addition, in their work, Rosner and colleagues (2011) described interactions between four rhesus macaque NK cell receptors, three inhibitory KIRs (3DLW03, 3DL11 and 3DL05) and one activating KIR (3DS05) with Mamu A1*001 and A3*13[108]. Additionally, Mamu A1*011 was identified as a ligand for inhibitory KIR3DW03 and Mamu A1*002 was also described as a ligand for KIR3DL05[108,109].

Furthermore, in the work of Albrecht and colleagues (2014), cohorts of animals were analysed regarding their KIR transcripts and it was recognized that the progression of AIDS in SIV infected macaques was influenced by the KIR transcripts present in each animal. In this context, one activating and two inhibitory KIRs were identified as being associated with certain outcomes of the infection. Herein, presence of *KIR3DS02* was associated with high viral loads, whereas *KIR3DSW08* and *KIR3DL02* were associated with lower viral loads[110]. However, the specificity of interaction between these receptors and MHC-class-I ligands is unknown.

2 Aim of the study

The interaction between killer cell immunoglobulin-like receptors (KIR) and major histocompatibility complex class I (MHC-class-I) ligands influences the response of NK cells and can be associated with higher or lower viral load, thus the progression of AIDS. Understanding the interactions and the mechanism that provide a protective response in SIV infection in rhesus macaques (*Macaca mulatta*) is of great interest, since this species is the most important animal model used in infectious disease and could, for this reason, provide insides that would allow a translation to human research.

The effect of the ligation of KIR3DL02 with Mamu allotypes known for protective responses (e.g. Mamu-A1*001 and Mamu-B*017), and with Mamu allotypes that have been associated with non-protective responses (e.g. Mamu-A1*004) is still unclear. The aim of this study is twofold: (1) study the interaction between NK cell receptor, KIR3DL02 and MHC-I of rhesus macaque to identify potential ligands, and (2) to expand the spectrum of the study by providing new Mamu mammalian expression constructs that were not within the already provided by the Primate Genetics Laboratory (DPZ), as for example Mamu B*008.

To accomplish these goals, recombinant KIR-Fc multimerized proteins were used to stain, Mamu surface expressing cells. Analysis of interaction was made by flow cytometry. Construction of new expression vectors required amplification of MHC-I alleles from cDNA of rhesus macaques using sequence specific primers and cloning.

3 Materials

3.1 Equipment

Equipment	Type	Manufacturer
Autoclave	Varioklav ® 400E	H+P Labortechnik
Balance	BP 310 s	Sartorius
Blotter (Semi-dry)	V20-SDB	Scie-PLAS
Centrifuge	5415 R	Eppendorf
	5424	Eppendorf
	5810 R	Eppendorf
	Biofuge pico	Heraeus
	Fresco 21	Heraeus
	Multifuge 1 S	Heraeus
	Multifuge 1 S-R	Heraeus
Cell sorter	SH800S	Sony Biotechnology
Electronic Pipette	Pipetus ®	HIRSCHMANN LABORGERÄTE
	Pipetboy acu 2	Integra
Electrophoresis combs (agarose)	Horizon 58	Gibco BRL
Electrophoresis combs (SDS-PAGE)	EPH-1010-V	Bridge
Electrophoresis Chamber (agarose)	Horizon 58	Life Technologies
Electrophoresis Chamber (SDS-PAGE)	Novex	LifeTechnologies
Flow Cytometer	LSR II	BD Biosciences
Freezer (-20 ºC)	Premium	Liebherr
Freezer (-80 ºC)	U 725-86	NB Scientific
Freezer (-140 ºC)	ULT-10140	Thermo Fisher Scientific
Freezing container	Mr. Frosties	Nalgene
Fridge (4 ºC)	Easy Electronic	Privileg
Gel documentation equipment	Gel Jet Imager 2000	INTAS
Hemocytometer	Neubauer improved	Marienfeld superior
Ice system	AF103	Scotsman®
Incubator		
- **Bacteria**	B12	Heraeus
	3033	GFL
	1083	GFL

- **Cell Culture**	Heraeus HERA cell 150	Thermo Scientific Thermo Electro Corporation
Magnet stirring equipment	M32 MR30001 K	GLW Heidolph
MACS multistand		Miltenyi Biotec
Microscope - **Fluorescence**	CK40 Observer A1	Olympus Zeiss
Microwave	SS-4F2H	Panasonic
pH measurement equipment	HI 221	HANNA instruments
Pipettes	(2.5 µL; 10 µL; 100 µL; 1000 µL)	Eppendorf
Photo printer	P93D	MITSUBISHI
Power supply - **Agarose Gel** - **SDS-PAGE**	 Power pack P25 Power pack P25T	 Biometra ® Biometra ®
Pump	TL 10	Medorex
Sequencing equipment	ABI3100avant	Applied Biosystems
Shaker	Duomax 1030	Heidolph
Spectrophotometer	NanoDrop 1000	Peqlab
Sterile Hood - **Bacteria** - **Cell culture**	 KR-125 Safety HERA safe KS 12 HERA safe KS 18	 KOJAIR Thermo Electro Corporation
Speed Vac	Concentrator plus	Eppendorf
Thermoblock	M32	GLW
Thermocycler	Labcycler	SensoQuest
Thermomixer	Eppendorf ThermoMixer® C	Eppendorf
UV light tables	IL-350-M	H. SAUR laboratories
Vacuum concentrator system	Concentrator Plus	Eppendorf
Vortex	G560 E	Scientific Industries, Inc
Water bath	1083	GFL

3.2 Consumables

Consumables	Manufacturer
6, 12, 24 and 96 well plate	Greiner Bio-one
Air-vented tubes, 12 mL	Greiner Bio-one
Cassettes	Novex Life Technologies
Cell culture flasks (T 25; T 75; T 175)	Sarstedt
Cryotubes	Sarstedt
FACS tubes	BD Falcon
Falcon tubes (15 mL; 50 mL)	Cell Star ®
Filter (0.22 µm)	Heinemann Labortechnik
Filtropur V50 (0.45 µm)	Sarstedt
HiTrap Protein G HP	GE Healthcare
MACS columns	Miltenyi Biotec
Nitrocellulose transfer membrane 0.45 µm	GE Healthcare Life Sciences
Petri Dishes	Cell Star ®
Pipette tips, 2.5 µL	Biozym
Pipette tips, 100 µL	Sarstedt
Pipette tips, 1000 µL	Roth
Plates (10 cm^2)	Sarstedt
Reaction tubes (0.2 mL; 0.5 mL; 1.5 mL; 2.0 mL)	Sarstedt
Serological pipettes (5 mL, 10 mL, 25 mL)	Sarstedt
Sorting chip 100 µm	Sony Biotechnology
Syringes 20 mL	HSW NORM-Ject
Whatman Paper 3MM	Fisher Scientific
Thermal paper (High density paper)	Mitsubishi electric

3.3 Chemicals

Chemicals	Manufacturer
β-mercaptoethanol **For cell culture**	Sigma Gibco
ε- aminocaprionic acid	Sigma
1-Step™ Ultra TMB-Blotting Solution	Pierce™
5-Brom-4-chlor-3-indoxyl-β-D-galactopyranosid (X-Gal)	Roth

Acetic acid	Roth
Acrylamide/Bis-acrylamide (30 %/0.8 % w/v)	BioRad
Agar agar	Roth
Agarose	Biozym
AppliClear-Water	AppliChem
Ammonium persulfate (APS)	Sigma
Big Dye®	Applied Biosystems
BioTherm Buffer (10 x)	GeneCraft
BioTherm Taq Polymerase	GeneCraft
Biotin Protein A	Pierce™
Boric Acid	Merck
Bromophenol Blue	Sigma-Aldrich
Bovine Serum Albumin (BSA)	PAA Laboratories
Calcium chloride ($CaCl_2$)	Merck
Coomassie (Bradford) Protein Assay Reagent	Pierce™
dATPs	Fermentas
Dimethyl sulfoxide (DMSO)	Sigma-Aldrich
Disodium phosphate (Na_2HPO_4)	Merck
Dulbecco's Phosphate-Buffered Saline (DPBS)	Thermo Fisher Scientific
Dulbecco's modified eagle medium (DMEM)	Thermo Fisher Scientific
dNTPs	GeneCraft
Ethylenediaminetetraacetic acid (EDTA)	Roth
Ethidium Bromide (EtBr)	AppliChem
Ethanol (pure) (EtOH)	Merck
Fetal Bovine/Calf Serum (FCS)	Merck
Formaldehyde 37 %	Roth
FreeStyle™ 293 Expression Medium	Thermo Fisher Scientific
Glacial acetic acid (CH_3CO_2H)	Roth
Glucose	Sigma
Glycine	Sigma
Glycerol	Roth
High deionized (HI-DI™) Formamid	Life Technologies
HPLC Water (LiChroslov ®) (H_2O)	Merck

Human IgG	Sigma
Hydrochloric acid (HCl)	Roth
Isopropanol	AppliChem
Isopropyl β-D-1-thiogalactopyranoside (IPTG)	Biomol
Lipofectamine 2000	Invitrogen
Magnesium chloride ($MgCl_2$)	Merck
Magnesium sulfate ($MgSO_4$)	Merck
Methanol (MeOH)	Roth
Milk Powder	Roth
Mycoplasma off	Minerva Biolabs
OptiMEM	Thermo Fisher Scientific
Pfu buffer with $MgSO_4$	Fermentas
Pfu DNA polymerase	Fermentas
Phosphoric Acid (H_3PO_4)	Roth
Potassium Acetate (KAc)	Roth
Potassium Chloride (KCl)	Merck
RNase A	Sigma
Saccharose	Merck
Shrimp alkaline phosphatase (SAP)	USB Athymetrix
Sodium acetate (NaAc)	Sigma Aldrich
Sodium azide (NaN_3)	Merck
Sodium dodecyl sulfate (SDS) pellets	Roth
Sodium chloride (NaCl)	AppliChem
Sodium hydroxide (NaOH)	Roth
Sodium iodide (NaI)	Merck
Sodium phosphate ($NaPO_4$)	Fulka
Sodium phosphate dibasic ($Na_2H_2PO_4$)	Merck
Tetramethylethylenediamine (TEMED)	Sigma
Tris-hydrochlorid (Tris-HCl)	Promega
Tris	Roth
Trisodium phosphate (Na_3PO_4)	Merck
Triton X-100	Sigma
Trypan Blue	Gibco
Trypsin/EDTA	Pan Biotech

Trypton/Pepton	Roth
Tween 20	Sigma
Yeast extract	Becton, Dickinson

3.4 Antibiotics

Antibiotics	**Manufacturer**
Ampicillin	Sigma
G418	Sigma
Gentamycin	Biochrom
Kanamycin	Sigma
Penicillin/Streptomycin	Pan Biotech
Zeocin	InvivoGen

3.5 Enzymes and buffers

Enyzmes and buffers	**Manufacturer**
ApaLI 10 000 U/mL	New England Biolabs
BamHI 20 000 U/mL	New England Biolabs
CutSmart buffer	New England Biolabs
EcoRI 20 000 U/mL	New England Biolabs
HindIII 20 000 U/mL	New England Biolabs
KpnI 10 000 U/mL	New England Biolabs
NEBuffer 1.1	New England Biolabs
NEBuffer 2.1	New England Biolabs
NEBuffer 3.1	New England Biolabs
NEB U buffer	New England Biolabs
T4-DNA-Ligase 400 000 U/mL	New England Biolabs
T4-DNA-Ligase 10 x Buffer	New England Biolabs
XhoI 20 000 U/mL	New England Biolabs

3.6 Kits

Kits	Manufacturer
Big Dye Terminator® v1.1 CycleSequencing Kit	Applied Biosystems
NEB Gel extraction kit	New England Biolabs
pGEM-T Easy Cloning kit	Promega
QIAquick gel extraction kit	QIAGEN
QIAquick plasmid kit	QIAGEN

3.7 Bacterial strains

For this work *Escherichia coli* JM 109 competent cells (#L2005, Promega) were used.

JM109 Genotype: *end*A1, *rec*A1, *gyr*A96, *thi, hsd*R17 (r_k^-, m_k^+), *rel*A1, *sup*E44, Δ(*lac-pro*AB), [F´ *tra*D36, *pro*AB, *laq*I^{q}ZΔM15]

3.8 Cell lines

The human cell lines HEK 293 and K-562 were cultured in DMEM media supplemented with 10 % FCS and 0.1 % Gentamycin at 37 °C and 5 % CO_2 atmosphere.

3.9 Plasmids

3.9.1 pGEM®-T Easy

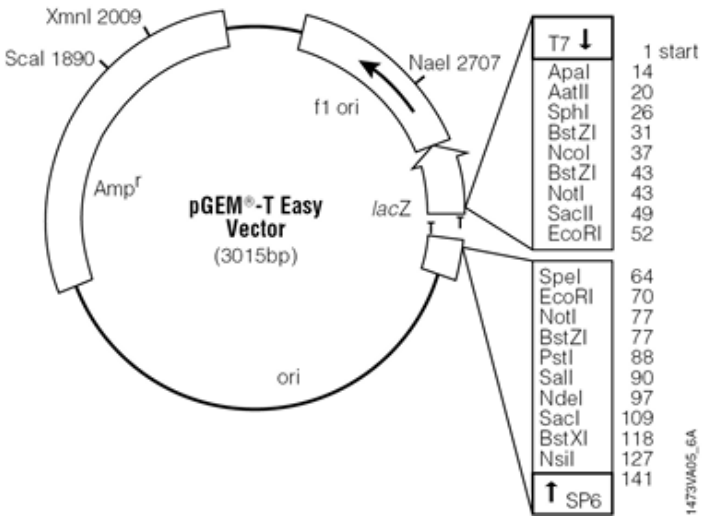

Figure 3 - Illustration of the pGEM®-T Easy vector (Promega #A1360)

3.9.2 pFUSE-hIgG1-Fc2

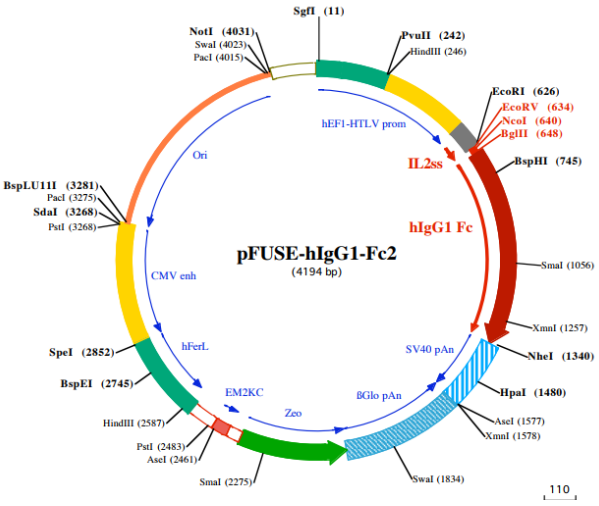

Figure 4 - Illustration of the pFUSE-hIgG1-Fc2 (InvivoGen #06G05-MT)

3.9.3 pAcGFP-N1

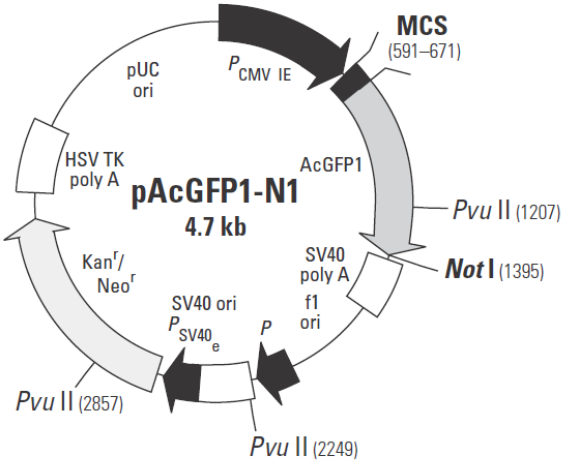

Figure 5 - Illustration of the pAcGFP-N1 vector (ClonTech #632469).

3.10 DNA ladder

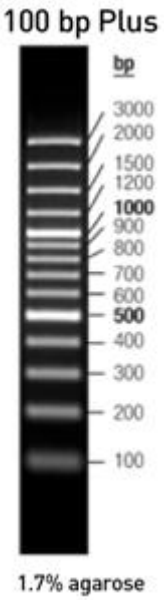

Figure 6 - Illustration of the Plus Gene Ruler DNA ladder (Fermentas #SM0321)

3.11 Protein ladder

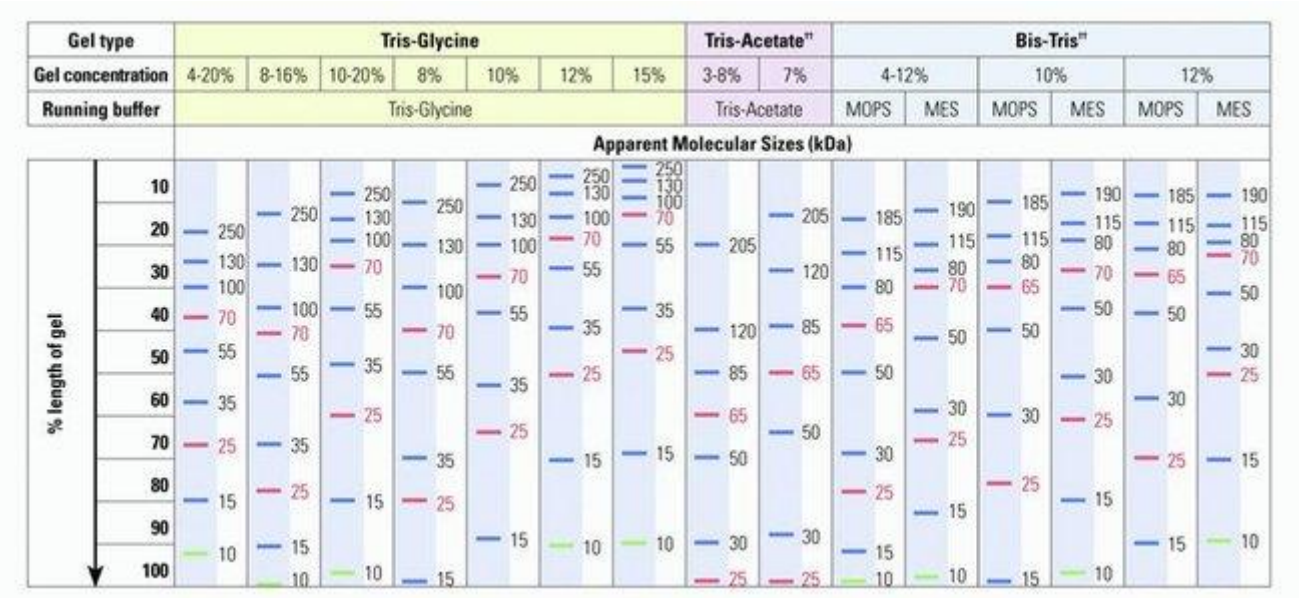

Figure 7 - Illustration of the PageRuler prestained protein ladder (Thermo Fisher Scientific, # 26619)

3.12 Solutions and buffer

Solutions and buffers	***Setting***
BT buffer	500 mg BSA 350 mg Triton-X-100 adjust volume to 50 mL with HPLC-H_2O
$CaCl_2$ solution	60 mM $CaCl_2$ 15 % Glycerol
Cell sorting buffer	1 x PBS 2 % heat inactivated (45 min 56 °C) FCS 2 mM EDTA (pH 7.2)
DNA Loading dye	1.93 M Saccharose 5.97 mM Bromophenol blue
Flow cytometry fixing solution	1 % Formaldehyde solution in PBS
Flow cytometry washing solution	1 x PBS 1 % BSA
Immunoblot – Blocking solution	1 x TBS-T 5 % milk powder
Immunoblot – TBS (10 x)	1.37 M NaCl 100 mM Tris-HCl (pH 7.2)
Immunoblot - TBS-T	1 x TBS 0.05 % Tween 20
MACS buffer	1 x PBS 0.5 % heat inactivated (45 min 56 °C) FCS 2 mM EDTA (pH 7.2)
Mini prep - P1 solution	50 mM Glucose 25 mM Tris-HCl, pH 8.0 10 mM EDTA, pH 8.0 add 100 µL/mL RNase A [10 mg/mL] before use
Mini prep - P2 solution	Solution P2A: 400 mM NaOH Solution P2B: 2 % SDS mix 1:1 before use
Mini Prep - P3 solution	3 M KAc Adjust pH to 4.8 using Glacial acetic acid
Protein Purification - Binding buffer (10 x)	20 mM Na_3PO_4 Adjust pH to 7.0 using H_3PO_4
Protein Purification - Elution buffer (10 x)	0.1 M Glycine/HCl Adjust pH to 2.7 using HCl
Protein Purification - Neutralizing buffer	1 M Tris/HCl Adjust pH to 9.0 using HCl
Semi-Dry Anode buffer (10 x)	750 mM Tris/HCl Adjust pH to 7.4 using HCl
Semi-Dry Anode transfer buffer (1 x)	100 mL Semi-dry Anode buffer 200 mL MeOH 700 mL H_2O
Semi-Dry Cathode buffer (10 x)	400 mM ε-aminocaprionic acid 200 mM Tris/HCl Adjust pH to 9.0 using HCl

Semi-Dry Cathode transfer buffer (1 x)	100 mL Semi-dry Cathode buffer 200 mL MeOH 700 mL H_2O
SDS-PAGE - Laemmli buffer (2 x)	374 mM Tris 416 mM SDS 438 mM Saccharose Adjust to pH 6.8 using HCl add 1.34 mM Bromphenol blue
SDS-PAGE - Running buffer (10x)	250 mM Tris 2 M Glycine 10 % SDS
SDS-PAGE - SDS separation gel (4 x) (15%)	14.4 mL H_2O 30 mL Acrylamide/Bis-acrylamide (30 %/0.8 % w/v) 15 mL 1.5 M Tris/SDS (pH 8.8) 300 µL 10 % SDS 300 µL 10 % APS 150 µL TEMED
SDS-PAGE - SDS stacking gel (4x)	6.15 mL H_2O 1.34 mL Acrylamide/Bis-acrylamide (30 %/0.8 % w/v) 2.50 mL 1.5 M Tris/SDS (pH 6.8) 50 µL 10 % SDS 100 µL 10 % APS 50 µL TEMED
SDS-PAGE - Tris/SDS (pH 6.8) (4 x)	1.5 M Tris 13.9 mM SDS pH 6.8 Adjust to pH 8.8 using HCl
SDS-PAGE - Tris/SDS (pH 8.8)	1.5 M Tris 13.9 mM SDS Adjust to pH 8.8 using HCl
SB buffer (10 x)	352 mM Boric Acid 100 mM NaOH pH 8.0 with HCl
SB agarose gel (1.5 %)	1 x SB buffer 1.5 % Agarose 0.5 µg/mL EtBr
Trypan blue	0.2 % Trypan blue [0.4 % v/v] 1 x PBS

3.13 Media

Media	***Setting***
Freezing medium	50 % complete culture medium 40 % heat inactivated (45 min 56 °C) FCS 10 % DMSO [1.10 g/mL]
DMEM-Genta medium	DMEM 10 % heat inactivated (45 min 56 °C) FCS 0.1 % Gentamycin [10 mg/mL]

DMEM-Zeo	DMEM 10 % heat inactivated (45 min 56 °C) FCS 0.1 % Gentamycin [10 mg/mL] 300 µg/mL Zeocin [100 000 µg/mL]
DMEM- G418 [2 mg/mL] medium	DMEM 10 % heat inactivated (45 min 56 °C) FCS 0.1 % Gentamycin [10 mg/mL] 2 mg/mL G418 [50 mg/mL]
LB-medium	1 % Tryptone 0.5 % Yeast extract 1 % NaCl autoclave at 121 ºC and 1.5 bar
LB-Amp medium	LB medium 0.1 % of Ampicillin [50 mg/mL]
LB-Kana medium	LB medium 0.1 % Kanamycin [50 mg/mL]
LB-Amp agar plates with IPTG and X-Gal	LB medium 1.5 % Agar agar, autoclave at 121 ºC and 1.5 bar 0.1 % Amp [50 mg/mL] 0.2 % X-Gal (2 % in Dimethylformamid) 0.1 % ITPG [24 mg/mL]
LB-Kana agar plates	LB medium 1.5 % Agar agar, autoclave at 121 ºC and 1.5 bar 0.1 % Kanamycin [50 mg/mL]
SOC medium	2 % Trypton 0.5 % Yeast extract 10 mM NaCl 2.5 mM KCl 10 mM $MgCl_2$ 10 mM $MgSO_4$ 20 mM Glucose autoclave at 121 ºC and 1.5 bar

3.14 Antibodies

Antibody	Clone	Manufacturer	Application
α-human IgG/HRP	-	Agilent – DAKO	Immunoblot
α-human IgG/APC	HP6017	BioLegend	Flow cytometry
α-mouse IgG/APC	Poly4053	BioLegend	Flow cytometry
α-mouse IgG/PE	Polyclonal	BioLegend	Flow cytometry
CD14/BV570	M5E2	BioLegend	Flow cytometry
CD56/FITC	NCAM16.2	BioLegend	Flow cytometry
CD45/APC	MB4-6D6	Miltenyi Biotec	Flow cytometry
CD159a/NKG2a	-	Beckman Coulter	Flow cytomtery
Streptavidin/BV570	-	BioLegend	Flow cytometry
α -MHC class I	W6/32	A. Ziegler, Berlin	Flow cytometry

3.15 Oligonucleotides

Primer	*Primer specificity*	*Sequence of recognition*	*Tm ºC*
G23	pGem-T Easy fw	5’-GTTTTCCCAGTCACGAC-3’	53
G24	pGem-T Easy rev	5’-GGATAACAATTTCACACAGG-3’	53
2970	pAcGFP2f	5’-CAAATGGGCGGTAGGCGTG-3’	50
2971	pAcGFP2r	5’-GTGGCCATTCACATCGCCAT-3’	49
5280	pFuse-IgG1-Fc2fw	5'-GCGCCTACCTGAGATCACC-3'	62
8333	hIgG1-rev	5’ ACCTTGCACTTGTACTCCTT 3'	56
2614	MYC1F	5’ ACACCATGGGAGCTGGTAAT 3'	55
2615	MYC1R	5’CTTCWTCGACTTYCAGACCCAAGGCAT 3'	55
2616	MYC2F	5’ GTTCTTTGAAAACTGAAT 3'	55
2617	MYC2R	5’ GCATCCACCAWAWACTCT 3'	55
2880	MAS-EcoRI-F	5’ GCTCGAATTCATGGCGCCCCGAACCCTCC 3'	66
2881	MAS-BamHI-R	5’ GATAAGGATCCTCCACTTTACAAGCCATAAGAGA 3'	60
3833	MBS-HindIII-F	5’ GCTCAAGCTTCGGTCATGCGGGTCATGGCGCCCC 3'	69
3834	MBS-KpnI-R	5’ CGTAGGTACCTTAGCCGTGAGAGACACATCA 3'	60
9828	MBS-EcoRI	5’ GAATTCGAGTCTCCTSAGACGCCGAGATG 3’	73
9829	MBS-KpnI	5’ GGTACCTTAGCCGTGAGAGACACATCA 3’	70
4159	MIS-HindIII-F	5’ GCTCAAGCTTCGGTCATGCGGGTCATGGCGCCCG 3'	69
4160	MIS-KpnI-R	5’ CGTAGGTACCCAAGCTGTGAGAGACACATCAG 3'	64

3.16 Databases, computer programs and versions

For the development of this work the following computer programs were used:

BioEdit version 7.1.9

(http://www.mbio.ncsu.edu/BioEdit/bioedit.html)

FlowJo version 10, v10

(https://www.flowjo.com)

GraphPad Prism 7

(https://www.graphpad.com)

And the following online databases were also needed:

NCBI BLAST

(https://blast.ncbi.nlm.nih.gov/Blast.cgi?PAGE_TYPE=BlastSearch)

Databases

(ftp://ftp.ebi.ac.uk/pub/databases/ipd/mhc/nhp/)

4 Methods

4.1 Molecular biology methods

4.1.1 Polymerase chain reaction (PCR)

4.1.1.1 Mamu amplification from cDNA of rhesus macaques

For amplification of Mamu alleles from cDNA of rhesus macaques, polymerase chain reactions (PCR) were performed. Since Mamu alleles were used for transfecting cells using an expression vector to perform interaction studies, accuracy of the amplified fragments is essential. Hence, Pfu DNA polymerase was used due to its proof reading capacity. For this, a master mix was prepared, containing all constituents needed for enabling the amplification reaction. The master mix preparation was performed on ice to avoid formation of unspecific products. A total of 29 µL was used for each reaction. The master mix was constituted by 19 µL HPLC H_2O, 3 µL 10 x Pfu reaction buffer with $MgSO_4$, 3 µL primer forward and primer reverse [10 pMol/µL] sequence specific, 0.6 µL dNTPs [10 mM] and 0.4 µL Pfu DNA polymerase [2.5 U/µL]. Lastly the DNA template was added, and a PCR run was performed as described in table 1.

Table 1 - PCR program for amplification of Mamu alleles form cDNA of rhesus macaques*. x ºC represents the annealing temperature of the primers used in the reaction.*

Phase	Temperature	Duration	Cycles
Initial denaturation	95 °C	2 min	1
Denaturation	95 °C	1 min	35
Annealing	x °C	1 min	
Elongation	72 °C	1.5 min	
Terminal elongation	72 °C	10 min	1

The PCR run was composed by three main steps, namely a denaturing, annealing and elongation or polymerase extension phase. The annealing temperature was calculated in accordance to the melting temperature (Tm), which is primer dependent and is determined using the formula shown below.

$$Tm = (C+G) \times 4\ ºC + (A+T) \times 2\ ºC$$

4.1.1.2 Colony PCR

Colony PCRs were performed after transformation of *E. coli* JM109 to ascertain which colonies presented the insert of interest. For this a master mix with a total volume of 30 µL per sample was prepared which contained 20.3 µL HPLC H_2O, 3 µL 10 x BioTherm™ buffer, 4 µL BT buffer (BSA [10 mg/mL] / Tx [7 mg/mL]), 1 µL primer forward and primer reverse [10 pMol/µL] sequence specific, 0.5 µL dNTPs [10 mM] and 0.2 µL BioTherm™ Taq Polymerase. DNA was added by stirring a tip with a picked colony into the master mix.

The PCR program applied for identification of positive colonies is presented in table 2.

Table 2 - PCR program for amplification of DNA from E.coli colonies. *x ºC represents the annealing temperature of the primers used in the reaction.*

Phase	Temperature	Duration	Cycles
Initial denaturation	94 °C	2 min	1
Denaturation	94 °C	1 min	30
Annealing	x °C	1 min	
Elongation	72 °C	y* min	
Terminal elongation	72 °C	5 min	1

*y= 1min/1kb

4.1.1.3 Mycoplasma PCR

Mycoplasma PCRs were regularly performed on the cell cultures used throughout this work as described in protocol 4.2.6. This was accomplished using the hot start protocol in order to diminish occurrence of non-specific products, as are the example of primer dimers. The hot start PCR is composed by two master mixes which are pipetted into a reaction tube separated by a wax layer, avoiding in this way the amplification of unspecific products by keeping the polymerase separated from the remaining constituents until the critical temperature is achieved. For this 1 µL 10 x BioTherm™ buffer, 1 µL primer forward and primers reverse and 0.5 µL dNTPs [10 mM] were pipetted into a reaction tube containing 6.5 µL HPLC H_2O. Then a wax layer was added, melted and cooled down. The second master mix was constituted by 2 µL 10 x BioTherm™ buffer, 4 µL BT buffer (BSA [10 mg/mL] / Tx [7 mg/mL]), 0.2 µL Taq-DNA polymerase mixed into 12.8 µL HPLC H_2O. To each reaction tube, 1 µL of cell culture supernatant was then added. For the first reaction, primers MYC1 were used (Table 3).

The PCR program used for Mycoplasma detection is presented below.

Table 3 - PCR program for amplification of Mycoplasma DNA from the supernatant of cell cultures.

Phase	Temperature	Duration	Cycles
Initial denaturation	94 °C	4 min	1
Denaturation	94 °C	30 sec	35
Annealing	72 °C	1 min	
Elongation	72 °C	1 min	
Terminal elongation	72 °C	6 min	1

The PCR product obtained from this reaction was then used to perform a Nested PCR, using MYC2 primers following PCR program on table 3.

4.1.2 Agarose gel electrophoresis for separating DNA fragments

Visualization and separation of DNA fragments according to size was achieved performing agarose gel electrophoresis. For this, 1.5 % agarose gels were prepared by mixing 1.5 g agarose with 100 mL 1 x SB buffer. The solution was boiled and cooled down with constant agitation. When temperature reached 55 °C, 3 µL of Ethidium Bromide [10 mg/ml] were added and homogenized. The prepared solution was then placed into an electrophoresis chamber with combs and left to gelfie, after which the combs were taken out and the gel was covered with 1 x SB buffer. DNA samples, previously mixed with loading dye, were pipetted into the wells, as well as a DNA ladder for determination of DNA fragment weight lengths. The gels were run at a charge of 120 V, and the results were visualized under UV-light (250 nm) and archived through and image processing system.

4.1.3 Sequencing analysis

Confirmation of the authenticity and correctness of constructs produced and used for this work as well as identification of new Mamu alleles amplified from cDNA of rhesus macaque was achieved via Dideoxy Method of DNA, also known as Sanger technique. For this, 1 µL primer [3.3 pMol/µL] was mixed into 6.5 µL aqueous DNA template, to which 1.5 µL of 5 x sequencing buffer and 1 µL of Big Dye™ v1.1 Terminator were added. DNA sample concentrations for sequencing should be 100 ng/kb sequence for PCR products, 200-300 ng for sequences under 1 kb of plasmid DNA and 400 ng for sequences over 1 kb of plasmid DNA.

The samples were run in a sequencing PCR program (Table 4).

Table 4 - Program for sequencing PCR.

Phase	Temperature	Duration	Cycles
Denaturation	96 °C	30 sec	25
Annealing	50 °C	15 sec	
Elongation	60 °C	4 min	

For DNA precipitation, the PCR products were shortly centrifuged and diluted in 90 µL of H_2O. DNA templates were mixed into previously prepared reaction tubes containing 250 µL of 100 % ethanol and 10 µL of NaAc (3 M pH 4.8). The samples were centrifuged for 15 min at 20238 x g and the supernatant was discarded. In order to wash the DNA sample, 250 µL of 70 % ethanol were added and templates again centrifuged at 20238 x g for 5 min. The supernatant was discarded and the pellet containing the DNA was dried using a vacuum concentrator for 10 min and was then stored at 4 ºC until sequencing analysis was performed.

For sequencing analysis, the pellets were resuspended in 10 µL Hi-Di™ formamide and DNA fragments were split by their length through electrophoretic capillarity, using ABI3130xl sequencer.

Herein, the fluorescent dyes in the dNTPs ligated to the DNA sequence were excited through a laser and the signal was captured by a detector. Data could then be read and analyzed using BioEdit computer software.

4.1.4 Poly A tailing of Pfu-DNA-polymerase-derived Mamu alleles

Proof-reading enzymes, like Pfu-DNA polymerase, produce blunt-end fragments on their amplified products. Therefore, an additional step of poly A tailing was required for ligation of Pfu-derived inserts to the pGEM-T Easy vector. The latter is a linearized vector with single terminal thymidines at each end which complement an A overhang usually conferred by Taq-polymerases. For this, the Pfu-amplified fragment were mixed with 3.5 µL HPLC H_2O, 3 µL 10 x BioTherm buffer, 3 µL dATPs [10 mM] and 0.5 µL Taq-DNA polymerase. The reaction mix was incubated for 30 min at 70 °C. The PCR product was then purified using QIAGen PCR purification kit according to the manufacturer's instructions. DNA was diluted in a final volume of 20 µL of HPLC H_2O.

4.1.5 Ligation of Mamu alleles to pGEM-T easy vector

For cloning of PCR products, a pGEM®-T Easy cloning kit (Promega) was used. This is a linearized vector which possesses a single 3'-terminal thymidine at both ends. In the ligation mix 5 µL of 2 x Rapid ligation buffer were mixed with 3 µL of the DNA insert, 1 µL of pGEM®-T Easy vector [60 ng/µL] and 1 µL of T4-DNA-Ligase. The reaction mix was then incubated overnight at 4°C. The product of the ligation was used to transform *E. coli* JM 109 cells (4.1.9).

4.1.6 DNA restriction by endonucleases

To allow ligation of insert DNA into plasmids, restriction reactions using endonucleases were performed. For this, a reaction of a total volume of 15 µL was set, containing 5 µg DNA, 1.5 µL of the appropriate buffer and 1 µL of restriction enzyme (3.5). In situations in which a greater volume was needed, reaction settings were appropriately adjusted. The reaction mix was incubated for 2 h at the optimal temperature for the enzymes to react, after which, enzymes were heat inactivated or removed according to manufacturer's instructions and DNA templates were purified using QIAGEN PCR purification kit, following the manufacturer's instructions.

4.1.7 Ligation reaction of DNA inserts to plasmids

For the ligation of restricted DNA fragments into expression vectors, 300 µg of DNA and 100 µg of the digested expression vector were incubated with 1 µL 10 x T4-Ligase-buffer and 1 µL T4-Ligase and the reaction was incubated overnight at 4 °C.

4.1.8 Production of chemically competent JM109 *E.coli* cells

For production of chemically competent cells, 5 mL LB medium were inoculated from a cryo glycerol stock of *E. coli* JM109 and incubated at 37 ºC and 170 rpm overnight. On the following day, 4 mL of the culture were inoculated in 400 mL LB medium and grown until reaching an OD_{590} of 0.375, corresponded to the exponential growth phase. The cell suspension was then incubated 10 min on ice and the cells were pelleted at 1 600 x g for 7 min at 4 ºC in eight 50 mL Falcons. The pellets were resuspended in 10 mL ice cold Calcium chloride ($CaCl_2$) solution each, pooled into two Falcons to 40 mL suspension and centrifuged at 1 100 x g for 5 min at 4 ºC. After discarding the supernatant, the pellets were again resuspended in 40 mL ice cold $CaCl_2$ solution each and incubated for 30 min on ice. After this, the cells were again centrifuged at 1 100 x g for 5 min at 4 ºC. Supernatants were discarded, and pellets were resuspended in 8 mL ice cold $CaCl_2$ solution each. JM109 chemically competent cells were stored in 500 µL aliquots at – 80 ºC until needed for transformation protocols (protocol 4.1.9).

4.1.9 Transformation of chemically competent JM109 *E. coli* cells

For plasmid DNA production, chemically competent *E. coli* cells were transformed. For this, JM109 cells were thawed on ice. The ligation reaction mix was added to the cells, mixed by stirring and the preparation was incubated on ice for 20 min. After this, the cells were incubated at 42 °C for 50 sec, and again on ice for 2 min. Lastly, 800 µL of SOC medium were added, the bacterial cells were placed into air-vented tubes and incubated for 1 h at 37°C and 170 rpm. Transformed bacterial cultures were plated in agar plates with appropriate antibiotic and incubated overnight at 37 °C. On the following day clones were picked for colony PCR (4.1.1.2) and culturing in selective LB medium for plasmid DNA purification through mini-preparations.

4.1.10 Mini-preparation of plasmid DNA

For recombinant plasmid DNA isolation from bacterial cultures mini-preparations were made following the principle of alkaline lysis. Transformed bacterial cultures were grown overnight in LB-antibiotic medium at 37 °C and 170 rpm. On the following day 2 mL of the bacterial cultures were centrifuged at 16000 x g for 1 min. The supernatant was discarded, and the pellet was resuspended in 150 µL of P1 solution containing 100 µg/mL RNase A [10 mg/mL]. To this, 150 µL of P2 solution were added. The samples were mixed by inverting and incubated for 5 min at RT, after which 150 µL of P3 solution were added and again mixed by inverting. Samples were centrifuged at 16000 x g for 10 min and the supernatant was placed in a new reaction tube. For higher purity, this step was

repeated. For DNA precipitation, 500 µL of isopropanol were added to the sample and mixed by inverting. Samples were centrifuged at 4 °C, 16000 x g for 30 min. The supernatant was discarded and 250 µL of 70% ethanol were added to wash the pellet. The samples were centrifuged at 16000 x g for 5 min, the supernatant was discarded. Samples were dried using a vaccum concentrator for 10 min, resuspended in HPLC H_2O and lastly DNA concentration was measured through spectrophotometry.

4.1.11 Midi-preparation of plasmid DNA

For plasmid DNA purification for posterior transfection, a midi-preparation using QIAquick plasmid DNA kit (QIAGEN) was performed according to the manufacturer's instructions.

4.1.12 Linearization of pAcGFP Mamu constructs for transfection

In order to achieve higher efficiency in posterior stable transfections, linearization of the plasmid DNA was performed using ApaLI enzyme. This allows the creation of a known breakage point in the plasmid that ensures expression of both, the MHC class I DNA and the GFP tag. For this, a total volume of 20 µL reaction mix was prepared and incubated for 2 h at 37 ºC. In this, 16.5 µL of the plasmid midi-preparation (5 µg DNA) were mixed with 2 µL of CutSmart buffer and 1.5 µL of ApaLI enzyme [10 U/µL]. In situation in which a greater volume was needed, reaction settings were appropriately adjusted. After the incubation, linearized DNA was purified using QIAGEN PCR purification kit, following the manufacturer's instructions.

4.2 Cell culture methods

4.2.1 Cell cultures

4.2.1.1 HEK 293 cell line

The human embryonic kidney cell line, HEK 293, was cultured in Dulbecco's Modified Eagle Medium (DMEM), supplemented with heat inactivated fetal calf serum (FCS) (10 % (v/v)) and Gentamycin (0.1 % (v/v)) at 37 °C under 5 % CO_2. HEK 293 cells transfected with pAcGFP constructs were grown in DMEM supplemented with heat inactivated fetal calf serum (FCS) (10 % (v/v)), Gentamycin (0.1 % (v/v)) and G418 [1 mg/mL], and HEK 293 cells transfected with pFUSE-hIgG2-Fc constructs were grown in DMEM supplemented with heat inactivated fetal calf serum (FCS) (10 % (v/v)), Gentamycin (0.1 % (v/v)) and Zeocin [300 µg/mL] selection medium.

4.2.1.2 K-562 cell line

The K-562 cell line was cultured in DMEM supplemented with heat inactivated fetal calf serum (FCS) (10 % (v/v)) and Gentamycin (0.1 % (v/v)) at 37 °C under 5 % CO_2. For K-562 cells transfected with pAcGFP constructs, DMEM medium supplemented with heat inactivated fetal calf serum (FCS) (10 % (v/v)), Gentamycin (0.1 % (v/v)) and G418 [2 mg/mL] was used for selection of transfected cells.

4.2.2 Applying cell cultures

For cell culture application, DMEM medium was pre-warmed to 37 °C in a water bath. Frozen cells were thawed in the water bath with gentle agitation and then resuspended in the pre-warmed DMEM medium. Cells were centrifuged at 200 x g for 5 min, the supernatant was discarded and the pellet was resuspended in appropriate medium with antibiotics, plated in T75 flasks and incubated at 37 °C and 5 % CO_2.

4.2.3 Determination of the viable cell number

For determination of the number of viable cells in a suspension, 10 µL of the cell suspension were mixed into 90 µL of 0.2 % trypan blue solution. From this, 10 µL were pipetted into a Neubauer chamber. Uncolored living cells of the four big squares were counted and the cell number contained in 1 mL of the cell suspension was calculated using the following equation

$$n\ of\ cells\ in\ 1\ mL = \frac{n\ of\ cells\ counted\ in\ 4\ big\ squares}{4} \times Chamber\ factor \times Dilution\ factor$$

*Chamber factor: 10 000

*Dilution factor: 10

4.2.4 Splitting of adherent cell cultures

For splitting of adherent cell, cells were washed with 1 x DPBS, detached using Trypsin/EDTA and resuspended in DMEM medium 1:1 ratio to Trypsin/EDTA. The desired amount of cell suspension was then centrifuged at 200 x g for 5 min the pellet was resuspended in fresh culture medium and plated.

4.2.5 Splitting of suspension cell cultures

For splitting of suspension cell, the desired amount of cell suspension was centrifuged at 200 x g for 5 min, the supernatant was discarded the pellet was resuspended in fresh culture medium and plated.

4.2.6 Mycoplasma PCR

Mycoplasma are the smallest free-living organisms, considered the simplest of bacteria and are a common cause of contamination in cell culture. Therefore, the cell cultures used in this work were regularly tested for contamination by Mycoplasma PCR, allowing by this means, the detection of this type of contaminations which are not observable by eye. For this, 200 µL of cell culture supernatant, which was in contact with cells for at least 48 h was collected, boiled to 95 °C for 5 min, thoroughly vortexed and centrifuged at 4000 rpm for 1 min. From this 1 µL was used to perform a Mycoplasma PCR (4.1.1.3) using primers MYC1. Followed by a nested PCR with the product of the first PCR, using PCR primers MY2 (oligonucleotide list in 3.15). An agarose gel (4.1.2) was run and cultures that presented bands between the weight lengths of 200 to 500 bp were immediately discarded. In each Mycoplasma PCR test a known mycoplasma-contaminated culture sample and a known mycoplasma-free culture sample were used as positive and negative control, respectively. For a representative example of the results obtained here, please see 9.1.

4.2.7 Transfection of HEK 293

For transfection 2 mL of HEK 293 cells (6.25 x 10^5 per mL) were plated in a 6 well plate and incubated overnight. On the following day cells were transfected via DNA-Lipofectamine complexes. For this, for each transfection, 7.5 µL Lipofectamine® 2000 reagent were diluted into 125 µL Opti-MEM® (Reduced Serum Medium). Separately, 2.5 µg linearized plasmid DNA were diluted in 125 µL Opti-MEM®, both were mixed carefully and incubated for 5 min at RT. The diluted DNA was then added to the Lipofectamine reagent, mixed gently and incubated for 15 min at RT. Lastly, DNA-lipid complexes were added carefully to the cells, mixed gently, and incubated for 48 h at 37 °C and 5 % CO_2.
Selection of transfected HEK 293 cultures was accomplished by antibiotic resistance conferred by the vector used for transfection. Cells were cultured in selection medium, with the appropriate antibiotic, in which only successfully transfected cells could survive and replicate.

4.2.8 Transfection of K-562

For transfection, 2 mL of K-562 cells (5 x 10^5 per mL) were plated in a 6 well plate and incubated for 2 h at 37 °C and 5 % CO_2, after which the cells were transfected via DNA-Lipofectamine complexes. For this, for each transfection, 12 µL Lipofectamine® 2000 were diluted into 200 µL Opti-MEM® (Reduced Serum Medium). Separately, 4 µg linearized plasmid DNA were diluted in 200 µL Opti-MEM®. Transfection protocol followed as described for HEK 293 cells (4.2.7).

4.2.9 Selection of stable transfected clones from HEK 293 and K-562 cell lines

Selection of pAcGFP transfected HEK 293 and K-562 cultures was accomplished by antibiotic resistance, using DMEM 10 % FCS, 0.1 % Gentamycin, G418 as selection medium. Transfection efficiency was checked through fluorescence microscopy (HBO-GFP/FITC 38 filter) and flow cytometry using the W6/32 antibody for MHC class I expression analysis.

4.2.10 Magnetic cell isolation and cell separation (MACS) of pAcGFP MHC class I transfected K-562

With the purpose of enriching the MHC-I transfected cell population, magnetic cell isolation and cell separation (MACS) was performed. For this, K-562 Mamu pAcGFP cells were counted, washed twice with 1 x PBS and resuspended in 100 µL PBS per 10^7 cells. Cells were then incubated with 1.5 µg W6/32 antibody per 10^6 cells, for 20 min at 4 °C. After incubation the cell suspension was washed twice with PBS, resuspended in 80 µL MACS buffer per 10^7 cells and incubated with 60 µL goat α-mouse microbeads per 10^7 cells for 15 min at 4 °C. During this incubation cells were regularly mixed. Then cells were washed twice with MACS buffer and resuspended in 500 µL buffer. Separation was accomplished by running the labelled cell suspension through a MS column placed on a separator under the forces of a strong magnet. For this, the MS column was first equilibrated with 500 µL MACS buffer. Cells were then run through the column and the flow-through containing unlabeled cells was collected for control analysis. The MS column was then washed 3 times with 500 µL MACS buffer. For collection of labelled cells, the MS column was removed from the separator and placed over a collection tube containing DMEM medium. Cells were eluted in 500 µL MACS buffer with the aid of the plunger supplied with the column, immediately centrifuged and resuspended in appropriate medium for plating. Efficiency of the separation was checked through fluorescence microscopy and FACS assays.

4.2.11 Cell sorting of pAcGFP K-562 cells

The homogeneity of the K-562 Mamu pAcGFP population was of vital importance for this study. Since in some cell populations MACS was not as efficient as in others, cell sorting was performed using the SH800S Cell sorter from Sony Biotechnology. For this, 1 x 10^7 K-562 pAcGFP cells were washed with 1 x PBS and resuspended in 500 µL sorting buffer. Cell suspensions were then run through the cell sorter using a 100 µm sorting chip and at least 1 x 10^5 GFP positive cells were collected for each cell line. The collected cells were then centrifuged at 200 x g for 5 min and resuspended in appropriate medium for plating and expansion.

4.2.12 Cryoconservation of eukaryotic cell lines

For cryoconservation of eukaryotic cell lines, cells were centrifuged at 200 x g for 10 min and carefully resuspended in DMEM freezing medium (3.13) and 1 mL of cell suspension was placed in each cryotube. These were placed in a freezing container, which contained isopropanol allowing the cooling process to occur at the rate of 1 °C per minute in the – 80 °C freezer for 48 h and then transferred to the – 140 °C freezer.

4.2.13 FACS: W6/32 assay

W6/32 is an antibody which recognizes MHC class I ligands and was for this reason used for accessing the level of Mamu surface expression levels of Mamu pAcGFP transfected HEK 293, K-562 cells. For this, 5 x 10^5 cells were incubated with 1 µg W6/32 for 1 h at 4 °C, after which cells were washed with 1 x PBS. After this, the secondary antibody, α-mouse IgG/APC, was given to the cells and these were incubated for 30 min at 4 °C.

In each assay a negative control, in which the cells were not incubated with W6/32 nor with the secondary antibody, and an unspecific binding control, in which the cells were only incubated with the secondary antibody, α-mouse IgG/APC, were performed. Assays were repeated at least three times.

4.2.14 FACS: KIR3DL02 – MHC-I binding studies

In order to investigate if the NK cell receptor KIR3DL02 is able to ligate with different Mamu alleles, FACS assays were performed in which Mamu pAcGFP transfected cells were incubated with multimerized KIR-Fc proteins stained with ECD in binding studies with HEK 293 and Brilliant Violet 570-coupled Streptavidin for binding studies with K-562 (4.3.3). For this, 2 x 10^5 Mamu pAcGFP transfected cells were washed twice with 1 x PBS 1% BSA, incubated with 20 µg of multimerized KIR-Fc protein for 45 min at 4 °C. After incubation cells were washed once with 1 x PBS 1 % BSA and lastly resuspended in 1 x PBS and immediately measured using an LSR II flow cytometer.

In each assay, a negative control, in which cells were untreated, an unspecific binding control, in which cells were incubated with Biotin-Protein A + Strep BV570, a positive control, in which Mamu A1*001 pAcGFP cells were incubated with KIR3DL05 protein were performed. Assays were repeated at least three times.

4.2.15 FACS analysis

4.2.15.1 MHC class I surface expression

Cell surface expression of Mamu alleles in the pAcGFP transfected cultures was determined by analyzing data obtained from FACS using FlowJo V10 software. For this, cell populations were gated as shown in figure 8. Firstly, cells were gated for considering only singlets (A). Selection of the target cell population was achieved by gating cells according to their size and granularity (B). And lastly cells were gated using the four-quadrant tool to distinguish GFP positive populations and APC stained cells (C and D). From these, Median fluorescence intensities (MFIs) were determined for the APC filter.

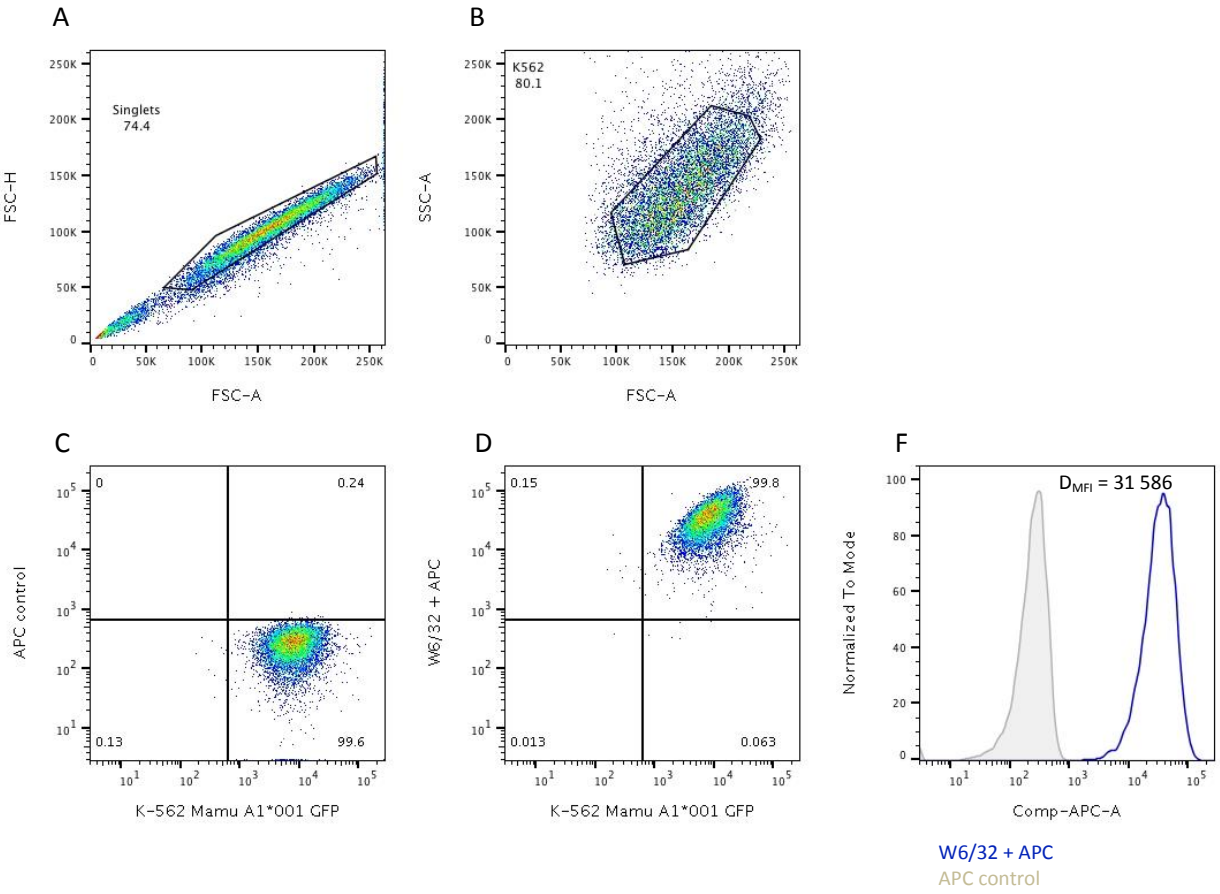

***Figure 8 - Gating scheme for analyzing MHC-I expression level flow cytometry data**. **(A)** Singlets gating; **(B)** K-562 living cells gating; **(C and D)** four-quadrant gating for identification of GFP positive cells and MHC class I expressing intensity; **(F)** Histogram display overlay of K-562 Mamu A1*001 GFP cells stained with W6/32 over the secondary antibody control.*

Figure 8 (F) shows a histogram overlay of the normalized median fluorescence intensity of K-562 Mamu A1*001 GFP stained with W6/32-APC (Blue) over K-562 Mamu A1*001 GFP α-mouse IgG/APC unspecific binding control. Finally, relative expression intensity was calculated according to the equation below.

$$Relative\ expression\ intensity = \frac{MFI\ of\ W6/32 - MFI\ of\ APC\ control\ for\ MHC\ class\ I\ transfected\ cells}{MFI\ of\ W6/32 - MFI\ of\ APC\ control\ for\ mock\ transfected\ cells}$$

4.2.15.2 Binding assays

Binding between KIR3DL02 and Mamu alleles was determined by analyzing data obtained from FACS using FlowJo V10 software. For this, cell populations were gated as described for the MHC class I surface expression. In this case, median fluorescence intensities were determined for the Qdot 585 filter. Herein, four-quadrant gating allows the identification of GFP positive populations and KIR stained populations figure 9 (A and B). Figure 9 (C) is a histogram demonstration of the increase in fluorescence intensity K-562 Mamu A1*004 GFP cells stained with KIR3DL02 in regard to the Biotin + StrepBV570 control.

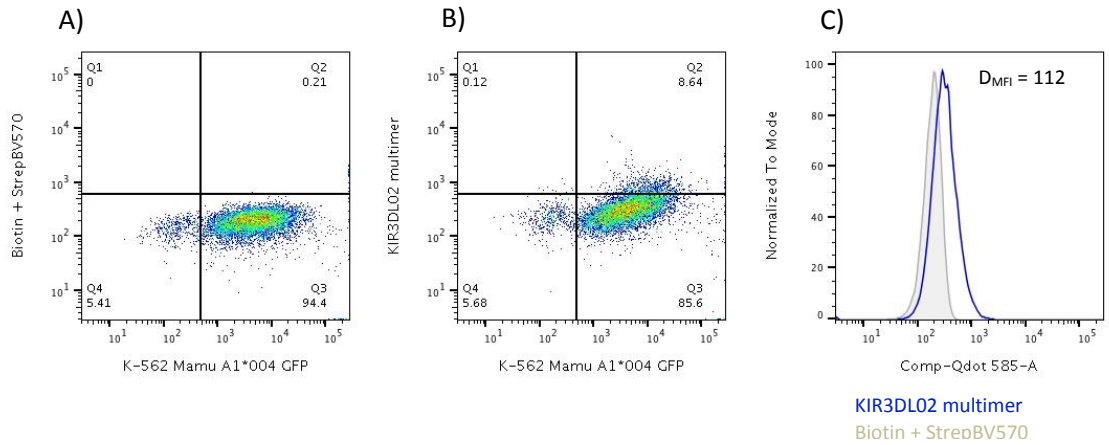

Figure 9 - Gating scheme for analyzing binding assay flow cytometry data. (A) (B) *four-quadrant gating for identification of GFP positive cells and KIR binding intensity;* ***(C)*** *Histogram display overlay of K-562 Mamu A1*004 GFP cells stained with KIR over the Biotin + StrepBV570 control.*

Finally, relative binding intensity was calculated according to the following equation.

$$Relative\ binding\ intensity = \frac{MFI\ of\ KIR - Fc - MFI\ of\ Biotin + StrepBV570\ control\ for\ MHC\ class\ I\ transfected\ cells}{MFI\ of\ KIR - Fc - MFI\ of\ Biotin + StrepBV570\ control\ for\ mock\ transfected\ cells}$$

4.3 Biochemical methods

4.3.1 G-Protein Affinity chromatography

For protein purification HEK 293 pFUSE-hIgG2-Fc KIR transfected cultures, these were cultured five days in Freestyle expression medium. After incubation, the medium was harvested and KIR-Fc fusion proteins were purified using HiTrap Protein G HP affinity columns following the manufacturer's

instructions. KIR-Fc protein fractions were then concentrated using a Vivaspin®20 concentrator, following the manufacturer's instructions and after quantification of protein concentrations (4.3.2), used for binding studies to Mamu pAcGFP transfected cells (4.2.14).

4.3.2 Quantification of protein concentrations

For determination of the concentration of purified Fc-fusion KIR proteins, Bradford assays were performed using the Coomassie protein assay reagent (Pierce™) following the manufacturer's instructions for the micro test tube protocol.

4.3.3 Multimerization of KIR-Fc fusion proteins

For increasing binding probability between KIR-Fc proteins and their potential Mamu ligands on Mamu pAcGFP transfected cells, 20 µg of KIR-Fc protein were mixed with 1.4 µg of biotinylated protein A [1 mg/mL in PBS] and incubated for 30 min at RT. After this, the biotinylated proteins were stained with 10 µL ECD, for binding studies with HEK 293, and 0.2 µg Brilliant Violet 570-coupled Streptavidin, for binding studies with K-562 cells, for 15 min at 4 ºC in the dark. Multimerized KIR3DL05 receptor, known to bind Mamu-A1*001, was used as a positive control and as negative control Biotin + StrepBV570 was used. Multimerized KIR-Fc proteins were then used to perform binding assays with Mamu pAcGFP transfected cells (4.2.14).

4.3.4 SDS-PAGE

Protein separation was accomplished using sodium dodecyl sulfate polyacrylamide gel electrophoresis (SDS-PAGE). For this, samples were mixed with 6 x Laemmli buffer containing β-mercaptoethanol, boiled for 5 min at 95 °C and run on a 15 % SDS gel under reducing conditions for 2 h at 120 V.

4.3.5 Immunoblot

After separation of the proteins through the SDS-PAGE, proteins were transferred to nitrocellulose membranes by semi-dry western blotting for 1:10 h at 48 mA. The membranes were blocked with 5% non-fat milk in Tris-buffered saline-Tween 20 (TBS-T) for 1 h, probed with α-human IgG/HRP overnight at 4 °C, and developed by incubation with 1-Step™ Ultra TMB-Blotting Solution which allowed protein bands visualization. Lastly, reaction was stopped with water and data were archived through and image processing system.

5 Results

As described previously, the MHC class I family is a highly polymorphic gene family. Growing evidence points towards a co-evolution of killer cell immunoglobulin-like receptors and their MHC-I ligands and emphasizes the complexity of the interactions established between these. In the rhesus macaque, being the main animal model for studying HIV/SIV, the interactions between KIRs and MHC-I (Mamu) are poorly described. With the prospect of broadening the knowledge in this field, this work focuses on studying the interaction between the NK cell receptor KIR3DL02, present in elite controller animals with lower viral loads and slower progression of the disease upon SIV infection, with different Mamu alleles.

5.1 Immunoblot analysis of purified KIR-Fc fusion proteins

In order to study the interaction between the NK cell receptor KIR3DL02 and diverse MHC class I molecules from rhesus macaque, HEK 293 cells stably transfected with the mammalian expression vector pFUSE-hIgG1-Fc2 including the extracellular parts of KIR3DL02 or KIR3DL05, respectively, were provided by the Primate Genetics Laboratory (DPZ). These were expanded and cultured in Freestyle expression medium to enable the secretion of the receptors by the transfected cells as Fc-fusion proteins. Freestyle expression medium was used for protein purification because it does not contain any human or animal serum and has been designed for recombinant protein production and purification. After five days of incubation the medium was harvested and the KIR-Fc fusion proteins were purified using HiTrap Protein G columns (GE Healthcare) (4.3.1).

Purified proteins were tested for accuracy by western blotting (4.3.4; 4.3.5). Figure 10 shows an example of a western blot containing load, flow-through and wash control as well as the eluted protein already concentrated using Vivaspin®20 centrifugal concentrators. Load is the supernatant that is harvested from the HEK 293 transfected cells before going through the HiTrap column. Flow-through is the solution dropping through the column and the wash control is taken after elution of the proteins in the column. Moreover, IgG samples were loaded as positive controls for the western blot.

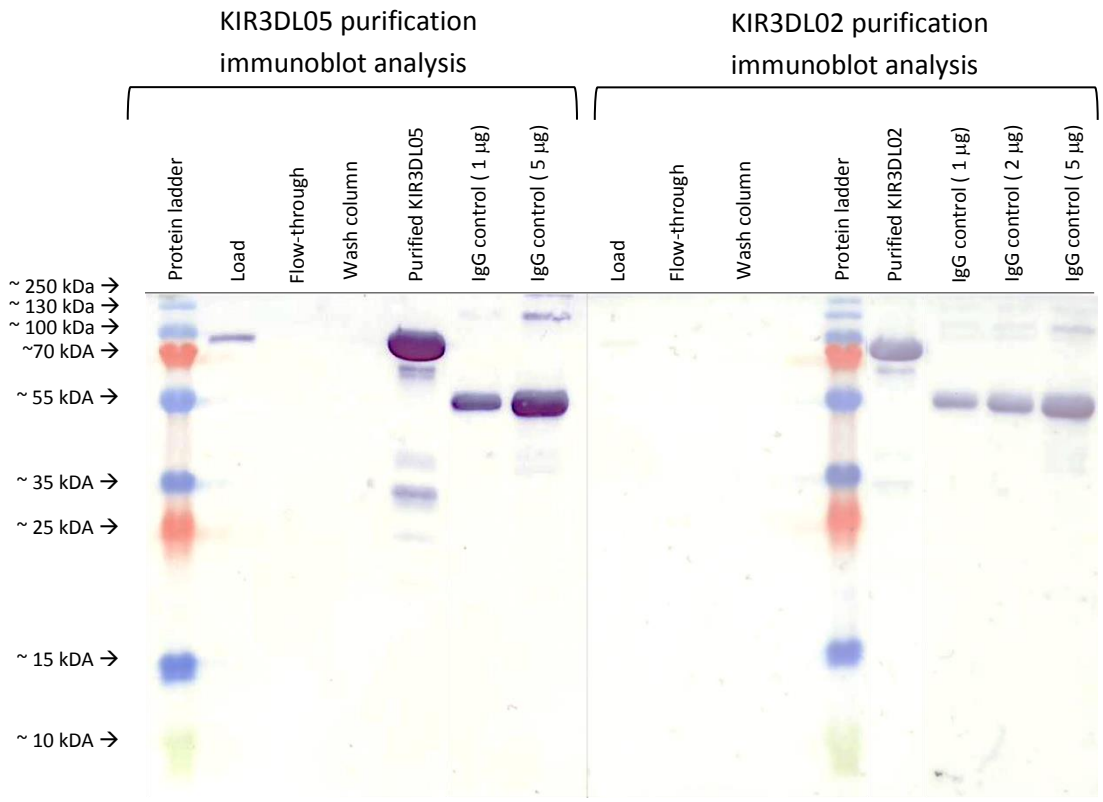

Figure 10 - Protein purification control of KIR3DL05-Fc and KIR3DL02-Fc fusion proteins. *Immunoblot analysis of ten microliters of each load, flow-through, wash control and KIR-Fc purified concentrated fractions. Human IgG samples with known concentrations were used as positive controls. Probes were run through a 15 % SDS acrylamide gel, blotted onto a nitrocellulose transfer membrane and incubated over night at 4 ºC with α-human IgG / HRP antibody (1:2500) and developed using 1-Step Ultra™ TMB-blotting solution. The figures show the KIR3DL05/02-Fc load fractions display a band with an approximate weight of 90 kDa which shows that already before purification the target protein is visible. Flow-through and wash controls present no bands, indicating that purification and elution were successful. Purified KIR3DL05/02 fractions show the highly concentrated glycosylated proteins at the same weight as seen in the load fraction (~ 90 kDa). Lower bands are degraded protein from the proteases released by dying cells. IgG controls, two last lanes on the left side western blot and three last lanes on the right side western blot, show that the protocol was successful and the immunoblot worked.*

Purification of KIR-Fc fusion proteins from the supernatant of HEK 293 KIR3DL05/02-Fc cultures was achieved with success. According to the amino acid constitution of the KIR-Fc fusion recombinant proteins these should have a molecular weight of 61.5 kDa. However, since KIR have several glycosylation sites there is a significant increase in protein weight because of this post-transcriptional modification. Here, the purified KIR-Fc fusion proteins show a molecular weight of approximately 90 kDa (visible in both load samples and purified KIR3DL05/3DL02). Bands with a lower weight are degraded KIR-Fc fusion proteins. Degradation might occur due to the release of proteases to the supernatant by the dying cells. As the Freestyle expression medium is serum free, longer incubation periods cause cell death of the transfected HEK 293 cells. This leads to the release of proteases which degrade the secreted Fc-fusion proteins. Flow-through samples show that all KIR-Fc fusion proteins in the supernatant were bound to the column and wash controls show that elution was accomplished with success and the columns were clean afterwards. IgG samples with known concentrations were

run as a positive control for the immunoblot protocol and show that the method was accomplished with success. Fresh recombinant KIR-Fc fusion proteins were purified for every binding assay.

5.2 Binding assays using the HEK 293 cell line

To study the interaction between MHC-I and KIR of rhesus macaque, the HEK 293 cell line was transfected with linearized Mamu pAcGFP-N1 expression vectors (4.1.12) via lipofectamine complexes (4.2.1.1). Successfully transfected cells were grown under selection medium and efficiency of transfection was checked by fluorescence microscopy and FACS W6/32 assay (4.2.13).

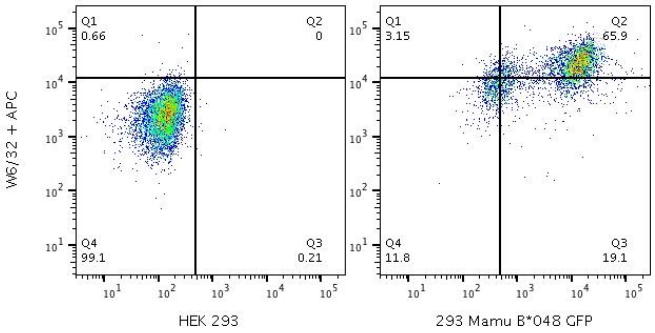

***Figure 11 - MHC-I expression on Mamu AcGFP transfected HEK 293 cells**. Flow cytometry data showing MHC-I surface expression increase on Mamu B*048 GFP (right picture) transfected culture compared to untransfected control HEK 293 cells (left picture). The X axis shows the increase in GFP fluorescence, the Y axis shows the increase in APC fluorescence. From each cell line, 5 x 10^5 cells were incubated with 1 µg of the monoclonal MHC-I antibody W6/32 and stained with α-mouse IgG / APC antibody.*

Figure 11 contains representative dotplots showing the increase of MHC-I cell surface expression associated with the transfection of Mamu allele B*048, when compared to HEK 293 untransfected cells.

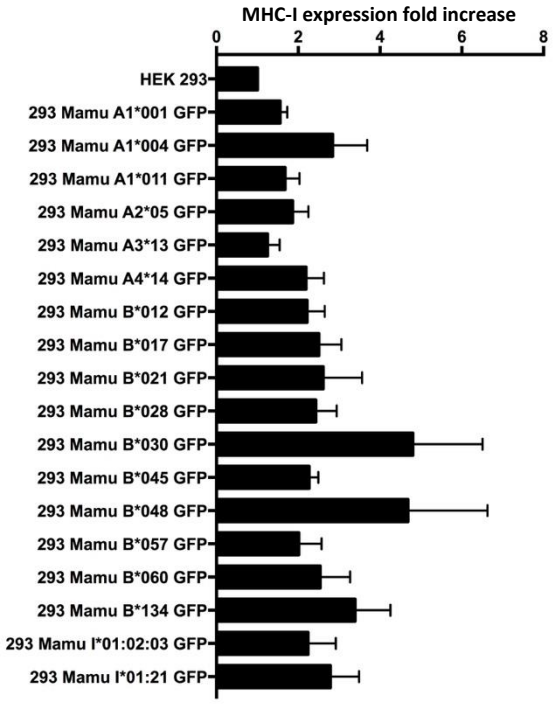

Figure 12 - MHC-I surface expression fold increase over control cell line, unstransfected HEK 293, from Mamu AcGFP transfected HEK 293 cultures. *Relative surface expression intensities from Mamus were calculated as described in 4.2.15.1 using MFI values of W6/32 + APC. Mean and standard error of the mean (SEM) are shown. Data is representative of at least three individual experiments.*

All eighteen Mamus provided were transfected into HEK 293 cells and MHC-I surface expression was tested in at least three independent experiments with the W6/32 FACS assay. The bar graph in figure 12 shows the fold increase of the Mamu AcGFP transfectants over the untransfected HEK 293 control. After verifying that Mamu AcGFP transfected cells presented an increase in MHC-I surface expression, binding studies using KIR3DL05, which is known to bind to Mamu A1*001, as a positive control, were performed.

First, 1 μg KIR-Fc fusion protein was added to 5 x 10^5 cells and incubated for 1 h at 4 ºC. Excess of Fc-fusion protein that did not bind to the cells was rinsed with 1 x PBS and cells were stained with α-human IgG / APC antibody for 15 min at 4 ºC. Excess of the secondary antibody was rinsed with 1 x PBS and probes were measured using an LSR II flow cytometer (BD Biosciences). Figure 13 shows representative dotplots.

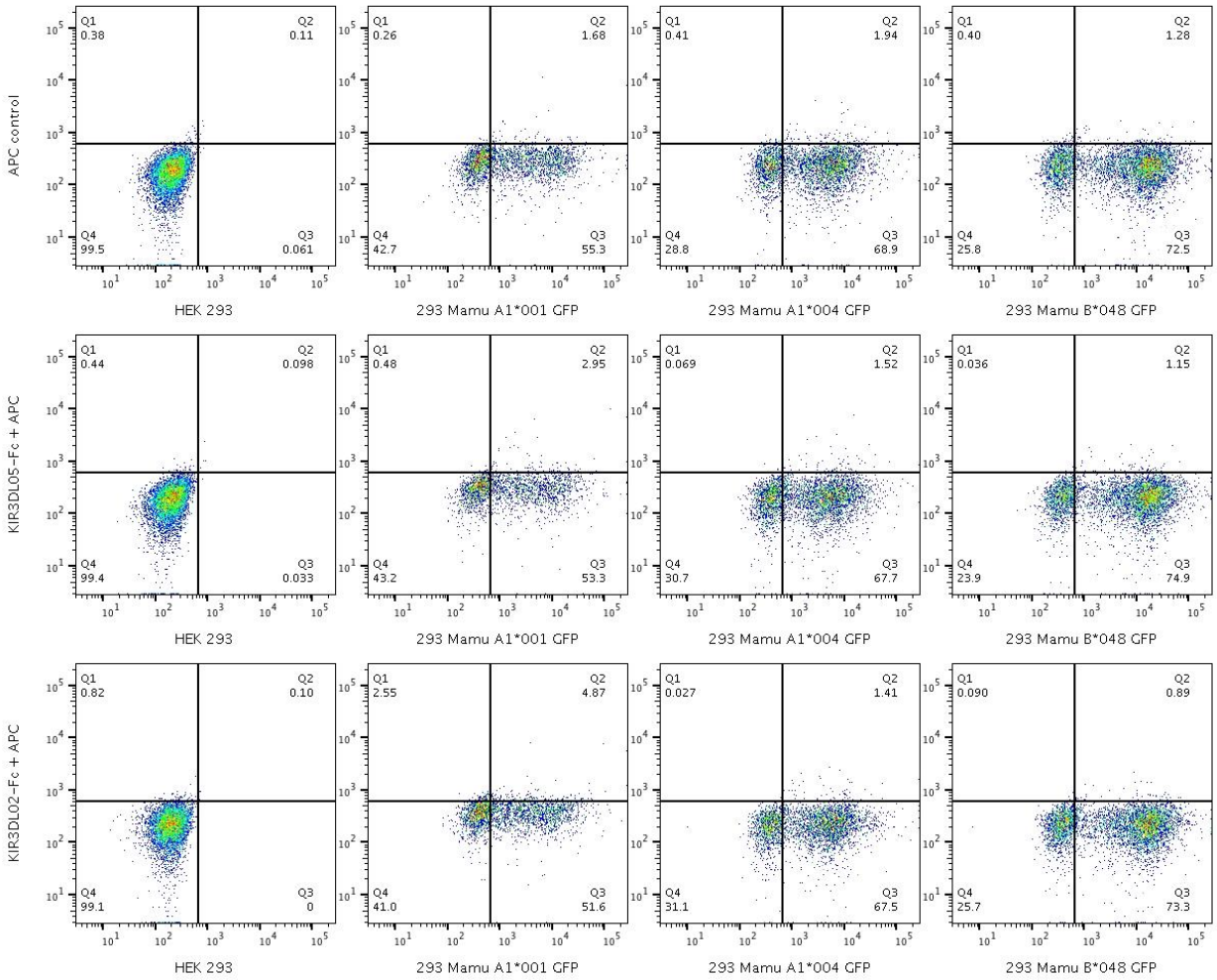

Figure 13 - No binding between unmultimerized KIR-Fc fusion proteins and MHC-I ligands on HEK 293 cells. *Flow cytometry data showing the results obtained in binding assays performed with unmultimerized Fc-protein. The X axis shows the increase in GFP fluorescence, the Y axis shows the increase in APC fluorescence. From the left to the right, untransfected HEK 293 cells, HEK 293 Mamu- A1*001 GFP, A1*004 GFP and B*048 GPF cell lines. From the upper to the lower row, α-human IgG / APC secondary antibody control, KIR3DL05-Fc stained with APC and KIR3DL02-Fc stained with APC.*

As no binding was found using Fc-fusion proteins to stain transfected cells directly, another approach with multimerized KIR Fc-fusion proteins as described in 4.2.14 was performed. Figure 14 displays representative dotplots.

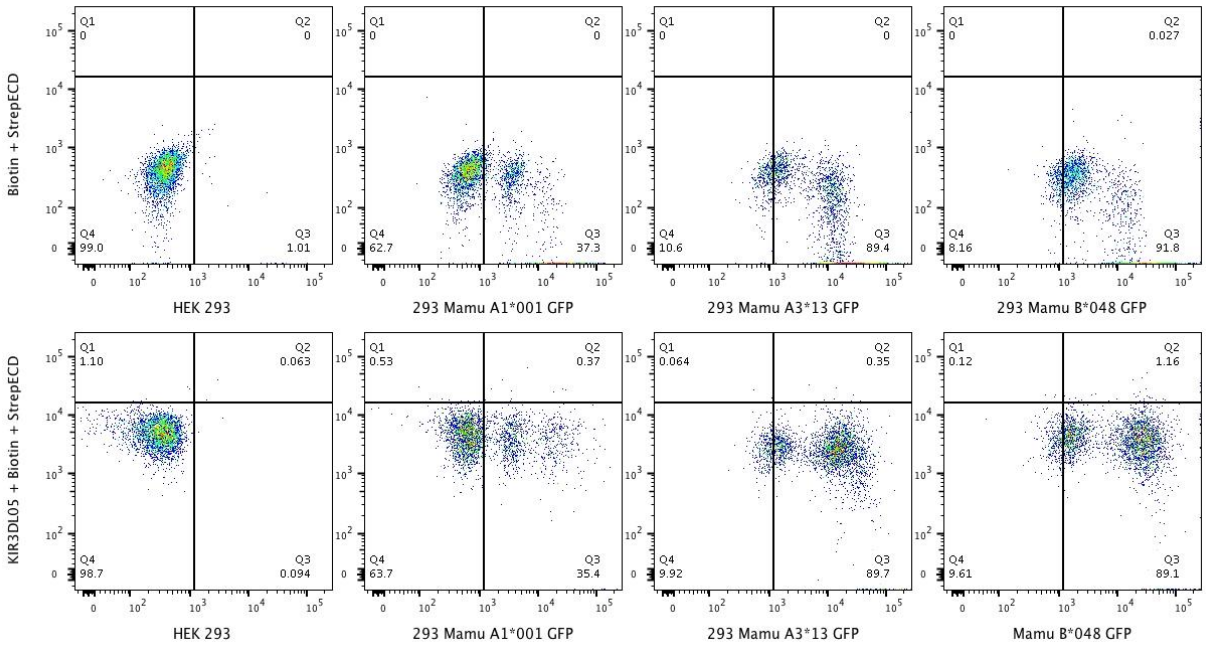

Figure 14 - Binding assays between multimerized KIR-Fc proteins and MHC-I transfected HEK 293 cells did not show any interaction. *Flow cytometry data of binding assays using multimerized KIR-Fc proteins and HEK 293 Mamu AcGFP cells. The X axis shows the increase in GFP fluorescence, the Y axis shows the increase in ECD fluorescence. From the left to the right, untransfected HEK 293, HEK 293 Mamu- A1*001 GFP, A3*13 GFP and B*048 GFP. From the upper to the lower row, Biotin + Strep ECD control and KIR3DL05 multimer coupled with Strep ECD.*

Binding assays using HEK 293 cells transfected with Mamu AcGFP expression vectors did not prove to be efficient. The results obtained from Rosner and colleagues (2011) were not replicable with this cell line. Hence, a comparison of HEK 293 and the human K-562 cell line followed[108].

5.3 Comparison between MHC-I levels of HEK 293 and K-562 human cell lines

As binding assays were not being successful in replicating the results of Rosner and colleagues (2011) work, a comparison between HEK 293 and K-562 cell lines was required[108]. Here, MHC class I basal surface expression level was compared. For this, untransfected HEK 293 and K-562 cells were incubated with the MHC-I specific monoclonal antibody W6/32 as described in 4.2.13.

Figure 15 shows the dotplots and histograms comparing the MHC-I surface expression levels of both cell lines.

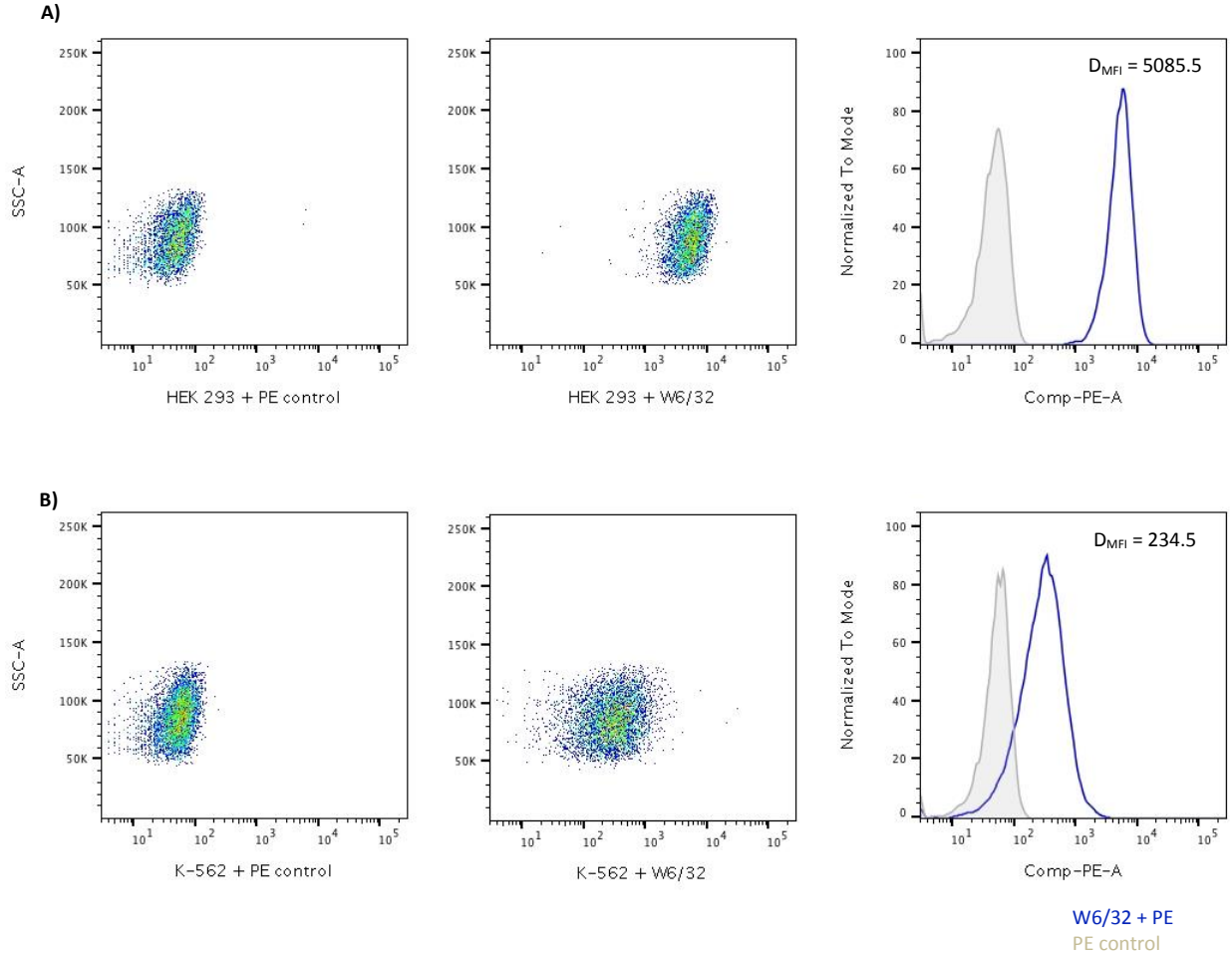

***Figure 15 - MHC-I surface expression level on HEK 293 and K-562 cells**. Dotplots and histograms showing the MHC-I surface expression in both cells lines. In the dotplots the X axis shows the increase in PE fluorescence, the Y axis shows the increase in granularity. From the left to the right, cells only with PE as a control, marked with the monoclonal antibody W6/32 with PE and the histogram overlay showing the increase in PE fluorescence W6/32 over PE control. **(A)** shows results of HEK 293 cells and **(B)** from K-562 cells. D_{MFI}, represent the differences in the median fluorescence intensity (MFI) measured with the W6/32 antibody to the secondary antibody control.*

As shown in figure 15, K-562 cells present a lower MHC-I surface expression level when compared to HEK 293 cells. Herein, MFI differences drop from 5085.5 for HEK 293 to 234.5 for K-562 cells. It was already expected that HEK 293 cells would have a higher MHC-I surface expression when compared to K-562. This could be an important factor influencing the different results obtained in the binding assays performed with HEK 293 Mamu AcGFP transfectants compared to Rosner *et al*. (2011)[108]. For this reason, K-562 cells were used to continue this work.

5.4 Enrichment of K-562 Mamu AcGFP positive population

In order to use the K-562 cell line for binding studies, these cells were transfected with the Mamu AcGFP expression constructs (4.2.8). As transfection efficiency was only between the 20 – 40 %, the GFP positive population should be increased for the binding assays. Therefore, Mamu positive cells were selected and isolated by magnetic cell separation and isolation (MACS) (4.2.10) and by cell sorting (4.2.11). Here, targeting the higher MHC-I surface expressing population and the GFP positive population, respectively. Both methods aimed towards obtaining more homogeneous populations that expressed the Mamu ligands stably.

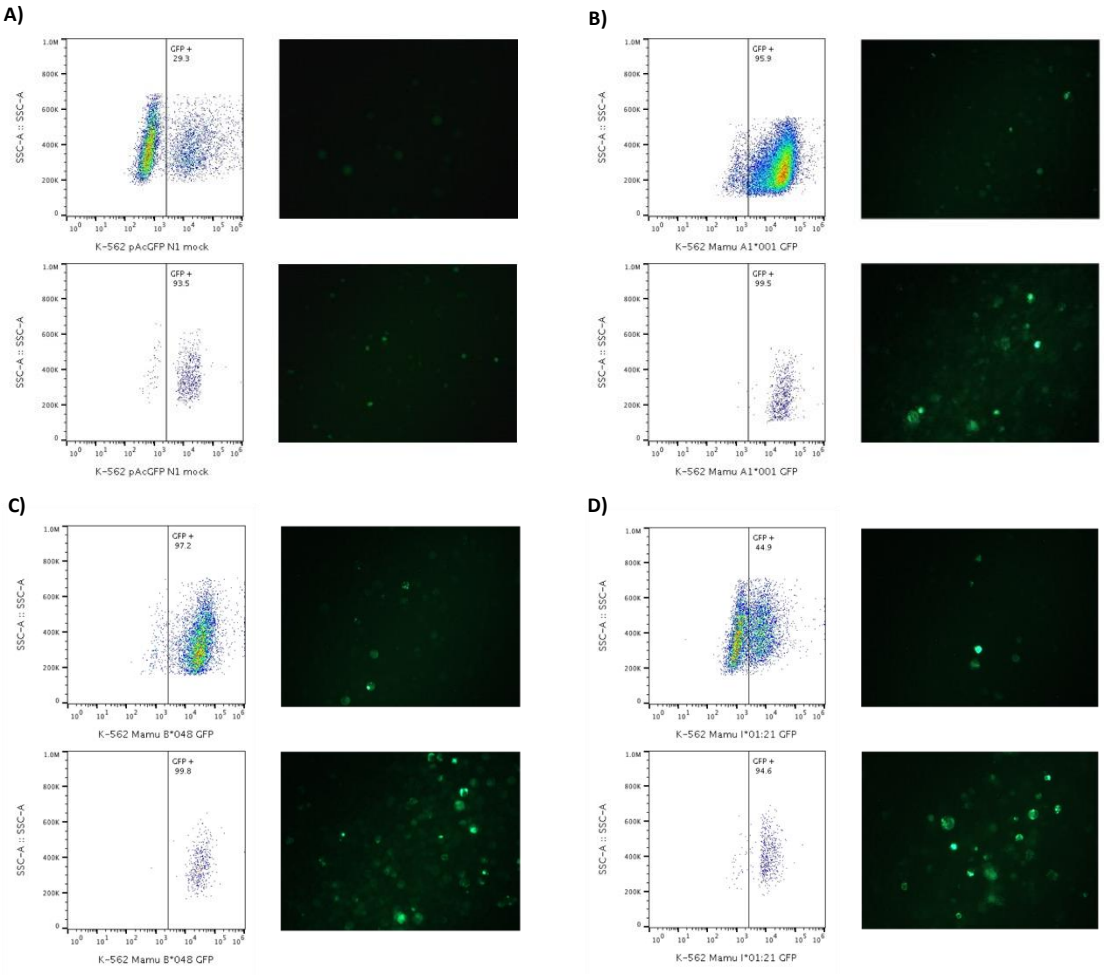

Figure 16 - Cell sorting was successful in the enrichment of Mamu AcGFP transfected cultures. (A), (B), (C) *and* ***(D)*** *show dotplots and one representative picture of each culture before and after cell sorting. Upper figures represent cultures before sorting, lower figures represent cultures after sorting. Cell sorting data shows 10 000 events counted before sorting and 1000 after sorting. For microscopy per each condition 2 x* 10^5 *cells were plated* ***(A)*** *shows K-562 pAcGFP-N1 transfected cells;* ***(B)*** *shows K-562 Mamu A*001 GFP transfected cells;* ***(C)*** *shows K-562 Mamu B*048 GFP transfected cells;* ***(D)*** *shows K-562 Mamu I*01:21 GFP transfected cells.*

Figure 16 shows flow cytometry and microscopy data of the enrichment efficiency of Mamu AcGFP transfected K-562 cells. Enrichment through MACS was tested by W6/32 FACS assay (4.2.13) and proved to be able to increase the MHC-I surface expressing population from 20 - 40 % to 80 - 90 % only for some cultures. Enrichment by MACS was only efficient in cells that had a transfection efficiency over 20 %. In cases in which transfected cells represented less than 20 % of the whole population MACS led to unspecific separation of untransfected K-562 cells. K-562 Mamu-A1*001 GFP and B*048 GFP were successfully enriched by MACS, presenting approx. 80 - 100 % of GFP positive cells. The remaining cells had to be separated by cell sorting since MACS did not prove to be efficient. Cell sorting allowed the increase in the GFP positive population from approx. 80 – 100 % to 90 – 100 %. The cells that were not successfully enriched by MACS, as was the example of K-562 Mamu I*01:21, were enriched by cell sorting, presenting final GFP positive cells of 70 – 90 %. Cultures that were successfully enriched were tested for MHC-I surface expression with the W6/32 FACS assay (4.2.13) and those that showed good MHC class I expression were further used for binding assays (4.2.14).

5.5 MHC class I surface expression of enriched K-562 Mamu AcGFP cell lines

In order to analyze the MHC-I surface expression of the enriched Mamu transfectants, FACS assays using the monoclonal MHC-I antibody W6/32 (4.2.13) were performed. Figure 17 shows representative dotplots and a bar graph with the MHC-I surface expression fold increase of the sorted Mamu AcGFP positive K-562 cells over the mock (K-562 pAcGFP-N1) transfectant control. Transfection with the empty vector caused and increase in MHC-I surface expression level of K-562 cells. A comparison between K-562 unstransfected and pAcGFP-N1 transfected cells is shown in appendix 9.2. The increase in MHC-I surface expression is observable in all Mamu AcGFP transfected cultures presented below. The increase of MHC-I surface expression is associated with the increase in GFP fluorescence.

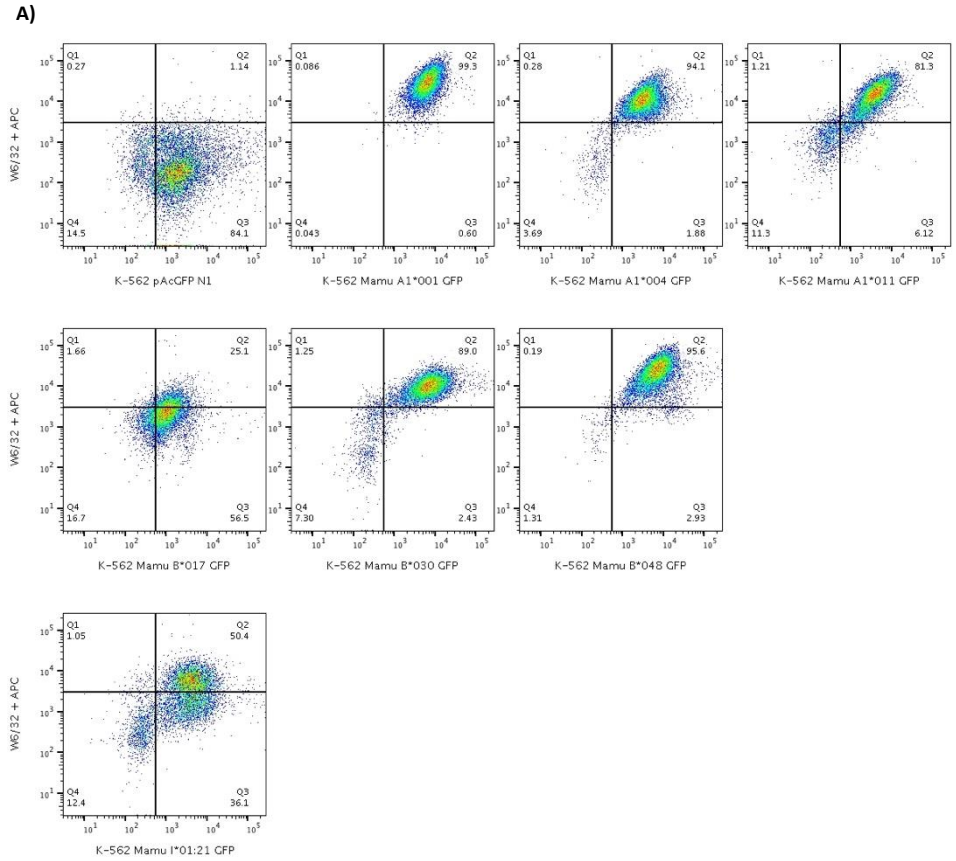

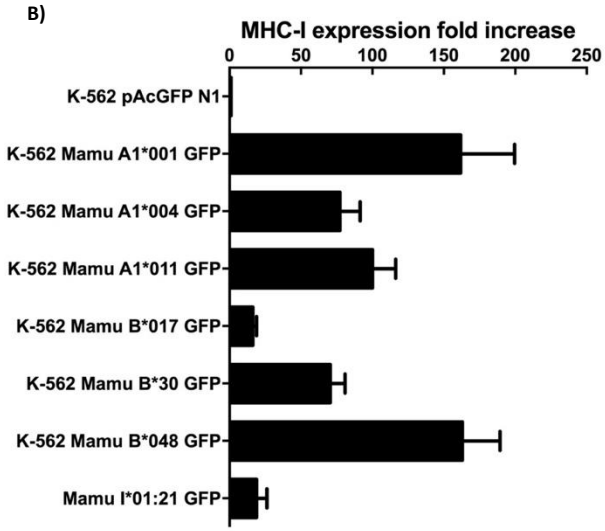

Figure 17 - K-562 Mamu AcGFP cell lines successfully express the Mamu alleles at the cell surface. (A) *Flow cytometry data showing MHC-I surface expression increase in K-562 Mamu AcGFP transfected cultures compared to K-562 pAcGFP-N1 transfected cell line. The X axis shows the increase in GFP fluorescence, the Y axis shows the increase in APC fluorescence. In the upper row, from the left to the right, K-562 pAcGFP-N1, K-562 Mamu- A1*001 GFP, A1*004 GFP, A1*011 GFP. In the middle row, from the left to the right, K-562 Mamu- B*017 GFP, B*030 GFP and B*048 GFP. In the lower row, K-562 Mamu I*01:21 GFP. From each cell line, 5 x 10^5 cells were incubated with the monoclonal MHC-I antibody, W6/32, and stained with α-mouse IgG/APC.* ***(B)*** *MHC-I surface expression fold increase of K-562 Mamu AcGFP cultures. Mean and SEM of at least three independent experiments are shown. Relative surface expression intensities from Mamus were calculated as described in 4.2.15.1 using MFI of W6/32 + APC.*

Of all eighteen Mamu contructs available seven were stably transfected and sorted with success. From these, all, except Mamu I*01:21, have statistically significant higher MHC-I surface expression levels compared to the mock transfected cell line. Regarding the remaining eleven constructs, although these presented GFP expressing cells, transfection efficiencies were not optimal. Troubleshooting here included lost expression of their MHC-I allele on the cell surface over time, low percentage of GFP positive population after transfection or low efficiency in cell sorting. In the case of Mamu I, it is known that these MHC-I alleles are not usually expressed on the cell surface.

5.6 Binding assays using the human K-562 cell line

After transfection and successful enrichment of the Mamu expressing K-562 cells, cultures with 80-100 % GFP positive cells were used for binding assays. Optimization of the protocol was required since the multimerization complex bound unspecificially to the K-562 Mamu AcGFP cell lines. Therefore, a FcR-blocking reagent, 1 x PBS 0.05 % azide and 1 x PBS 1 % BSA were tested for diminishing unspecific binding. Figure 18 shows the unspecific binding of Biotin + StrepBV570 to K-562 Mamu A1*001 GFP cell line when using FcR blocking reagent.

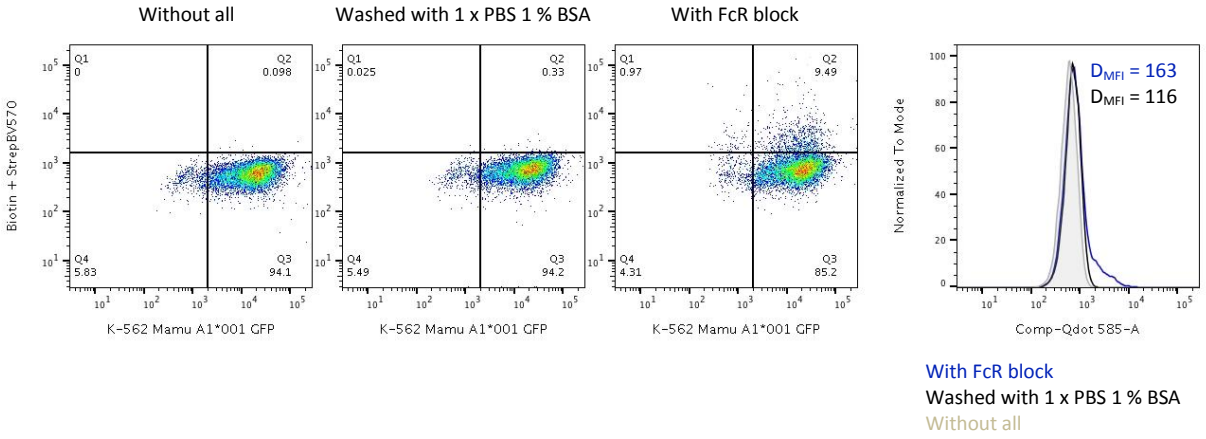

***Figure 18 - FcR blocking reagent causes unspecific binding of the Biotin + StrepBV570 complex**. In the dotplots the X axis represents the increase in GFP fluorescence and the Y axis the increase in BV570 fluorescence. From the left to the right, K-562 Mamu A1*001 GFP without all, K-562 Mamu A1*001 GFP washed with 1 x PBS 1 % BSA, K-562 Mamu A1*001 GFP with FcR blocking reagent and histogram display of the overlay of the three dotplots showing the increase in BV570 fluorescence when using FcR block (blue line) compared to washing with 1 x PBS 1 % BSA (black line). Cells without all are represented in grey.*

Additionally, figure 19 shows that using 1 x PBS 1 % BSA for washing the cells is more efficient in diminishing the unspecific binding of Biotin + StrepBV570 than using 1 x PBS 0.05 % azide.

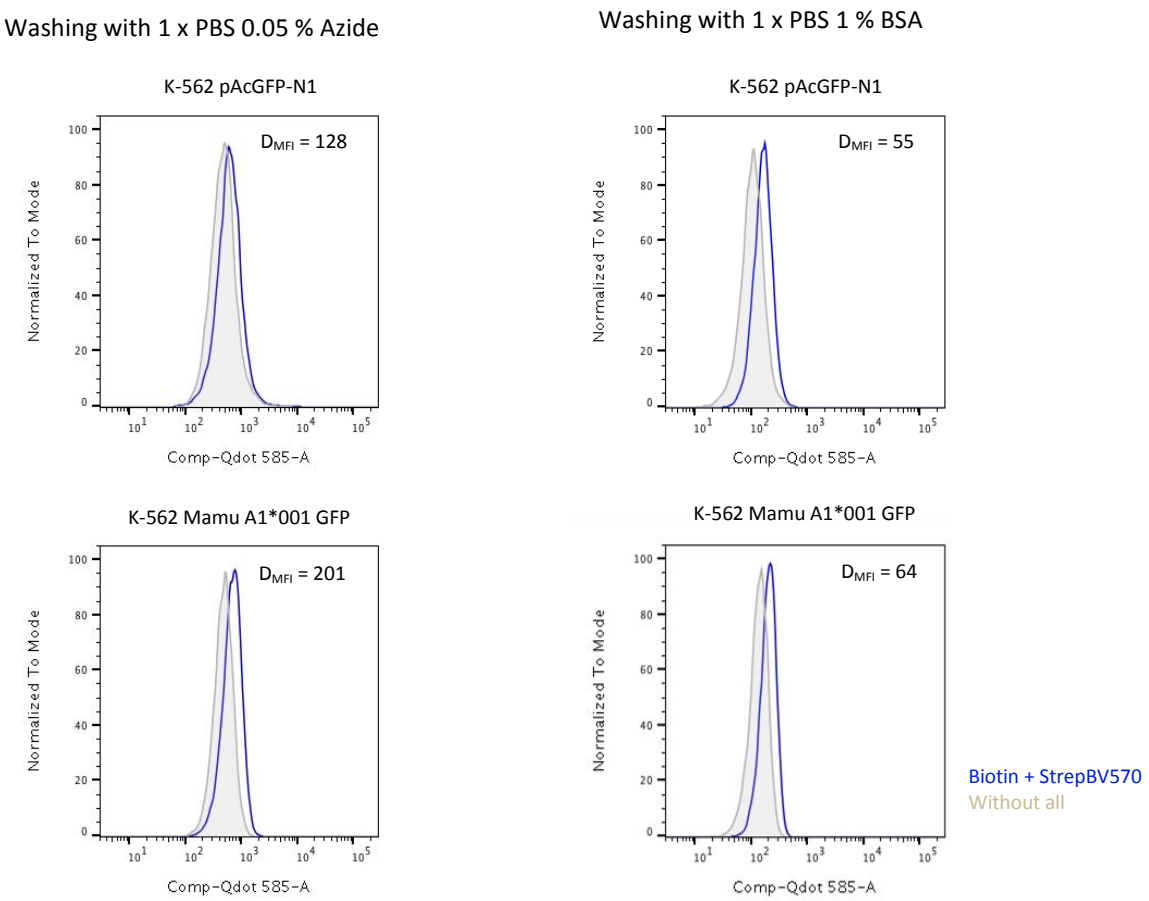

Figure 19 - Washing with 1 x PBS 1 % BSA is better for reducing unspecific binding to K-562 AcGFP cells than with 1 x PBS 0.05 % azide. *Histograms showing unspecific binding of Biotin + StrepBV570 to transfected cells, K-562 pAcGFP-N1 (upper histograms) and to K-562 Mamu A1*001 GFP (lower histograms) when washing with 1 x PBS 0.05 % azide (left side histograms) and with 1 x PBS 1 % BSA (right side histograms). Blue lines represent the Biotin + StrepBV570, grey lines are cells without everything.*

Here, the MFI of the unspecific binding of Biotin + StrepBV570 diminishes from an MFI of 128 to 55 for the mock transfectants and from 201 to 64 for the K-562 Mamu A1*001 GFP cell line. For this reason, it was considered to be optimal to wash the cells twice with 1 x PBS 1 % BSA before binding assays and one time after incubation with the KIR multimer to rinse excess of unbound multimer in order to diminish unspecific binding of the multimerization complex.

Next, the seven stably transfected, sorted Mamu AcGFP K-562 cultures were tested for binding KIR3DL05 and KIR3DL02. K-562 cell line transfected with the empty vector was used as a control and the increase in binding over the mock transfectant was calculated as described in 4.2.15.2.

A)

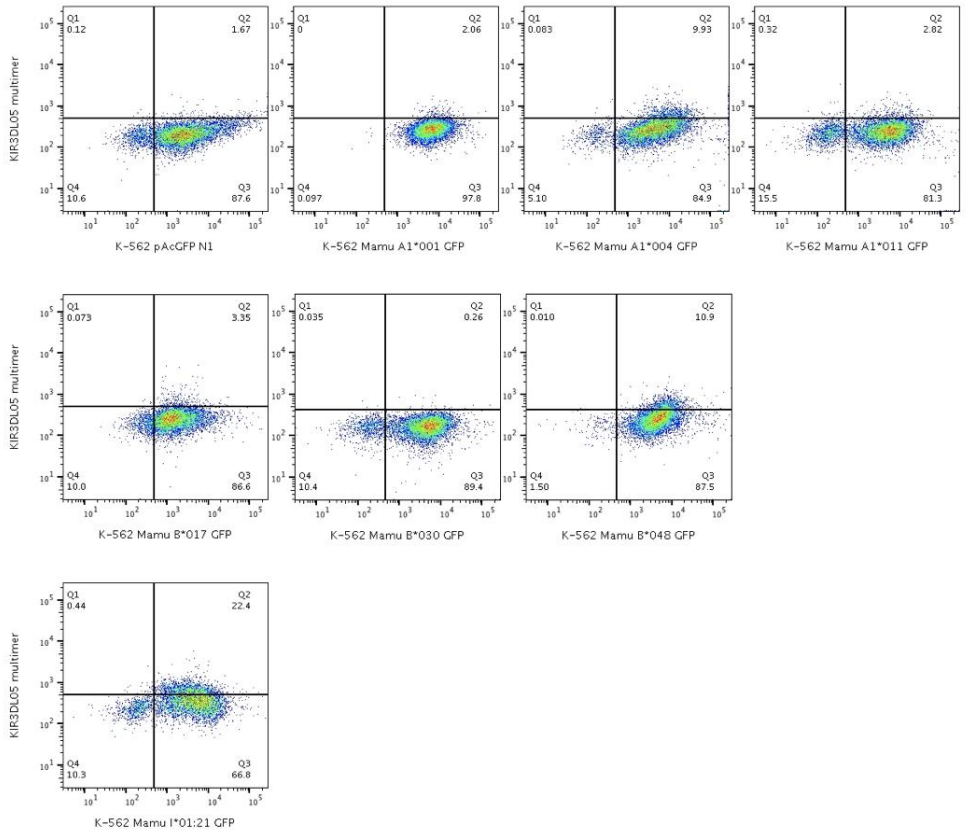
KIR3DL05 multimer
Q1 0.12
Q2 1.67
Q4 10.6
Q3 87.6
K-562 pAcGFP N1
Q1 0
Q2 2.06
Q4 0.097
Q3 97.8
K-562 Mamu A1*001 GFP
Q1 0.083
Q2 9.93
Q4 5.10
Q3 84.9
K-562 Mamu A1*004 GFP
Q1 0.32
Q2 2.82
Q4 15.5
Q3 81.3
K-562 Mamu A1*011 GFP
Q1 0.073
Q2 3.35
Q4 10.0
Q3 86.6
K-562 Mamu B*017 GFP
Q1 0.035
Q2 0.26
Q4 10.4
Q3 89.4
K-562 Mamu B*030 GFP
Q1 0.010
Q2 10.9
Q4 1.50
Q3 87.5
K-562 Mamu B*048 GFP
Q1 0.44
Q2 22.4
Q4 10.3
Q3 66.8
K-562 Mamu I*01:21 GFP

B)

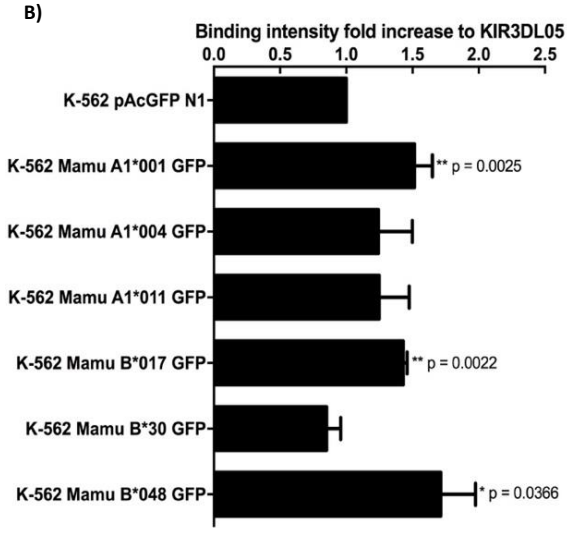
Binding intensity fold increase to KIR3DL05
0.0
0.5
1.0
1.5
2.0
2.5
K-562 pAcGFP N1
K-562 Mamu A1*001 GFP
** p = 0.0025
K-562 Mamu A1*004 GFP
K-562 Mamu A1*011 GFP
K-562 Mamu B*017 GFP
** p = 0.0022
K-562 Mamu B*30 GFP
K-562 Mamu B*048 GFP
* p = 0.0366

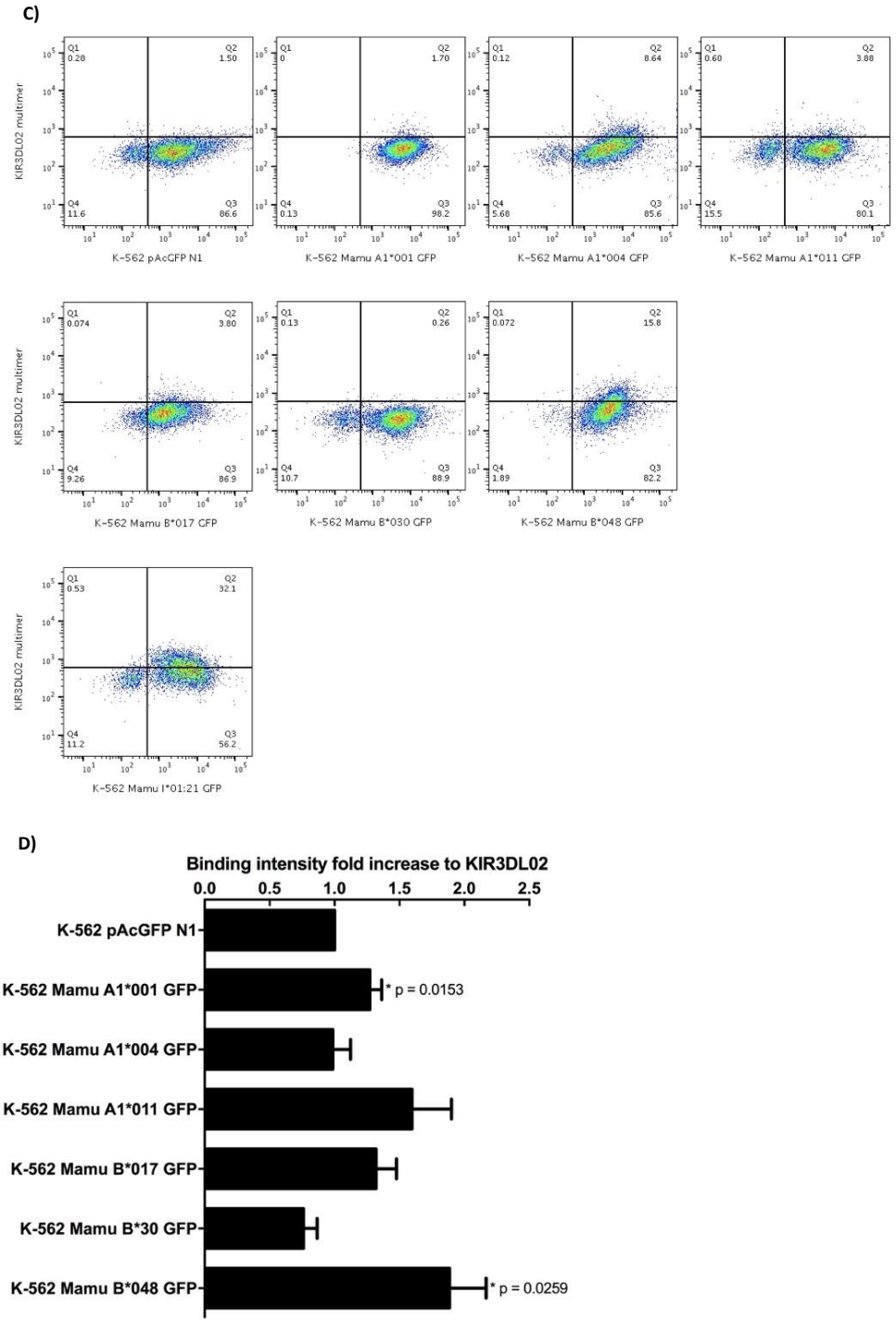

Figure 20 - Multimerized KIR3DL05/02-Fc proteins bind differently to Mamu alleles. (A) *and* ***(C)*** *Flow cytometry data shown as dotplots in which the X axis represents the increase in GFP fluorescence and the Y axis the increase in BV570 fluorescence.* ***(A)*** *shows results of KIR3DL05 binding studies.* ***(C)*** *shows results for KIR3DL02 binding studies. Binding assay followed as described in 4.2.14. In the upper row, from the left to the right, K-562 pAcGFP-N1, K-562 Mamu A1*001 GFP, A1*004 GFP, A1*011 GFP. In the middle row, from the left to the right, K-562 Mamu B*017 GFP, B*030 GFP and B*048 GFP. In the lower row, K-562 Mamu I*01:21 GFP.* ***(B)*** *and* ***(D)*** *Relative binding intensities of KIR3DL05 and 3DL02-Fc fusion multimerized proteins to rhesus macaque MHC-I alleles. Binding intensities were calculated as described in 4.2.15 using MFI values measured for BV70.* ***(B)*** *histogram showing fold increase over the mock transfected cells of KIR3DL05 binding to different Mamu AcGFP transfected K-562 cells.* ***(D)*** *histogram display for KIR3DL02. Statistical significance was found for KIR3DL05 and 3DL02 with Mamu A1*001 and B*048. And for KIR3DL05 with Mamu B*017. Mean and SEM are shown in the histograms. Data shown in representative of at least three independent experiments. P values were calculated with unpaired one-sided t-student tests with Welch's correlation.*

Figure 20 (A) and (C) shows representative dotplots of the mock transfected K-562 cell line and the seven Mamu AcGFP transfected cells incubated with KIR3DL05/02 multimer stained with BV570-coupled Streptavidin. Binding to MHC-I ligands Mamu-A1*001, A1*004 and B*048 is observable by the increase in fluorescence in BV570 with the increase in fluorescence in GFP. In the case of Mamu I*01:21 fluorescence intensity of BV570 diminishes with the increase of GFP fluorescence. (B) and (D) are bar graphs showing the increase in binding intensity for KIR3DL05/02, respectively. Binding to Mamu I*01:21 is not shown in bar graphs because it diminishes with the increase o MHC-I surface expression of the allele.

Higher relative binding intensities compared to control experiments were observed for KIR3DL05 and ligand Mamu A1*001 (p=0.0025), reproducing Rosner and colleagues (2011) published data[108]. However, higher relative binding intensities for KIR3DL05 with Mamu B*017 (p=0.0022) and B*048 (p=0.0366) were also found which were not reported in Rosner's study. This could arise from the higher MHC-I surface expression of each of these ligands in the cell lines used for the present study. Higher relative binding intensities for KIR3DL05 and Mamu A1*004 were also observed, nonetheless variability between individual experiments did not allow statistical support (p=0.2063).

For KIR3DL02 higher relative binding intensities compared with those of control experiments were found for binding to Mamu A1*001 (p=0.0153) and B*048 (p=0.0259). Although higher relative binding intensities were also observed for KIR3DL02 with Mamu A1*004, values varied between individual experiments and failed statistical support (p=0.9320).

5.7 Binding of KIR proteins depends on the surface expression of their Mamu ligands

In order to understand the impact of MHC-I surface expression in the binding of KIRs, FACS binding assays were analyzed with GFP intensity gatings.

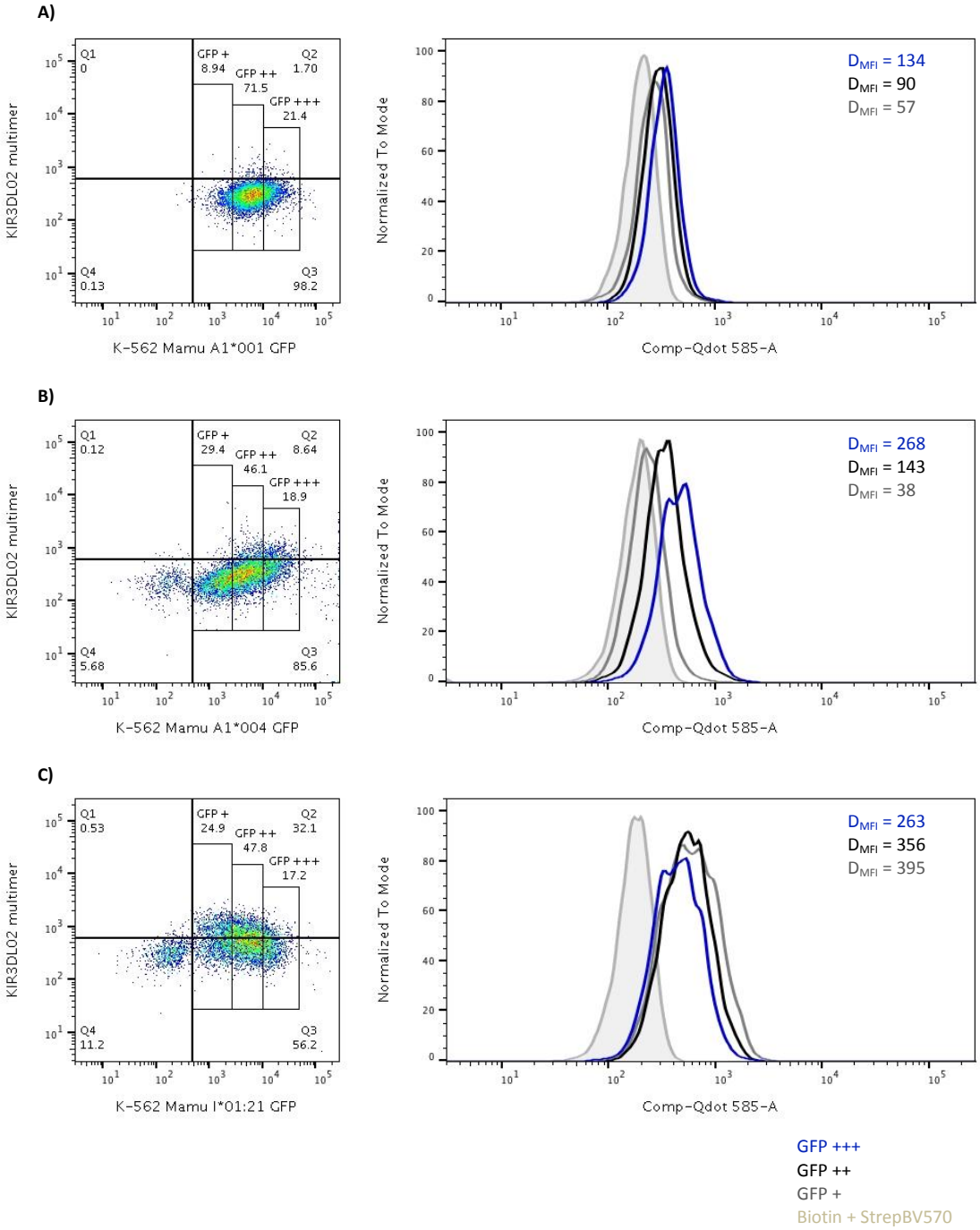

Figure 21 - Binding of multimerized KIR3DL02-Fc protein to Mamu AcGFP transfected K-562 cells is dependent on the MHC-I surface expression. *Flow cytometry data analysis from binding assays between multimerized KIR3DL02 protein and* ***(A)*** *K-562 Mamu A1*001 GFP,* ***(B)*** *K-562 Mamu A1*004 GFP and* ***(C)*** *K-562 Mamu I*01:21 GFP. On the left side of* ***(A), (B)*** *and* ***(C),*** *dotplots show in the X axis the increase in GFP fluorescence and in the Y axis the increase in BV570 fluorescence. On the left side, histograms with the overlay of Biotin + StrepBV570 (light grey), GFP + population (dark grey line), GFP ++ population (black line) and GFP +++ population (blue line) BV570 fluorescence measurements are shown. Binding of multimerized KIR3DL02 protein increases with the increase of Mamu- A1*001 and A1*004 and diminished with the increase of Mamu I*01:21 expression*

In MHC-I surface expression level assays (W6/32 FACS assays, 5.5) it was shown that expression of individual Mamu ligands increases with the enhancement of GFP expression (see Figure 17). The data obtained from these assays were gated so that three different GFP populations were identified; the lower GFP expressing population, designated GFP +, the median GFP expressing population, GFP ++, and the population which expressed the most GFP, GFP +++. As a consequence, cells that had the lowest expression of GFP were considered to express less MHC-I at their cell surface than cells that expressed more GFP. Figure 21 presents dotplots showing the GFP gating strategy and histograms with the overlay of the three GFP populations and the Biotin + StrepBV570 for each individual Mamu AcGFP cell line. For both, Mamu A1*001 and A1*004 ligands, KIR binding increases with the increase of GFP fluorescence. For Mamu A1*001, the difference in MFI increases from 57 for the GFP + population to 134 for the GFP +++ population. In the same way, for Mamu A1*004, the difference in MFI increases from 38 for GFP + to 268 for the GFP +++ population. On the contrary, for Mamu I*01:21 MFI diminishes with the increase of GFP fluorescence, going from 395 for the GFP + population to 263 for the GFP +++ population.

5.8 Amplification and cloning of MHC-I alleles from rhesus macaque cDNA into the mammalian expression vector pAcGFP-N1

Rhesus macaque KIRs predominantly have three IgG domains and bind MHC-I A and B as their main ligands. For this work, eighteen Mamu constructs, C-terminally fused to a GFP tag (pAcGFP-N1, Clontech) were provided by the Primate Genetics Laboratory (DPZ). Herein, six Mamu A, ten Mamu B and two Mamu I constructs, all previously checked for their accuracy by Sanger sequencing. Within these, the known protective Mamu A1*001 and Mamu B*017 as well as the non-protective Mamu A1*004 allele.

With the intent of widening the spectrum of this study, new Mamu alleles were amplified from cDNA of rhesus macaque using sequence specific primers. For this, both forward and reverse primers contained specific restriction enzyme cutting sites.

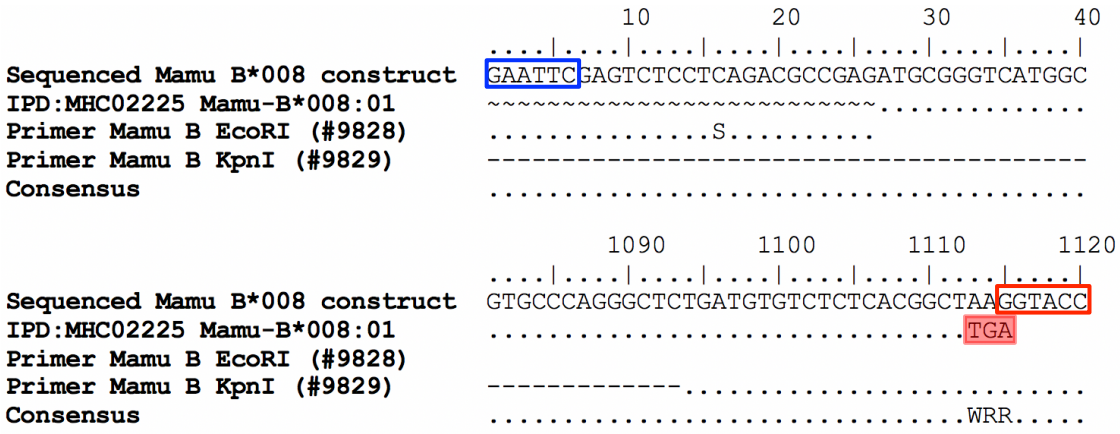

Figure 22 - Primer binding sites of the sequenced Mamu-B*008:01 construct. *Alignment shows parts of the here sequenced construct, the Mamu-B*008:01 consensus sequence obtained from the IDP MHC-I database as well as forward and reverse primers used to amplify the DNA fragment. Marked in blue and red the restriction sites, EcoRI and KpnI, respectively. In the forward primer, S allows the amplification of G or C nucleotides. The reverse primer was built to mutate the stop codon at the end of the Mamu B*008:01 fragment.*

Forward primers were designed to bind the start codon. Reverse primers were built to allow the amplification of complete Mamu allele sequences, creating a mutation of the stop codon. Different cutting sites were used in forward and reverse primers to enable directional cloning of the Mamu alleles into the pAcGFP-N1 expression vector. As an example, figure 22 shows primers used for Mamu B amplification from rhesus macaque cDNA. The complete Mamu B*008:01 sequence is shown in 9.3.

Mamu A and B alleles were amplified by PCR (4.1.1.1). PCR products were run on a 1.5 % agarose gel (4.1.2) and bands with approximately 1100 bp were extracted and purified using QIAquick gel extraction kit (3.6), following the manufacturer's instructions. Figure 23 shows an example of a 1.5 % agarose gel with MHC-I amplification products.

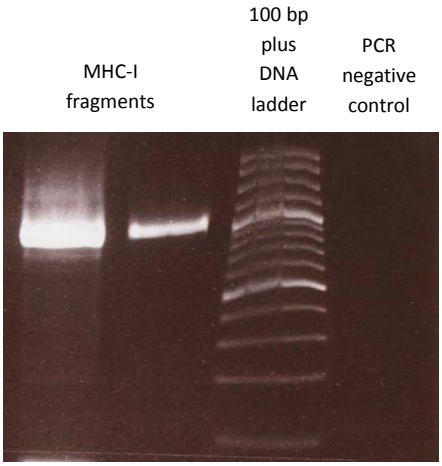

Figure 23 - Mamu amplification from cDNA of rhesus macaque. *1.5 % agarose gel showing the DNA fragments amplified with Mamu specific primers (two lanes on the right), the DNA ladder (third lane) and the PCR negative control (left lane). cDNA of rhesus macaque was used as template in the PCR reaction (4.1.1.1)*

As the MHC-I alleles were amplified using a proof reading DNA polymerase, an additional poly A tailing step (4.1.4) was required to add an adenine tail complementary to the thymidine tail of the bacterial cloning vector pGEM®-T Easy cloning vector (Promega). After poly A tailing, the products were ligated into the pGEM®-T Easy vector and used to transform *E. coli* JM109 chemically competent cells (4.1.5; 4.1.9).

Success of the transformation was tested by colony PCR (4.1.1.2) using a Mamu specific forward primer and a vector specific reverse primer. Colonies that showed a positive result for containing the insert were grown over night and plasmid DNA was extracted (4.1.10).

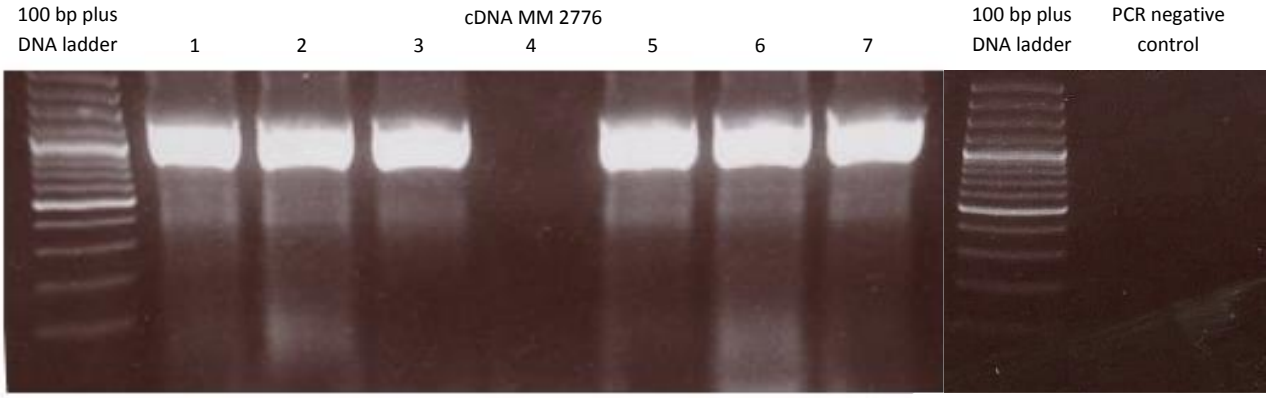

Figure 24 - Integration control of Mamu-sequences into p-GEM®-T Easy vector. *1.5 % agarose gel showing the DNA ladder (first lane on the left side of each picture) and the colony PCR products (lanes one to seven on the picture on the left side). Colonies were used as templates in a PCR reaction (program for amplification of DNA from E. coli JM109 colonies) with a Mamu-specific forward primer and a vector-specific reverse primer (#9828 and #G24 respectively, 3.15). Clones 1 to 3 and 5 to 7 present a band at approximately 1100 bp. Clone 4 is negative. PCR negative control is shown on the right-side picture, last lane.*

Figure 24 is a representative example of the colony PCR results. Here, clones 1 to 3 and 5 to 7 are positive as these present a band at 1100 bp, in contrast to clone 4 and the negative control which do not present any PCR product.

Plasmid DNA purified from the transformed cells was sequenced (4.1.3) in order to identify the amplified Mamu alleles for further cloning. In total, cDNA from four animals was used and from these, seven different Mamu alleles that were not among the previously provided were found (Table 5).

Table 5 - MHC-I alleles isolated from cDNA of rhesus macaque. *Alleles designation followed by the number of the animal from which it was isolated and the respective identification number in the IDP MHC database.*

Mamu Allele	Animal number	Number on MHC-I data base
Mamu A1*008:01:01	2222	MHC01903
Mamu B*001:01:01	2727	MHC02219
Mamu B*006:01	2776	MHC02223
Mamu B*008:01	2776	MHC02225
Mamu B*069:03	2260	MHC02316
Mamu B*072:02	2727	MHC02321
Mamu B*075:01	2260	MHC02323

Apart from these, the pseudogene *Mamu B*074:02 v1* as well as certain other Mamu alleles presenting frameshifts and nucleotide changes, that would lead to incompatible amino acid expression were amplified.

Clones that showed accuracy were cloned into the mammalian expression vector pAcGFP-N1 (Clontech). For this, both, the respective insert and the expression vector, were restricted with specific restriction enzymes (4.1.6) and ligated (4.1.7) in order to transform JM109 cells (4.1.9).

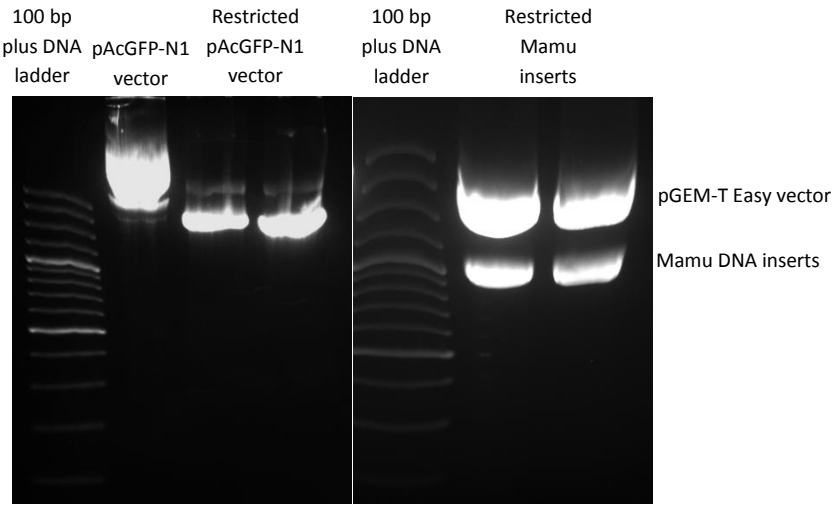

Figure 25 - Restriction of pAcGFP-N1 vector and amplified Mamu inserts with specific restriction enzymes. *1.5 % agarose gel showing DNA ladder on the first lane of each picture. Following the pAcGFP-N1 vector control (second lane on the left picture) and restricted vector templates with EcoRI and BamHI (third lane) and EcoRI and KpnI (fourth lane). On the picture on the right, second and third lane show Mamu B inserts restricted with EcoRI and KpnI. Upper bands are restricted pGEM-T Easy vectors, lower lanes are the Mamu fragments (approx. 1100 bp in length).*

Figure 25 presents an example of a 1.5 % agarose gel in which the digested inserts and vector are displayed as well as the unrestricted vector as control. In contrast to the restricted plasmid, the uncut vector migrates slower during electrophoresis. DNA fragments of the correct size were cut out of the gel, purified using QIAquick gel extraction kit following the manufacturer's instructions and ligated into the vector (4.1.7). After transformation of *E. coli* JM109 cells colonies were tested by colony PCR (4.1.1.2). Positive colonies were grown for plasmid DNA extraction and sequencing (4.1.10; 4.1.3). Clones verified by sequencing were regrown for MIDI plasmid DNA extraction for higher quantities and purer DNA templates (4.1.11). These Mamu pAcGFP-N1 constructs are ready for future transfection of the human K-562 cell line and binding studies.

6 Discussion

This study aimed towards understanding whether the NK cell receptor KIR3DL02 is able to bind MHC-I of rhesus macaques. For this, binding studies were performed using multimerized KIR-Fc fusion proteins and Mamu AcGFP cell cultures. Also, with the intent of broadening the study, MHC-I alleles were amplified from cDNA of rhesus macaques.

As a first approach, HEK 293 cells were stably transfected with linearized Mamu AcGFP mammalian expression constructs. Linearization ensured the integrity of all necessary gene elements of the vector and therefore higher efficiency in obtaining transfected cells that expressed the MHC-I insert in conjunction with the GFP tag. Success of transfection was verified by fluorescence microscopy and W6/32 FACS assays. Although HEK 293 cells could be transfected, transfection efficiencies were low. Moreover, the MHC-I surface expression was not much higher when compared to the untransfected cell line.

Binding studies performed using HEK 293 Mamu AcGFP transfected cell lines did not prove to be successful. Here, binding of KIR with MHC-I was tested with KIR-Fc fusion recombinant unmultimerized and multimerized proteins, nonetheless, results published in Rosner and colleagues work (2011) could not be replicated in either of the approaches[108]. In the assays in which unmultimerized protein were used no signal at all was recorded. Binding between KIR3D proteins is known to be weaker than KIR2D proteins[111]. Using unmultimerized KIR-Fc fusion proteins to stain directly Mamu AcGFP cells might, for this reason, not allow a binding signal. While using multimerized protein, although there was no unspecific binding of the multimerization complex, HEK 293 untransfected cells showed high binding intensities whereas Mamu AcGFP transfected cells did not show an increase in binding compared to the control. As the study conducted by Rosner *et al.* (2011) used K-562 cells to express the Mamu alleles, a comparison between HEK 293 and K-562 cells concerning their basal MHC-I surface level followed[108].

Although both cell lines derive from human, these have distinct origins that confer them different characteristics. The HEK 293 is an embryonic kidney cell line, whereas the K-562 originated from chronic myeloid leukemia. K-562 cells are an erythroleukemia cells which have multipotential and hematopoietic properties. These can spontaneously differentiate into progenitors of erythrocytes, granulocytes or monocytes. For this reason, the HEK 293 cell line was tested in the first place for this study. The comparison showed that HEK 293 cells present a higher basal level of MHC-I surface expression than K-562. As this work is focused on understanding KIR3DL02 capacity to bind to certain MHC-I of rhesus macaques, a high basal MHC-I surface expression level on the cell line used to

transfect with the Mamu constructs is not optimal and could be the reason for the different results obtained in this approach.

Binding between rhesus KIR and human HLA class I has been described by Aguilar and colleagues (2011)[112]. Here, it was found that rhesus macaque KIRs can bind human MHC-I with broad specificity[112]. This could, for one, justify the high binding to the HEK 293 unstransfected cells using multimerized KIR protein. On the other hand, Rosner described that KIR binding to MHC-I of rhesus macaque is dependent on the surface expression level of the Mamu alleles[108,113]. Hence, the low Mamu surface expression efficiency of transfected HEK 293 cells could be a factor impairing the success of these experiments. Considering these facts, the K-562 cell line was used to proceed with this study. K-562 cells have been reported to be highly sensitive targets in *in vitro* studies for natural killer cells as in the CD107a degranulation assays[114,115].

In order to proceed, K-562 cells were stably transfected with linearized Mamu AcGFP mammalian expression vectors. As a control the empty vector, pAcGFP-N1, was also transfected. Since transfection efficiencies were below optimal, cell cultures were enriched by antibiotic resistance, followed by magnetic cell separation using the MHC class I specific W6/32 monoclonal antibody, and by cell sorting, targeting the GFP positive population. Herein, despite the presence of GFP positive cells only seven out of the eighteen Mamu constructs available were enriched with success. A reason for this might be poor surface expression of transfected MHC-I alleles. This has already been described to be characteristic of certain Mamu alleles. Low cell surface expression was most recently described for Mamu A2*05 by Groot and colleagues (2017) as well as for Mamu A4*14, Mamu B*012, B*028, B*030, B*057, I*01:02:02 and I*01:21 by Rosner and colleagues (2010) in their work concerning subcellular locations of MHC-I of rhesus macaques[116,117]. Here, it was shown that alleles that presented low cell surface expression have high intracellular expression[117]. This might explain the presence of GFP positive cells in the transfected cells that do not appear to increase MHC-I surface expression while testing with the W6/32 assay. Since the surface expression of the Mamu alleles is fundamental for the interaction with the KIR-Fc fusion multimerized receptors, cell lines that did not show a good cell surface expression were not used in further assays.

In this work, the rhesus macaque MHC-I alleles, Mamu- A1*001, A1*004, A1*011, B*017, B*030, B*048 and I*01:21 showed a good cell surface expression and were enriched with success. Cultures used for binding assays presented 80-100 % GFP positive cells. All of these Mamu alleles showed higher relative MHC-I surface expression intensities when compared to the mock transfected cell line. Mamu B*030 and Mamu I*01:21 were previously described as having low cell surface expression[117]. Nonetheless, in this study a fold increase over the mock transfectant in MHC-I surface

expression of around 70 % and 20 %, respectively, was shown. Here, Mamu A1*001 and B*048 presented an MHC-I expression with a fold increase of around 150 %. Mamu B*017 showed the lowest MHC-I expression of all seven transfected cell lines, with a fold increase of approximately 15 %, however, low recognition from the W6/32 antibody of this MHC-I allele cannot be excluded. Interestingly, transfecting K-562 cells with the empty vector already induced an increase in MHC-I surface expression. For this reason, K-562 pAcGFP-N1 transfected cells were used as a control in the binding assays. This was to discard the effect of transfection from the binding assays.

Binding assays with K-562 Mamu AcGFP transfected cell lines were performed using multimerized Fc-fusion protein. For more accurate results, the assay was optimized with the purpose of diminishing unspecific binding to the multimerization complex. Although hydrophobic interactions are important for epitope-antibody interaction, in some cases this can also promote unspecific binding. Because of this, additives are used in buffers as protein blockers. Amongst these, FcR blocking reagent, 0.05 % azide and 1 % BSA are common choices and were tested in this work. It was found that the use of FcR blocking reagent and 1 x PBS 0.05 % azide are both not efficient methods to diminish unspecific binding of the Biotin + StrepBV570 complex. In contrast, washing cells with 1 x PBS 1 % BSA proved to be very efficient. Bovine serum albumin (BSA) is a globular protein with hydrophilic and hydrophobic subgroups which can surround the KIR-Fc multimers impairing the unspecific binding of these to other proteins, charged surfaces, glass and plastic. Also, BSA helps in stabilizing proteins in solution. Hence, 1 x PBS 1 % BSA was used to wash the cells before the binding assay and to rinse after incubation with multimerized proteins.

Using K-562 cells, a clear improvement in the binding assays when compared to the assays performed with HEK 293 Mamu AcGFP transfected cells was achieved. However, using K-562 transfected cells, an increase in binding intensity when compared to Biotin + StrepBV570 for the K-562 pAcGFP-N1 empty vector cells was still observed. Here, it can be suggested that the KIRs used in this work bound human MHC-I molecules expressed by the K-562 cells. Aguilar and colleagues (2011) studied the interaction between certain rhesus macaque KIRs and human MHC-I. It was shown that although rhesus KIRs bind human MHC-I, binding has broad specificity and is higher to HLA-C than HLA-A or -B[112]. However, binding to different Mamu alleles could still be verified with success.
Rosner and colleagues (2011) showed that the NK cell receptor KIR3DL05 was able to bind Mamu A1*001[108]. Here, this was used as a positive control. With K-562 cells transfected with the Mamu AcGFP constructs, KIR3DL05 bound successfully to Mamu A1*001, as described previously. However, binding to Mamu B*17 and B*048 was also observed. This had not been reported in the publication. Nonetheless, in their paper, Rosner and colleagues state that low expression of certain Mamu alleles at the cell surface might compromise binding of KIR receptors. As here MHC-I surface expression of

the individual Mamus was higher compared to the MHC-I surface expression in Rosner's work this might influence the binding assay results. It was described before that binding of KIR-Fc fusion multimerized proteins is dependent on the expression intensities of Mamu alleles at the cell surface[108]. The higher expressions of Mamu- B*017 and B*048 might have allowed binding of KIR3DL05 to be detected. Also, important to keep in mind are possible differences in the cells used. Compared to Rosner's study, a newly purchased batch of K-562 cells was used here and this needs to be considered when comparing results obtained in both studies. As described before, K-562 cells are undifferentiated cells from the bone marrow. Due to this, batches are more prone to have variations when compared to cell lines from differentiated cells, as for example HEK 293.

The KIR3DL02 receptor was described in Albrechts work to be associated with better outcomes in SIV infections and lower viral loads[110]. Because of this, it was expected that this receptor would be able to bind Mamu alleles already associated with a protective effect in simian immunodeficiency virus infection and slower development of AIDS[110,118]. This class of alleles include the here tested, Mamu A1*001 and B*017. Additionally, Mamu A1*004, which is mostly associated with a detrimental effect during SIV infection was included in the study. Higher binding intensities when compared to the control cells were observed with Mamu A1*001 and B*048 alleles. Mamu B*048 has not yet been described in the literature for having neither a protective nor a detrimental effect. Due to this, no suggestions can be drawn from the results obtained concerning this Mamu allele. Interestingly and although there is no statistical support, the results obtained throughout this work appear to support that KIR3DL02 might bind to Mamu A1*004. This was not expected since KIR3DL02 was present in a cohort of macaques with lower viral loads and slower progression of AIDS, whereas Mamu A1*004 has been identified to negatively influence SIV[119]. Here, it becomes important to keep in mind that these protective and non-protective effects of KIR3DL02 and Mamu A1*004, respectively, were studied separately, and no association between the presence of both allele and receptor was made yet. It is possible that the presence of both, receptor and ligand, in the same individual leads to a protective effect, whereas the absence of the receptor could lead to a detrimental effect of the ligand. In human, studies showed that, the presence of the HLA-Bw4 80I ligand is associated with a protective effect when KIR3DL1 is highly expressed[33,120]. Whereas, presence of KIR3DL1 in the absence of HLA-Bw4-80I leads to weaker responses of the NK cells[120]. In another perspective, considering data published by Albrecht and colleagues (2014), Mamu A1*004 was mostly found in animals with high viral loads, even in the presence of KIR3DL02 receptor[110]. This suggests that Mamu A1*004 is a bad ligand of KIR3DL02, binding with low avidity.

Binding intensities were compared with MHC-I surface expression to evaluate the effect of the surface expression of the ligands. An increase in binding associated with an increase in MHC-I surface

expression was verified for Mamu A1*001, A1*004 as well as B*048. This suggests that binding of KIRs is dependent on the surface expression of their MHC-I ligands as already shown by Rosner[108,113]. On the contrary, binding of KIR3DL02 to Mamu I*01:21 diminished with the increase of surface expression of the ligand. This might suggest that KIR3DL02 evolved to bind Mamu A and B rather than Mamu I ligands, supporting already existing evidence for a co-evolution in KIR - MHC-I gene families. It has been demonstrated that in humans KIR2D receptors bind HLA-C alleles with higher affinity, while KIR3D proteins mainly ligate HLA-A and B[72,103].

Mamu I is part of Mamu B locus and is likely to have resulted from a duplication of this classical MHC-I locus[101]. This can be detected in macaques but not in other *Cercopithecine* genera, suggesting that it arose from a recent event[101]. Despite presenting characteristics of the classical MHC-I B gene family, Mamu I shows low variability and appears to have evolved as a consequence of purifying selection, features from the nonclassical MHC-I family[101,121]. Regarding the nonclassical MHC-I genes, on the one hand, it has been suggested that these genes are nonfunctional or pseudogenes. On the other hand, HLA-E, which requires binding of peptides derived from leader sequences of other class I molecules for surface stabilization, represents a ligand for CD94/NKG2 NK cell receptors[121]. Further, it was found that the HLA-G is involved in maternal-fetal tolerance[122]. Similarities between Mamu AG and HLA-G support the hypothesis that nonclassical MHC-I might develop to take on specific roles[123,124]. The Mamu I locus, as a very recent duplication, is still going through purifying selection. This explains the low sequence variation and the presence of classical MHC-I characteristics[72,101]. However, this might also suggest that this gene is evolving to take on more specific roles and is losing its classical MHC-I features, including binding to KIRs.

Binding between inhibitory receptors and MHC-I ligands leads to the inactivation of NK cell cytolytic activity[52,54]. Here, the higher the avidity of the binding, the stronger the signal transmitted to the NK cell[48,73]. This is important not only during infection but also NK cell development. During NK cell development, inhibitory receptors play a fundamental role in determining the activation status and the responsiveness of circulating NK cells. According to the licensing model, interaction between inhibitory KIRs and MHC-I molecules confers functional competence to the NK cells[38,86]. Moreover, according to the disarming model, only a NK cell that expresses an inhibitory receptor will become responsive[38,86]. Hence, an individual that presents inhibitory receptors in its repertoire that can bind MHC-I with high avidity will have functionally better and more responsive NK cells in circulation compared to one that does not possess these receptors. Because of this, these individuals are better fit to identify MHC-I devoid cells. Upon SIV/HIV infection, in order to escape from CD8+ T cell mediated immunity, the virus downregulates MHC-I expression of the host cell[21,29]. Here, NK cells play a vital role in identifying infected cells. In order to prevent being identified by NK cells, the HI

virus only downregulates MHC-I selectively[21,125]. The peptides presented by MHC-I A and B are downregulated, whereas MHC-I C and E are left to serve as ligands for NK cell inhibition[21]. The selection criteria by which MHC-I molecules are targeted to be downregulated are still unknown, however protective phenotypes of MHC-I and KIRs have been identified through epidemiology studies in humans[126–128]. In the rhesus macaques it is also known that Mamu- A1*001, B*017 and B*008 are associated with a protective effect[110,129,130]. The NK cells receptor KIR3DL02 was identified by Albrecht and colleagues (2014) as being present in animals with lower viral loads[110].

Considering the results obtained in the present work, it can be suggested that Mamu A1*001 is a ligand for KIR3DL02. It can be hypothesized that during NK cell development, presence of KIR3DL02 and its binding to Mamu A1*001 confers functional capacity to the cell, allowing the licensing of mature NK cells. Supporting evidence for binding between KIR3DL02 and Mamu B*048 was also found. This MHC-I allele has not been associated neither with protective nor with a detrimental effect, but little is known about this due to the high polymorphism and variability of rhesus macaques MHC-I gene families. Regarding Mamu A1*004, although it has been associated with a detrimental effect, data found here suggest that this MHC-I allele could be a ligand for KIR3DL02. Taking into account data published by Albrecht and colleagues (2014) it can be suggested that Mamu A1*004, although being a ligand for KIR3DL02, binds weakly to the receptor, which leads to weaker signals and as a consequence, NK cells become less responsive during development or disarmed[110].

Taking these findings into account, it is clear that there is much to be understood regarding the interaction between rhesus macaque KIR and MHC class I ligands. It is important to know which KIR can bind to which MHC-I molecules and the functional consequences of their binding. Only when these interactions are understood, will it be possible to comprehend how they can positively or negatively influence SIV infection and progression.

7 Conclusion and further perspectives

The rhesus macaque NK cell receptor KIR3DL02 was previously associated with lower viral loads and better outcomes of SIV. The aim of this work was, in the first place, to study the interaction between KIR3DL02 and diverse MHC-I molecules, with special interest in investigating the interaction between KIR3DL02 and known protective Mamu A1*001 and B*017 and detrimental associated Mamu A1*004. In the second place, to amplify new Mamu alleles from cDNA of rhesus macaque and clone these into mammalian expression vector for further interaction studies.

Results obtained in this study allowed the identification of possible MHC-I ligands for KIR3DL02. Protective Mamu A1*001 and also Mamu B*048 showed an increase in binding intensity when compared to the control. Mamu A1*004 also appeared to serve as a ligand, but statistical support failed. Binding between KIR3DL02 and Mamu A1*004 was not expected as the ligand has been associated with a detrimental effect while the receptor is present in animals with lower viral loads and is hypothesized to be protective. Nonetheless, KIR – MHC-I interaction in rhesus macaques are poorly described and further studies are required to support these findings.
Moreover, seven new Mamu alleles were successfully amplified and cloned into the pAcGFP-N1 mammalian expression vector. Among these, the protective Mamu B*008 which can now be used for binding and functional studies.

Throughout this work, FACS binding assays were optimized so that the unspecific binding signal would be minimal. Despite this, multimerized KIRs still showed an increase in binding intensity to the mock transfectants when compared to the Biotin + StrepBV570. Although the K-562 cell line presents very low basal levels of MHC-I surface expression, transfection with the empty vector lead to an increase in this basal surface expression. In order to better understand if MHC-I basal surface expression of mock transfected K-562 cells is affecting the results, binding studies using the MHC-I devoid 721.221 cell line transfected with Mamu AcGFP vectors should be performed.
Herein, within human MHC-I, the nonclassical HLA-E is not usually expressed at the cell surface. For surface expression, this MHC-I molecule needs to bind a peptide from the leader sequence of other HLA molecules. Binding between rhesus macaque KIRs and HLA E has not been studied and it is unlikely that HLA-E is a ligand for KIR receptors, as it has been described as a ligand for CD94/NKG2[131]. However, transfection with Mamu AcGFP constructs might cause surface expression of HLA E molecules by the K-562 cells. To understand whether KIR multimers have unspecific binding to HLA-E, binding assays with MHC-I devoid cells can be performed. Here, cells should be transfected with a Mamu E / HLA-E and a construct that would provide a leader peptide for surface expression of these MHC-I molecules.

Altogether, the use of Fc-fusion proteins to study the interaction between rhesus KIRs and MHC-I alleles transfected into K-562 cells presented several disadvantages that could not be overcome in this work. For one, it is time consuming and expensive. Also, the cell line used to transfect the Mamu construct is very unstable and possibly leads to unspecific binding and variation in results obtained in the present study compared to the study developed by Rosner and colleagues (2011)[108]. Because of this, another approach should be considered to proceed. Here, functional studies using co-cultures of stably KIR transduced NK cell lines and MHC-I devoid cells transduced with Mamu constructs as target cells are proposed. This would allow identification of KIR ligands as well as the understanding of the functional effect of the binding. For this CD107a degranulation studies should be performed with CD107a surface expression as a marker for NK cell activation. As a control untransduced target cells could be used. In the case of KIR3DL02 ligand binding, it can be speculated, that degranulation, and therefore CD107a surface expression, might be lower than in the control condition due to inhibited NK cell mediated lysis. Considering the results obtained here, it is expected that using co-cultures of KIR3DL02 transduced NK cells with Mamu- A1*001, A1*004 and B*048 as target cells will lead to lower NK cell activation reflected by reduced CD107a surface expression. To further corroborate the obtained results, KIR3DL02-specific antibodies could be used to block the interaction with the ligands.

8 References

1. Schultz, K. T. & Grieder, F. Structure and function of the immune system. Toxicol. Pathol. 15, 262–264 (1987).

2. Delves, P. J. & Roitt, I. M. The Immune System. N. Engl. J. Med. 343, 37–49 (2000).

3. Parkin, J. & Cohen, B. An overview of the immune system. Lancet 357, 1777–1789 (2001).

4. Medzhitov, R. & Janeway, C. A. How does the immune system distinguish self from nonself? Semin. Immunol. 12, 185–188 (2000).

5. Janeway, C. A. & Medzhitov, R. Innate immune recognition. Annu. Rev. Immunol. 20, 197–216 (2002).

6. Parish, C. R. & O'Neill, E. R. Dependence of the adaptive immune response on innate immunity: some questions answered but new paradoxes emerge. Immunol. Cell Biol. 75, 523–7 (1997).

7. Janeway, C. A. Jr, Travers, P., Walport, M., Capra, D. J. The Immune System in Health and Disease. New York: Garland Science (New York: Garland Science, 2001).

8. The MHC sequencing consortium. Complete sequence and gene map of a human major histocompatibility complex. Nature 401, 921–923 (1999).

9. Dausset, J. & Contu, L. Is the MHC a general self-recognition system playing a major unifying role in an organism? Hum. Immunol. 1, 5–17 (1980).

10. Hurt, P., Walter, L., Sudbrak, R., Klages, S., Müller, I., Shiina, T., Inoko, H., Lehrach, H., Günther, E., Reinhardt, R., Himmelbauer, H. The Genomic Sequence and Comparative Analysis of the Rat Major Histocompatibility Complex. Genome Res. 631–639 (2004). doi:10.1101/gr.1987704.6

11. Walter, L. Receptors and MHC Class I Ligands in Non-human Primates. in Natural Hosts of SIV 269–285 (2014).

12. Walter, L. Pas de deux: Natural Killer Receptors and MHC Class I Ligands in Primates. Curr. Genomics 51–57 (2007).

13. Trowsdale, J. & Knight, J. C. Europe PMC Funders Group Major Histocompatibility Complex Genomics and Human Disease. 301–323 (2015). doi:10.1146/annurev-genom-091212-153455.Major

14. Mak, T. W. & Saunders, M. E. MHC: The Major Histocompatibility Complex. in The Immune Response 247–277 (2006). doi:10.1016/B978-012088451-3.50012-0

15. Kelley, J., Walter, L. & Trowsdale, J. Comparative genomics of major histocompatibility complexes. Immunogenetics 56, 683–695 (2005).

16. Costantino, C. M., Spooner, E., Ploegh, H. L. & Hafler, D. A. Class II MHC self-antigen presentation in human B and T lymphocytes. PLoS One 7, (2012).

17. Alberts, B., Johnson, A., Lewis, J., Raff, M., Roberts, K., Walter, K.T Cells and MHC Proteins. in Molecular Biology of the Cell (New York: Garland Science, 2002).

18. Jones, E. Y. MHC class I and class II structures. Curr. Opin. Immunol. 9, 75–9 (1997).

19. Li, X. C. & Raghavan, M. Structure and function of major histocompatibility complex (MHC) class I antigens. Curr. Opin. Organ Transplant. 15, 499–504 (2010).

20. Natarajan, K., Li, H., Mariuzza, R. A. & Margulies, D. H. MHC class I molecules, structure and function. Rev Immunogenet. 32–46 (1999).

21. Petersen, J. L., Morris, C. R. & Solheim, J. C. Virus Evasion of MHC Class I Molecule Presentation. J. Immunol. 171, 4473–4478 (2003).

22. Arts, E. J. & Hazuda, D. J. HIV-1 antiretroviral drug therapy. Cold Spring Harb. Perspect. Med. (2012). doi:10.1101/cshperspect.a007161

23. Montessori, V., Press, N., Harris, M., Akagi, L. & Montaner, J. S. G. Adverse effects of antiretroviral therapy for HIV infection. Can. Med. Assoc. J. 170, 229–238 (2004).

24. Reust, C. E. Common adverse effects of antiretroviral therapy for HIV disease. Am. Fam. Physician 83, 1443–1451 (2011).

25. Wilen, C. B., Tilton, J. C. & Doms, R. W. HIV: Cell Binding and Entry. Cold Spring Harb. Perspect. Med. 2, 1–14 (2012).

26. Levy, J. A. Pathogenesis of Human Immunodeficiency Virus Infection. Microbiol. Rev. 57, 183–289 (1993).

27. Zhu, J. & Paul, W. E. CD4 T cells: fates, functions , and faults. Blood 112, 1557–1569 (2008).

28. Okoye, A. A. & Picker, L. J. CD4+ T-Cell Depletion In Hiv Infection: Mechanisms Of Immunological Failure. Immunol. Rev. 254, 54–64 (2013).

29. Guha, D. & Ayyavoo, V. Innate immune evasion strategies by human immunodeficiency virus type 1. ISRN AIDS 2013, (2013).

30. Février, M., Dorgham, K. & Rebollo, A. CD4 +T cell depletion in human immunodeficiency virus (HIV) infection: Role of apoptosis. Viruses 3, 586–612 (2011).

31. Carrington, M. & O'Brien, S. J. The influence of HLA genotype on AIDS. Annu. Rev. Med. 54, 535–551 (2003).

32. Kaslow RA, Carrington M, Apple R, Park L, Muñoz A, Saah AJ, Goedert JJ, Winkler C, O'Brien SJ, Rinaldo C, Detels R, Blattner W, Phair J, Erlich H, M. D. Influence of combinations of human major histocompatibility complex genes on the course of HIV-1 infection. Nat Med 2, 405–11 (1996).

33. Alter, G., Martin, M. P., Teigen, N., Carr, W. H., Suscovich, T. J., Schneidewind, A., Streeck, H., Waring, M., Meier, A., Brander, C., Lifson, J. D., Allen, T. M., Carrington, M., Altfeld, M. Differential natural killer cell–mediated inhibition of HIV-1 replication based on distinct KIR/HLA subtypes. J. Exp. Med. 204, 3027–3036 (2007).

34. Campbell, K. S. & Hasegawa, J. Natural killer cell biology: An update and future directions. J. Allergy Clin. Immunol. 132, 536–544 (2013).

35. Khakoo, S. I., Thio, C. L., Martin, M. P., Brooks, C. R., Gao, X., Astemborski, J., Cheng, J., Goedert, J. J., Vlahov, D., Hilgartner, M., Cox, S., Little, A. M., Alexander, G. J., Cramp, M. E., O'Brien, S. J., Rosenberg, W. M.C., Thomas, D. L., Carrington, M. HLA and NK cell Inhibitory Receptor Genes in Resolving Hepatitis C Virus Infection. Science (80-.). 305, 872–874 (2004).

36. Caligiuri, M. a. Human natural killer cells. Blood 112, 461–469 (2008).

37. Sun, J. C., Beilke, J. N. & Lanier, L. L. Adaptive immune features of natural killer cells. Nature 457, 557–561 (2009).

38. Orr, M. T. & Lanier, L. L. Natural Killer Cell Education and Tolerance. Cell 142, 847–856 (2010).

39. Yu, J., Freud, A. G. & Caligiuri, M. A. Location and cellular stages of natural killer cell development. Trends Immunol. 34, 573–582 (2013).

40. Lanier, L. L., Phillips, J. H., Hackett, J., Tutt, M. & Kumar, V. Natural Killer Cells: Definition of a Cell Type Rather Than a Function. J. Immunol. 137, 2735–2739 (1986).

41. Ljunggren, H. G. & Karre, K. In search of the missing self: MHC molecules and NK cell recognition. Immunol.Today 11, 237–244 (1990).

42. Bessoles, S., Grandclément, C., Alari-Pahissa, E., Urlaub, D., Gehrig, J., Jeevan-Raj, B., Held, W. Adaptations of natural killer cells to self-MHC class I. Front. Immunol. 5, 1–6 (2014).

43. Geiger, T. L. & Sun, J. C. Development and maturation of natural killer cells. Curr. Opin. Immunol. 39, 82–89 (2016).

44. Bozzano, F., Marras, F. & De Maria, A. Natural Killer Cell Development and Maturation Revisited: Possible Implications of a Novel Distinct Lin−CD34+DNAM-1brightCXCR4+ Cell Progenitor. Front. Immunol. 8, 6–13 (2017).

45. Poli, A., Michel, T., Thérésine, M., Andrès, E., Hentges, F., Zimmer, J. CD56bright natural killer (NK) cells: An important NK cell subset. Immunology 126, 458–465 (2009).

46. Moretta, L. Dissecting CD56dim human NK cells. Blood 116, 3689–3691 (2010).

47. Elliott, J. M. & Yokoyama, W. M. Unifying concepts of MHC-dependent natural killer cell education. Trends Immunol. 32, 364–372 (2011).

48. Brodin, P., Kärre, K. & Höglund, P. NK cell education: not an on-off switch but a tunable rheostat. Trends Immunol. 30, 143–149 (2009).

49. Lanier, L. L. NK cell receptors. Annu Rev Immunol 16, 359–393 (1998).

50. Pegram, H. J., Andrews, D. M., Smyth, M. J., Darcy, P. K. & Kershaw, M. H. Activating and inhibitory receptors of natural killer cells. Immunol. Cell Biol. 89, 216–224 (2011).

51. Carrillo-Bustamante, P., Keşmir, C. & de Boer, R. J. The evolution of natural killer cell receptors. Immunogenetics 68, 3–18 (2016).

52. Long, E. O. Negative signalling by inhibitory receptors: the NK cell paradigm. Immunol. Rev. 70–84 (2008). doi:10.1111/j.1600-065X.2008.00660.x.Negative

53. Lanier, L. L. Nk Cell Recognition. Annu. Rev. Immunol. 23, 225–274 (2005).

54. Long, E. O., Sik Kim, H., Liu, D., Peterson, M. E. & Rajagopalan, S. Controlling NK Cell Responses: Integration of Signals for Activation and Inhibition. Annu. Rev. Biochem. 31, 1–36 (2013).

55. Tomasello, E., Blery, M., Vely, E. & Vivier, E. Signaling pathways engaged by NK cell receptors: Double concerto for activating receptors, inhibitory receptors and NK cells. Semin. Immunol. 12, 139–147 (2000).

56. Yokoyama, W. M. & Seaman, W. E. The Ly-49 and NKR-P1 gene families encoding lectin-like receptors on natural killer cells: the NK gene complex. Annu. Rev. Immunol. 11, 613–635 (1993).

57. Mcqueen, K. L. & Parham, P. Variable receptors controlling activation and inhibition of NK cells. Curr. Opin. Immunol. 14, 615–621 (2002).

58. Trowsdale, J., Barten, R., Haude, A., Stewart, A. C., Beck, S., Wilson, M. J.The genomic context of natural killer receptor extended gene families. Immunol. Rev. 181, 20–38 (2001).

59. Kulkarni, S., Martin, M. P. & Carrington, M. The Yin and Yang of HLA and KIR in human disease. Semin. Immunol. 20, 343–352 (2008).

60. Chan, H. et al. Epigenetic Control of Highly Homologous Killer Ig-Like Receptor Gene Alleles 1. J Immunol 5966–5974 (2005). doi:10.4049/jimmunol.175.9.5966

61. Davies, G. E., Locke, S. M., Wright, P. W., Li, H., Hanson, R. J., Miller, J. S., Anderson, S. K Identification of bidirectional promoters in the human KIR genes. Genes Immun. 245–253 (2007).

62. Campbell, K. S. & Purdy, A. K. Structure/function of human killer cell immunoglobulin-like receptors: Lessons from polymorphisms, evolution, crystal structures and mutations. Immunology 132, 315–325 (2011).

63. Roe, D., Vierra-Green, C., Pyo, C. W., Eng, K., Hall, R., Kuang, R., Spellman, S., Ranade, S., Geraghty, D. E., Maiers, M. Revealing complete complex KIR haplotypes phased by long-read sequencing technology. Genes Immun. 18, 127–134 (2017).

64. Vilches, C. & Parham, P. KIR: Diverse, Rapidly Evolving Receptors of Innate and Adaptive Immunity. Annu. Rev. Immunol. 20, 217–251 (2002).

65. Manser, A. R., Weinhold, S. & Uhrberg, M. Human KIR repertoires: Shaped by genetic diversity and evolution. Immunol. Rev. 267, 178–196 (2015).

66. Uhrberg, M., Valiante, N. M., Shum, B. P., Shilling, H. G., Lienert-Weidenbach, K., Corliss, B., Tyan, D., Lanier, L. L., Parham, P. Human Diversity in Killer Cell Inhibitory Receptor Genes. Immunity 7, 753–63 (1997).

67. Vilches, C., Pando, M. J., Rajalingam, R., Gardiner, C. M. & Parham, P. Discovery of two novel variants of KIR2DS5 reveals this gene to be a common component of human KIR 'B' haplotypes. Tissue Antigens 56, 453–456 (2000).

68. Uhrberg, M. The KIR gene family: Life in the fast lane of evolution. Eur. J. Immunol. 35, 10–15 (2005).

69. Boyington, J. C. & Sun, P. D. A structural perspective on MHC class I recognition by killer cell immunoglobulin-like receptors. Mol. Immunol. 38, 1007–1021 (2002).

70. Kikuchi-Maki, A., Yusa, S., Catina, T. L. & Campbell, K. S. KIR2DL4 is an IL-2-regulated NK cell receptor that exhibits limited expression in humans but triggers strong IFN-gamma production. J. Immunol. 171, 3415–3425 (2003).

71. Marsh, S. G. E., Parham, P., Dupont, B., Geraghty, D. E., Trowsdale, J., Middleton, D., Vilches, C., Carrington, M., Witt, C., Guethlein, L. A., Shilling, H., Garcia, C. A., Hsu, K. C., Wain, H. (KIR) Nomenclature Report , 2002. Immunol. Rev. 8859, (2002).

72. de Groot, N. G., Blokhuis, J. H., Otting, N., Doxiadis, G. G. M. & Bontrop, R. E. Co-evolution of the MHC class I and KIR gene families in rhesus macaques: Ancestry and plasticity. Immunol. Rev. 267, 228–245 (2015).

73. Rajagopalan, S. & Long, E. O. Understanding how combinations of HLA and KIR genes influence disease. J. Exp. Med. 201, 1025–1029 (2005).

74. Colucci, F. The role of KIR and HLA interactions in pregnancy complications. Immunogenetics 69, 557–565 (2017).

75. Leone, P., De Re, V., Vacca, A., Dammacco, F. & Racanelli, V. Cancer treatment and the KIR–HLA system: an overview. Clin. Exp. Med. 17, 419–429 (2017).

76. Ahlenstiel, G., Martin, M. P., Gao, X., Carrington, M. & Rehermann, B. Distinct KIR / HLA compound genotypes affect the kinetics of human antiviral natural killer cell responses. J. Clin. Invest. 118, 1017–1026 (2008).

77. Yawata, M., Yawata, N., Draghi, M., Little, A., Partheniou, F., Parham, P. Roles for HLA and KIR polymorphisms in natural killer cell repertoire selection and modulation of eff ector function. J. Exp. Med. 203, 633–645 (2006).

78. Romero, V., Azocar, J., Joaquin, Z., Clavijo, O. P., Terreros, D., Gu, X., Husain, Z., Chung, R. T., Amos, C., Yunis, E. J. Interaction of NK inhibitory receptor genes with HLA-C and MHC class II alleles in Hepatitis C virus infection outcome u n. Mol. Immunol. 2429–2436 (2008). doi:10.1016/j.molimm.2008.01.002

79. Cook, M., Briggs, D., Craddock, C., Mahendra, P., Milligan, D., Fegan, C., Darbyshire, P., Lawson, S., Boxall, E., Moss, P. Donor KIR genotype has a major influence on the rate of cytomegalovirus reactivation following T-cell replete stem cell transplantation. Blood 107, 1230–1233 (2008).

80. Machuca, A., Tang, S., Hu, J., Lee, S., Wood, O., Vockley, C., Vutukuri, S. G., Deshmukh, R., Awazi, B., Hewlett, I. Killer Immunoglobulin- Like Receptor Genotype May Distinguish Immunodeficient HIV-Infected Patients Resistant to Immune Restoration Diseases Associated With Herpes Virus Infections. J Acquir Immune Defic Syndr 45, 359–369 (2007).

81. Price, P., Mathiot, N., Krueger, R., Stone, S., Keane, N. M., French, M. A Immune dysfunction and immune restoration disease in HIV patients given highly active antiretroviral therapy. J. Clin. Virol. 22, 279–87 (2001).

82. Martin, M. P., Gao, X., Lee, J., Nelson, G. W., Detels, R., Goedert, J.M., Buchbinder, S., Hoots, K., Vlahov, D., Trowsdale, J., Wilson, M., Brien, S. J. O., Carrington, M. Epistatic interaction between KIR3DS1 and HLA-B delays the progression to AIDS. Nat. Genet. 31, 429–434 (2002).

83. Qi, Y., Martin, M. P., Gao, X., Jacobson, L., Goedert, J. J., Buchbinder, S., Kirk, G. D., Brien, S. J. O., Trowsdale, J., Carrington, M. KIR / HLA Pleiotropism : Protection against Both HIV and Opportunistic Infections. PLoS Pathog. 2, (2006).

84. Long, B. R., Ndhlovu, L. C., Oksenberg, J. R., Lanier, L. L., Hecht, F. M., Nixon, D. F., Barbour, J. D. Conferral of Enhanced Natural Killer Cell Function by KIR3DS1 in Early Human Immunodeficiency Virus Type 1 Infection. J. Virol. 82, 4785–4792 (2008).

85. Sungjin, K., Poursine-laurent, J., Truscott, S. M., Lybarger, L., Song, Y., Yang, L., French, A. R., Sunwoo, J.B., Lemieux, S., Hansen, T. H., Yokoyama, W. M. Licensing of natural killer cells by host major histocompatibility complex class I molecules. Nature 436, 2–6 (2005).

86. Anfossi, N., Pascale, A., Guia, S., Falk, C. S., Roetynck, S., Stewart, C. A., Breso, V., Frassati, C., Reviron, D., Middleton, D., Romagné, F., Ugolini, S. Human NK Cell Education by Inhibitory Receptors for MHC Class I. Immunity 331–342 (2006). doi:10.1016/j.immuni.2006.06.013

87. Kim, S., Sunwoo, J. B., Yang, L., Choi, T., Song, Y-J., French, A. R., Vlahiotis, A., Piccirillo, J. F., Cella, M., Colonna, M., Mohanakumar, T., Hsu, K. C., Dupont, B., Yokoyama, W. M. HLA alleles determine differences in human natural killer cell responsiveness and potency. PNAS 105, 3053–3058 (2008).

88. Cooley, S., Xiao, F.M Pitt, M., Gleason, M., Mccullar, V., Bergemann, T. L., Mcqueen, K. L., Guethlein, L. A., Parham, P., Miller, J. S. A subpopulation of human peripheral blood NK cells that lacks inhibitory receptors for self-MHC is developmentally immature. Blood 110, 578–587 (2018).

89. Plenum, B., York, N., Gao, F., Bailes, E., Robertson, D. L., Chen, Y., Rodenburg, C. M., Michael, S. F., Cummins, L. B., Arthur, L. O., Peeters, M., Shaw, G. M., Sharp, P. M., Hahn, B. H. Origin of HIV-1 in the chimpanzee Pan troglodytes troglodytes. Nature 397, 436–441 (1999).

90. Neil, S. P. O., Novembre, F. J., Hill, A. B., Suwyn, C., Hart, C. E., Evans-strickfaden, T., Anderson, D. C., Herndon, J. G., Saucier, M., Mcclure, H. M. Progressive Infection in a Subset of HIV-1 – Positive Chimpanzees. J. Infect. Dis. 1051–1062 (2000).

91. Hatziioannou, T. & T. Evans, D. Animal models for HIV/AIDS research. Nat Rev Microbiol. 10, 852–867 (2015).

92. Morrow, W. J. W., Wharton, M., Lau, D. & Levy, J. A. Small Animals Are Not Susceptible to Human Immunodeficiency Virus Infection. J. gen. Virol. 2253–2257 (1987).

93. Shedlock, D. J., Silvestri, G. & Weiner, D. B. Monkeying around with HIV vaccines: using rhesus macaques to define 'gatekeepers' for clinical trials. Nat Rev Immunol 9, 717–728 (2015).

94. North, T. W., Villalobos, A., Hurwitz, S. J., Deere, J. D., Higgins, J., Chatterjee, P., Tao, S., Kauffman, R. C., Luciw, P. A., Kohler, J. J., Schinazi, R. F. Enhanced Antiretroviral Therapy in Rhesus Macaques Improves RT-SHIV Viral Decay Kinetics. Antimicrob. Agents Chemother. 58, 3927–3933 (2014).

95. Daza-vamenta, R., Glusman, G., Rowen, L., Guthrie, B. & Geraghty, D. E. Genetic Divergence of the Rhesus Macaque Major Histocompatibility Complex. Cold Spring Harb. Lab. Press 1501–1515 (2004). doi:10.1101/gr.2134504.1993

96. Miller, M. D., Yamamoto, H., Hughes, A. L., Watkins, D. I. & Letvin, N. L. Definition of an epitope and MHC class I molecule recognized by gag-specific cytotoxic T lymphocytes in SIVmac-infected rhesus monkeys. J. Immunol. 147, 320–329 (1991).

97. Boyson, J. E., Shufflebotham, C., Cadavid, L. F., Urvater, J. A., Knapp, L. A., Hughes, A. L., Watkins, D. I. The MHC class I genes of the rhesus monkey. Different evolutionary histories of MHC class I and II genes in primates. J. Immunol. 156, 4656–4665 (1996).

98. Knapp, L. A., Cadavid, L. F. & Watkins, D. I. The MHC-E Locus Is the Most Well Conserved of All Known Primate Class I Histocompatibility Genes. J Immunol 189–196 (1998).

99. Boyson, J. E., McAdam, S. N., Gallimore, A., Golos, T. G., Liu, X., Gotch, F. M., Hughes, A. L., Watkins, D. I. The MHC E locus in macaques is polymorphic and is conserved between macaques and humans. Immunogenetics 41, 59–68 (1995).

100. Ryan, A. F., Grendell, R. L., Geraghty, D. E. & Golos, T. G. A soluble isoform of the rhesus monkey nonclassical MHC class I molecule Mamu-AG is expressed in the placenta and the testis. J Immunol 169, 673–83 (2002).

101. Urvater, J., Otting, N., Loehrke, J. H., Rudersdorf, R., Slukvin, I. I., Piekarczyk, M. S., Golos, T. G., Hughes, A. L., Bontrop, R. E., Watkins, D. I. Mamu-I: a novel primate MHC class I B-related locus with unusually low variability. J Immunol 164, 1386–98 (2000).

102. Moffett, A. & Colucci, F. Co-evolution of NK receptors and HLA ligands in humans is driven by reproduction. Immunol. Rev. 267, 283–297 (2015).

103. Guethlein, L. A., Older Aguilar, A. M., Abi-Rached, L. & Parham, P. Evolution of killer cell Ig-like receptor (KIR) genes: definition of an orangutan KIR haplotype reveals expansion of lineage III KIR associated with the emergence of MHC-C. J Immunol 179, 491–504 (2007).

104. Hermes, M., Albrecht, C., Schrod, A., Brameier, M. & Walter, L. Expression Patterns of Killer Cell Immunoglobulin-Like Receptors (KIR) of NK-Cell and T-Cell Subsets in Old World Monkeys. PLoS One 8, 1–10 (2013).

105. Hershberger, K. L., Shyam, R., Miura, A. & Letvin, N. L. Diversity of the Killer Cell Ig-Like Receptors of Rhesus Monkeys. J. Immunol. 166, 4380–4390 (2001).

106. Parham, P. & Guethlein, L. A. Genetics of Natural Killer Cells in Human Health , Disease , and Survival. Annu. Rev. Immunol. 19.1-19.30 (2018). doi:10.1146/annurev-immunol-042617-053149

107. Nomura, T. & Matano, T. Association of MHC-I genotypes with disease progression in HIV/SIV infections. Front. Microbiol. 3, 1–6 (2012).

108. Rosner, C., Kruse, P. H., Hermes, M., Otto, N. & Walter, L. Rhesus Macaque Inhibitory and Activating KIR3D Interact with Mamu-A-Encoded Ligands. J. Immunol. 186, 2156–2163 (2011).

109. Colantonio, A. D., Bimber, B. N., Neidermyer, W. J., Reeves, R. K., Alter, G., Altfeld, M., Johnson, R. P., Carrington, M., O'Connor, D. H., Evans, D. T. KIR polymorphisms modulate peptide-dependent binding to an MHC class I ligand with a Bw6 motif. PLoS Pathog. 7, (2011).

110. Albrecht, C., Malzahn, D., Brameier, M., Hermes, M., Ansari, A. A., Walter, L. Progression to AIDS in SIV-infected rhesus macaques is associated with distinct KIR and MHC class I polymorphisms and NK cell dysfunction. Front. Immunol. 5, 1–16 (2014).

111. Khakoo, S. I. & Jamil, K. M. KIR/HLA interactions and pathogen immunity. J. Biomed. Biotechnol. 2011, (2011).

112. Aguilar, A. M. O., Guethlein, L. A., Hermes, M., Walter, L. & Parham, P. Rhesus macaque KIR bind human MHC class I with broad specificity and recognize HLA-C more effectively than HLA-A and HLA-B. Immunogenetics 63, 577–585 (2011).

113. Rosner, C. M. Funktionelle Analyse von MHC-Klasse-I-Genen des Rhesusaffen (Macaca mulatta). (2008).

114. Vitale, M., Zamai, L., Neri, L. M., Manzoli, L., Facchini, A., Papa, S. Natural killer function in flow cytometry: Identification of human lymphoid subsets able to bind to the NK sensitive target K562. Cytometry 12, 717–722 (1991).

115. Somanchi, S. S., McCulley, K. J., Somanchi, A., Chan, L. L. & Lee, D. A. A novel method for assessment of natural killer cell cytotoxicity using image cytometry. PLoS One 10, 1–15 (2015).

116. de Groot, N. G., Heijmans, C. M. C., de Ru, A. H., Janssen, G. M. C., Drijfhout, J. W., Otting, N., Vangenot, C., Doxiadis, G. G. M., Koning, F., van Veelen, P. A., Bontrop, R. E. A Specialist Macaque MHC Class I Molecule with HLA-B*27–like Peptide-Binding Characteristics. J. Immunol. 000–000 (2017). doi:10.4049/jimmunol.1700502

117. Rosner, C., Kruse, P. H., Lübke, T. & Walter, L. Rhesus macaque MHC class I molecules show differential subcellular localizations. Immunogenetics 62, 149–158 (2010).

118. Zhang, Z., Fu, T., Casimiro, D. R., Davies, M., Liang, X., Schleif, W. A., Tussey, L., Chen, M., Tang, A., Keith, A., Trigona, W. L., Freed, D. C., Tan, C. Y., Horton, M., Emini, E, A., Shiver, J. W. Mamu-A*01 Allele-Mediated Attenuation of Disease Progression in Simian-Human Immunodeficiency Virus Infection. J Virol 76, 12845–12854 (2002).

119. Walter, L. & Ansari, A. A. MHC and KIR polymorphisms in rhesus macaque SIV infection. Front. Immunol. 6, (2015).

120. Boudreau, J. E., Mulrooney, T. J., Le Luduec, J.-B., Barker, E. & Hsu, K. C. KIR3DL1 and HLA-B Density and Binding Calibrate NK Education and Response to HIV. J. Immunol. 196, 3398–3410 (2016).

121. Braud, V. M., Allan, D. S. & McMichael, A. J. Functions of nonclassical MHC and non-MHC-encoded class I molecules. Curr. Opin. Immunol. 11, 100–108 (1999).

122. Ferreira, L. M. R., Meissner, T. B., Tilburgs, T. & Strominger, J. L. HLA-G: At the Interface of Maternal–Fetal Tolerance. Trends Immunol. 38, 272–286 (2017).

123. Boyson, J. E., Iwanaga, K. K., Colas, G. & Watkins, D. Identification of a Novel MHC class I Gene, Mamu AG, Expressed in the Placenta of a Primate with an Inactive G Locus. Am. Assoc. Immunol. (1997).

124. Boyson, J. E., Iwanaga, K. K., Golos, T. G. & Watkins, D. I. Identification of the rhesus monkey HLA-G ortholog. Mamu-G is a pseudogene. J Immunol 157, 5428–5437 (1996).

125. Cohen, G. B., Gandhi, R. T., Davis, D. M., Mandelboim, O., Chen, B. K., Strominger, J. L., Baltimore, D. The Selective Downregulation of Class I Major Histocompatibility Complex Proteins by HIV-1 Protects HIV-Infected Cells from NK Cells. Immunity 10, 661–671 (1999).

126. Bashirova, A. A., Thomas, R. & Carrington, M. HLA / KIR Restraint of HIV : Surviving the Fittest. Annu Rev Immunol 295–317 (2011). doi:10.1146/annurev-immunol-031210-101332

127. Carrington, M., Martin, M. P. & Bergen, J. Van. KIR-HLA intercourse in HIV disease. Trends Microbiol. 16, 620–627 (2008).

128. Boulet, S. et al. HIV protective KIR3DL1 and HLA-B genotypes influence NK cell function following stimulation with HLA-devoid cells. J. Immunol. 184, 2057–64 (2010).

129. O'Connor, D. H., Mothe, B. R., Weinfurter, J. T., Fuenger, S., Rehrauer, W. M., Jing, P., Rudersdorf, R. R., Liebl, M. E., Krebs, K., Vasquez, J., Dodds, E., Loffredo, J., Martin, S., McDermott, A. B., Allen, T. M., Wang, C., Doxiadis, G. G., Montefiori, D. C., Hughes, A., Burton, D. R., Allison, D. B., Wolinsky, S. M., Bontrop, R., Picker, L. J., Watkins, D. I. Major histocompatibility complex class I alleles associated with slow simian immunodeficiency virus disease progression bind epitopes recognized by dominant acute-phase cytotoxic-T-lymphocyte responses. J. Virol. 77, 9029–9040 (2003).

130. Loffredo, J. T., Maxwell, J., Qi, Y., Glidden, C. E., Borchardt, G. J., Soma, T., Bean, A. T., Beal, D. R., Wilson, N. A., Rehrauer, W. M., Lifson, J. D., Carrington, M., Watkins, D. I. Mamu-B*08-Positive Macaques Control Simian Immunodeficiency Virus Replication. J. Virol. 81, 8827–8832 (2007).

131. Posch, P. E., Borrego, F., Brooks, A. G. & Coligan, J. E. HLA-E is the ligand for the natural killer cell CD94/NKG2 receptors. J. Biomed. Sci. 321–331 (1998). doi:10.1007/BF02253442

9 Appendix

9.1 Mycoplasma PCR

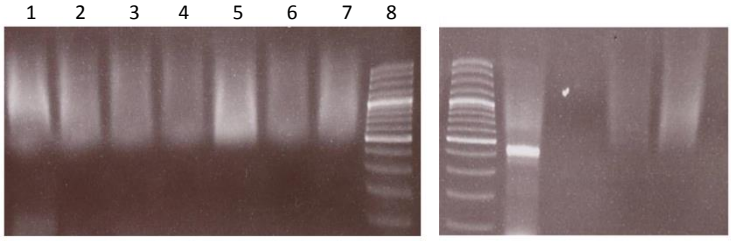

Figure 27 – Mycoplasma PCR results show only the positive control has contaminations in the first PCR. *1.5 % agarose gel showing results for the first mycoplasma PCR. Lanes one to seven show that no fragment was amplified from the supernatant of these cell lines, lane eight is the DNA ladder. On the right picture, the DNA ladder is on the first lane, followed by the mycoplasma positive control (supernatant from a cell culture that is contaminated), on the third lane, the mycoplasma negative control (supernatant from a clean cell culture), and on the fourth lane the PCR negative. Supernatant from different cell cultures was harvested after at least 48 h incubation with the cells, boiled for 5 min at 95 ºC, thoroughly vortexed, centrifuged down and 1 µL served as template in the PCR reaction (4.1.1.3) using primers #2614 and 2615. Supernatant from 1 – K-562, 2 - K-562 Mamu A1*001 GFP, 3 – K-562 Mamu B*048 GFP, 4 – K-562 Mamu A3*13 GFP, 5 - K-562 Mamu B*017 GFP, 6 – K-562 Mamu A1*011 GFP, 7 – K-562 Mamu A1*004 GFP*

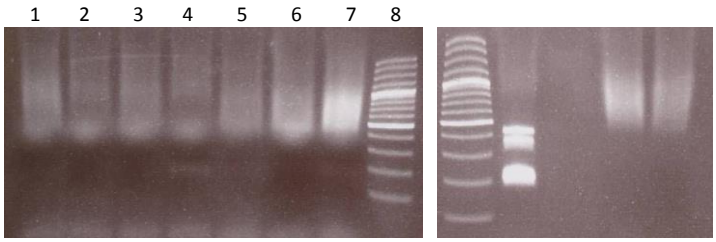

Figure 28 – Nested mycoplasma PCR results shows that all cultures are contamination free. *1.5 % agarose gel showing results for the nested mycoplasma PCR. Lanes one to seven show that no fragment was amplified from the supernatant of these cell lines, lane eight is the DNA ladder. On the right picture, the DNA ladder is on the first lane, followed by the mycoplasma positive control, on the third lane, the mycoplasma negative control, and on the fourth lane the PCR negative. For this PCR reaction, 1 µL of the previous mycoplasma PCR served as template in the PCR reaction (4.1.1.3) using primers #2616 and 2617. PCR product from 1 – K-562, 2 - K-562 Mamu A1*001 GFP, 3 – K-562 Mamu B*048 GFP, 4 – K-562 Mamu A3*13 GFP, 5 - K-562 Mamu B*017 GFP, 6 – K-562 Mamu A1*011 GFP, 7 – K-562 Mamu A1*004 GFP*

9.2 Transfection with pAcGFP-N1 empty vector increases MHC-I surface expression of K-562 cells

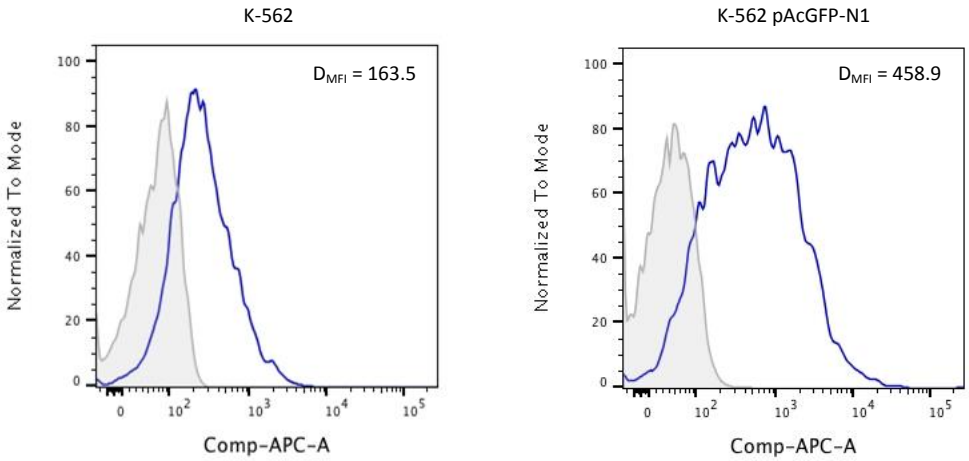

Figure 29 - Transfection with pAcGFP-N1 empty vector increases MHC-I surface expression of K-562 cells. *Flow cytometry data showing the increase in MHC-I surface expression of K-562 pAcGFP-N1 transfected cells compared to untransfected K-562. Histograms show the overlay of W6/32 + APC fluorescence intensity over the secondary antibody control, on the right side for untransfected K-562, on the left side for K-562 pAcGFP-N1 transfected cells. Grey lines show the increase in APC fluorescence due to the secondary antibody control, blue lines show the increase in APC fluorescence due to W6/32 binding to MHC-I surface molecules.*

9.3 Mamu B*008 complete sequence

```
                                          10        20        30
                                   ....|....|....|....|....|....|
Sequenced Mamu B*008 construct     GAATTCGAGTCTCCTCAGACGCCGAGATGC
IPD:MHC02225 Mamu-B*008:01         ~~~~~~~~~~~~~~~~~~~~~~~~~~~....
Primer Mamu B EcoRI (#9828)        ..............S..........
Primer Mamu B KpnI (#9829)         ------------------------------
Consensus                          ..............................

                                          40        50        60
                                   ....|....|....|....|....|....|
Sequenced Mamu B*008 construct     GGGTCATGGCGCCCCGAACCTTCCTCCTGC
IPD:MHC02225 Mamu-B*008:01         ..............................
Primer Mamu B EcoRI (#9828)
Primer Mamu B KpnI (#9829)         ------------------------------
Consensus                          ..............................

                                          70        80        90
                                   ....|....|....|....|....|....|
Sequenced Mamu B*008 construct     TGCTCTCGGGGGCCCTGGCCCTGACCGAGA
IPD:MHC02225 Mamu-B*008:01         ..............................
Primer Mamu B EcoRI (#9828)
Primer Mamu B KpnI (#9829)         ------------------------------
Consensus                          ..............................

                                         100       110       120
                                   ....|....|....|....|....|....|
Sequenced Mamu B*008 construct     CCTGGGCCGGCTCGCACTCCATGAGGTATT
IPD:MHC02225 Mamu-B*008:01         ..............................
Primer Mamu B EcoRI (#9828)
Primer Mamu B KpnI (#9829)         ------------------------------
Consensus                          ..............................

                                         130       140       150
                                   ....|....|....|....|....|....|
Sequenced Mamu B*008 construct     TCAGCACCTCCGTGTCCCGGCCCGGCCGCG
IPD:MHC02225 Mamu-B*008:01         ..............................
Primer Mamu B EcoRI (#9828)
Primer Mamu B KpnI (#9829)         ------------------------------
Consensus                          ..............................

                                         160       170       180
                                   ....|....|....|....|....|....|
Sequenced Mamu B*008 construct     GGGAGCCCCGCTTCATCTCCGTGGGCTACG
IPD:MHC02225 Mamu-B*008:01         ..............................
Primer Mamu B EcoRI (#9828)
Primer Mamu B KpnI (#9829)         ------------------------------
Consensus                          ..............................
```

```
                                  190       200       210
                                 ....|....|....|....|....|....|
Sequenced Mamu B*008 construct   TGGACGACACGCAGTTCGTGCGGTTCGACA
IPD:MHC02225 Mamu-B*008:01       ............................
Primer Mamu B EcoRI (#9828)
Primer Mamu B KpnI (#9829)       ----------------------------
Consensus                        ............................

                                  220       230       240
                                 ....|....|....|....|....|....|
Sequenced Mamu B*008 construct   GCGACGCCGAGAGTCCGAGAGAGGAGCCGC
IPD:MHC02225 Mamu-B*008:01       ............................
Primer Mamu B EcoRI (#9828)
Primer Mamu B KpnI (#9829)       ----------------------------
Consensus                        ............................

                                  250       260       270
                                 ....|....|....|....|....|....|
Sequenced Mamu B*008 construct   GGGCGCCGTGGATGGAGCAGGAGGGTCCAG
IPD:MHC02225 Mamu-B*008:01       ............................
Primer Mamu B EcoRI (#9828)
Primer Mamu B KpnI (#9829)       ----------------------------
Consensus                        ............................

                                  280       290       300
                                 ....|....|....|....|....|....|
Sequenced Mamu B*008 construct   AGTATTGGGAAGAGGAGACACGGAGAGCCA
IPD:MHC02225 Mamu-B*008:01       ............................
Primer Mamu B EcoRI (#9828)
Primer Mamu B KpnI (#9829)       ----------------------------
Consensus                        ............................

                                  310       320       330
                                 ....|....|....|....|....|....|
Sequenced Mamu B*008 construct   AGGGCCACGCACAGACTGACCGAGCGGACC
IPD:MHC02225 Mamu-B*008:01       ............................
Primer Mamu B EcoRI (#9828)
Primer Mamu B KpnI (#9829)       ----------------------------
Consensus                        ............................

                                  340       350       360
                                 ....|....|....|....|....|....|
Sequenced Mamu B*008 construct   TGGGGACCCTGCGCGGCTACTACAACCAGA
IPD:MHC02225 Mamu-B*008:01       ............................
Primer Mamu B EcoRI (#9828)
Primer Mamu B KpnI (#9829)       ----------------------------
Consensus                        ............................
```

```
                                  370       380       390
                                  ....|....|....|....|....|....|
Sequenced Mamu B*008 construct    GCGAGGCCGGGTCTCACACCCTCCAGACGA
IPD:MHC02225 Mamu-B*008:01        ..............................
Primer Mamu B EcoRI (#9828)
Primer Mamu B KpnI (#9829)        ------------------------------
Consensus                         ..............................

                                  400       410       420
                                  ....|....|....|....|....|....|
Sequenced Mamu B*008 construct    TGTACGGCTGCGACCTGGGGCCCGACGGGC
IPD:MHC02225 Mamu-B*008:01        ..............................
Primer Mamu B EcoRI (#9828)
Primer Mamu B KpnI (#9829)        ------------------------------
Consensus                         ..............................

                                  430       440       450
                                  ....|....|....|....|....|....|
Sequenced Mamu B*008 construct    GCCTCCTCCGCGGGTATCACCAGTACGCCT
IPD:MHC02225 Mamu-B*008:01        ..............................
Primer Mamu B EcoRI (#9828)
Primer Mamu B KpnI (#9829)        ------------------------------
Consensus                         ..............................

                                  460       470       480
                                  ....|....|....|....|....|....|
Sequenced Mamu B*008 construct    ACGACGGCAAGGATTACTTCGCCCTGAACG
IPD:MHC02225 Mamu-B*008:01        ..............................
Primer Mamu B EcoRI (#9828)
Primer Mamu B KpnI (#9829)        ------------------------------
Consensus                         ..............................

                                  490       500       510
                                  ....|....|....|....|....|....|
Sequenced Mamu B*008 construct    AGGACCTGCGCTCCTGGACCGCCGCGGACG
IPD:MHC02225 Mamu-B*008:01        ..............................
Primer Mamu B EcoRI (#9828)
Primer Mamu B KpnI (#9829)        ------------------------------
Consensus                         ..............................

                                  520       530       540
                                  ....|....|....|....|....|....|
Sequenced Mamu B*008 construct    TGGCGGCTCAGATAACCCAGCGCAAGTGGG
IPD:MHC02225 Mamu-B*008:01        ..............................
Primer Mamu B EcoRI (#9828)
Primer Mamu B KpnI (#9829)        ------------------------------
Consensus                         ..............................
```

```
                                        550       560       570
                                   ....|....|....|....|....|....|
Sequenced Mamu B*008 construct     AGGCGGCCCGTGAGGCGGAGCAGGTCAGAG
IPD:MHC02225 Mamu-B*008:01         ..............................
Primer Mamu B EcoRI (#9828)
Primer Mamu B KpnI (#9829)         ------------------------------
Consensus                          ..............................

                                        580       590       600
                                   ....|....|....|....|....|....|
Sequenced Mamu B*008 construct     CCTACCTGGAGGGGACGTGCGTGGAGTGGC
IPD:MHC02225 Mamu-B*008:01         ..............................
Primer Mamu B EcoRI (#9828)
Primer Mamu B KpnI (#9829)         ------------------------------
Consensus                          ..............................

                                        610       620       630
                                   ....|....|....|....|....|....|
Sequenced Mamu B*008 construct     TCCGCAGATACCTGGAGAACGGGAAGGAGA
IPD:MHC02225 Mamu-B*008:01         ..............................
Primer Mamu B EcoRI (#9828)
Primer Mamu B KpnI (#9829)         ------------------------------
Consensus                          ..............................

                                        640       650       660
                                   ....|....|....|....|....|....|
Sequenced Mamu B*008 construct     CGCTGCAGCGCGCGGATCCCCCAAAGACAC
IPD:MHC02225 Mamu-B*008:01         ..............................
Primer Mamu B EcoRI (#9828)
Primer Mamu B KpnI (#9829)         ------------------------------
Consensus                          ..............................

                                        670       680       690
                                   ....|....|....|....|....|....|
Sequenced Mamu B*008 construct     ACGTGACCCACCACCCCGTCTCTGACCATG
IPD:MHC02225 Mamu-B*008:01         ..............................
Primer Mamu B EcoRI (#9828)
Primer Mamu B KpnI (#9829)         ------------------------------
Consensus                          ..............................

                                        700       710       720
                                   ....|....|....|....|....|....|
Sequenced Mamu B*008 construct     AGGCCACCCTGAGGTGCTGGGCCCTGGGCT
IPD:MHC02225 Mamu-B*008:01         ..............................
Primer Mamu B EcoRI (#9828)
Primer Mamu B KpnI (#9829)         ------------------------------
Consensus                          ..............................
```

```
                                  730       740       750
                                  ....|....|....|....|....|....|
Sequenced Mamu B*008 construct    TCTACCCTGCGGAGATCACACTGACCTGGC
IPD:MHC02225 Mamu-B*008:01        ..............................
Primer Mamu B EcoRI (#9828)
Primer Mamu B KpnI (#9829)        ------------------------------
Consensus                         ..............................

                                  760       770       780
                                  ....|....|....|....|....|....|
Sequenced Mamu B*008 construct    AGCGGGATGGGGAGGACCAAACTCAGGACA
IPD:MHC02225 Mamu-B*008:01        ..............................
Primer Mamu B EcoRI (#9828)
Primer Mamu B KpnI (#9829)        ------------------------------
Consensus                         ..............................

                                  790       800       810
                                  ....|....|....|....|....|....|
Sequenced Mamu B*008 construct    CCGAGCTTGTGGAGACCAGGCCAGGAGGAG
IPD:MHC02225 Mamu-B*008:01        ..............................
Primer Mamu B EcoRI (#9828)
Primer Mamu B KpnI (#9829)        ------------------------------
Consensus                         ..............................

                                  820       830       840
                                  ....|....|....|....|....|....|
Sequenced Mamu B*008 construct    ATGGAACCTTCCAGAAGTGGGGAGCTGTGG
IPD:MHC02225 Mamu-B*008:01        ..............................
Primer Mamu B EcoRI (#9828)
Primer Mamu B KpnI (#9829)        ------------------------------
Consensus                         ..............................

                                  850       860       870
                                  ....|....|....|....|....|....|
Sequenced Mamu B*008 construct    TGGTGCCTTCTGGAGAAGAGCAGAGATACA
IPD:MHC02225 Mamu-B*008:01        ..............................
Primer Mamu B EcoRI (#9828)
Primer Mamu B KpnI (#9829)        ------------------------------
Consensus                         ..............................

                                  880       890       900
                                  ....|....|....|....|....|....|
Sequenced Mamu B*008 construct    CGTGCCATGTGCAGCACGAGGGGCTGCCGG
IPD:MHC02225 Mamu-B*008:01        ..............................
Primer Mamu B EcoRI (#9828)
Primer Mamu B KpnI (#9829)        ------------------------------
Consensus                         ..............................
```

```
                                        910       920       930
                                   ....|....|....|....|....|....|
Sequenced Mamu B*008 construct     AGCCCCTCACCCTGAGATGGGAGCCATCTT
IPD:MHC02225 Mamu-B*008:01         ..............................
Primer Mamu B EcoRI (#9828)
Primer Mamu B KpnI (#9829)         ------------------------------
Consensus                          ..............................

                                        940       950       960
                                   ....|....|....|....|....|....|
Sequenced Mamu B*008 construct     CCCAGTCCACCATCCCCATCGTGGGCATCG
IPD:MHC02225 Mamu-B*008:01         ..............................
Primer Mamu B EcoRI (#9828)
Primer Mamu B KpnI (#9829)         ------------------------------
Consensus                          ..............................

                                        970       980       990
                                   ....|....|....|....|....|....|
Sequenced Mamu B*008 construct     TTGCTGGCCTGGCTGTCCTAGGAGCTGTGT
IPD:MHC02225 Mamu-B*008:01         ..............................
Primer Mamu B EcoRI (#9828)
Primer Mamu B KpnI (#9829)         ------------------------------
Consensus                          ..............................

                                        1000      1010      1020
                                   ....|....|....|....|....|....|
Sequenced Mamu B*008 construct     TCATCGGAGCTGTGGTCGCTGCTGTGATGT
IPD:MHC02225 Mamu-B*008:01         ..............................
Primer Mamu B EcoRI (#9828)
Primer Mamu B KpnI (#9829)         ------------------------------
Consensus                          ..............................

                                        1030      1040      1050
                                   ....|....|....|....|....|....|
Sequenced Mamu B*008 construct     GGAGGAGGAAGAGCTCAGGTGGAAAAGGAG
IPD:MHC02225 Mamu-B*008:01         ..............................
Primer Mamu B EcoRI (#9828)
Primer Mamu B KpnI (#9829)         ------------------------------
Consensus                          ..............................

                                        1060      1070      1080
                                   ....|....|....|....|....|....|
Sequenced Mamu B*008 construct     GGAGCTACTCTCAGGCTGCGTCCAATGACA
IPD:MHC02225 Mamu-B*008:01         ..............................
Primer Mamu B EcoRI (#9828)
Primer Mamu B KpnI (#9829)         ------------------------------
Consensus                          ..............................
```

```
                                        1090      1100      1110
                                    ....|....|....|....|....|....|
Sequenced Mamu B*008 construct      GTGCCCAGGGCTCTGATGTGTCTCTCACGG
IPD:MHC02225 Mamu-B*008:01          ..............................
Primer Mamu B EcoRI (#9828)
Primer Mamu B KpnI (#9829)          -------------.................
Consensus                           ..............................

                                        1120      1130      1140
                                    ....|....|....|....|....|....|
Sequenced Mamu B*008 construct      CTAAGGTACCAATCACTAGTGAATTCGCGG
IPD:MHC02225 Mamu-B*008:01          ..TGA
Primer Mamu B EcoRI (#9828)
Primer Mamu B KpnI (#9829)          ..........
Consensus                           ..WRR........................
```